Point-by-point response to the reviews

Anonymous Referee #1

In this paper, which appears to be a follow-on from Guzman et al., 2017, the authors develop a simple approximation that allows them to estimate outgoing longwave radiation (OLR) using three parameters that are readily obtained from space-based lidar measurements: cloud top, cloud base (or, for opaque layers, apparent base) and cloud optical depths. Cloud altitudes are converted to temperatures using model data. The optical depths are used to compute emissivities. Since the current generation of space-based lidars cannot measure the optical depth of opaque layers, the emissivities for these clouds are assumed to be 1. For opaque clouds, OLR is approximated as a simple linear function of mid-layer temperature. The approximation for transparent clouds also uses mid-layer temperature, but is not as straightforward, as it also requires estimates of cloud emissivity and the OLR in clear sky conditions. Collocated CERES measurements are used to characterize the accuracy of both approximations.

The material presented in this paper is appropriate for AMT, and, after a few modifications are made, I believe the manuscript should eventually be published. The English language usage is, at times, somewhat (and occasionally very) awkward; however, the paper is well-organized, the figures are well-done and informative, the authors' derivation of their technique was clear and the steps taken to verify its performance were appropriate and straightforward. While the most interesting (and potentially useful) part of the manuscript was section 6, where the authors describe the limitations of their method, there are still a couple of issues that I believe deserve further investigation.

1. I had hoped to find a clear and convincing explanation for the rotation of the thin cloud data from the one-to-one line that is so evident in Figure 6b.

- **Response:**
  - The rotation of the thin cloud data from the one-to-one line does not affect the results of this study. Indeed, we did a sensitivity study to $CRE_{Thin}^{\boxplus\,(LID)}$ (Sect. 6.3): instead of computing the lidar-derived $CRE_{Thin}^{\boxplus\,(LID)}$ using the relationship used in Fig. 6b, we consider $CRE_{Thin}^{\boxplus}$ as the residual between CERES-derived total $CRE_{Total}^{\boxplus\,(CERES)}$ and lidar-derived $CRE_{Opaque}^{\boxplus\,(LID)}$: $CRE_{Thin}^{\boxplus} = CRE_{Total}^{\boxplus\,(CERES)} - CRE_{Opaque}^{\boxplus\,(LID)}$. This leads to Opaque clouds contributing to 74 % to the total CRE instead of 73 % in global mean. It is then not sensitive.
  - The rotation of the thin cloud data from the one-to-one line is the consequence of multiple effects. We examine hereafter the points raised by the reviewer. Thank you.

In particular,

(a) I'd like to know if this rotation is diminished in the "single-cloud-layer situations (not shown)", for which R increases from 0.89 to 0.92 (I suggest including the "not shown" plots in a future revision);

- **Response:** This rotation is not diminished in the "single-cloud-layer situations" (Fig. A4d).
- **Change made:**
  - In Sect. 6: Sect. 6.2 Multi-layer cloud and broken cloud situations has been added.
  - In Appendix: Fig. A4 has been added. It shows the decomposition of Fig. 6 in "single-layer cloud" and "multi-layer cloud" situations. The main text refers to Fig. A4 in Sect. 6.2.

(b) I'm intrigued by the differences in the sampling distributions for the opaque clouds vs. the thin clouds. For opaque layers, there is a noticeable skew in the distribution caused by (per line 518) "occurrences far from and over the identity line in Fig. 6a". But for the thin clouds in Fig. 6b the sampling distribution appears to be normally distributed about a single straight line). Do the authors have any thoughts or speculations about the root cause(s) for this difference in behavior?

- **Response:** The new Fig. A4e shows that the noticeable skew in the distribution is due to multi-layer cloud situations. In these situations, an optically thin cloud overlapping an optically opaque cloud will tend to significantly underestimate $T_{Opaque}^{|}$ as we do not consider the difference of emissivity between the two clouds. For thin clouds, in presence of multi-layer cloud situations (Fig. A4f), $T_{Thin}^{|}$ can be overestimated or underestimated depending on which cloud is optically thicker. The contrast between their emissivity is generally smaller than for an opaque multi-layer cloud situation. This is the reason why there is no noticeable skew in the distribution for the thin clouds.

2. How sensitive is the thin cloud OLR to emissivity errors introduced by aerosol contamination of “clear air” beneath the clouds detected by GOCCP?

- **Response:** The computation of the Thin cloud emissivity $\varepsilon^{|}_{Thin}$ used all the clear sky layers (without aerosol) located below the lowest cloud layer, in order to determine the optical thickness of the cloud layers. If, for example, an aerosol layer is present just below the cloud, $\varepsilon^{|}_{Thin}$ would be derived from the sum of the cloud layer optical thickness and the aerosol layer optical thickness. As this study is only over ocean, errors introduced by aerosol are essentially found during boreal summer over a limited area: the dust plume (Peyridieu et al., 2010 DOI:10.5194/acp-10-1953-2010). Moreover, with regards to this study, we are interested in CRE, which, over ocean, are far larger than aerosol direct radiative effect.

Minor issues:

Line 17 : how much does the “atmosphere opacity altitude” depend on the (a) capabilities of the lidar used to measure the cloud, (b) the ambient lighting conditions, and (c) the algorithms used to retrieve apparent cloud base?

- **Response:** The “atmosphere opacity altitude” $Z^{|}_{Opaque}$ indeed depends on these three aspect.
  (a) The accuracy of $Z^{|}_{Opaque}$ depends on the vertical resolution of the lidar, the telescope field of view, and the capabilities receiver sensor (noise). These uncertainty sources likely give error smaller than one 480 m bin.
  (b) $Z^{|}_{Opaque}$ retrieval is difficult during daytime because daytime conditions are much noisier than the nighttime conditions in CALIOP data. This is the reason why we only use nighttime data in this study.
  (c) $Z^{|}_{Opaque}$ depends on the algorithm used to retrieve apparent cloud base. It depends on the horizontal and vertical averaging choice (Chepfer et al., 2013; Cesana et al., 2016).
    · Chepfer et al. (2013) – DOI:10.1175/JTECH-D-12-00057.1
    · Cesana et al. (2016) – DOI:10.1002/2015JD024334
- **Change made:**
  ➢ In Sect. 2.1 (1st §): “$Z^{|}_{Opaque}$ depends on the horizontal and vertical averaging used in the retrieval algorithm. It is also affected by sunlight noise during daytime. At 480 m vertical resolution, it poorly depends on the lidar characteristics.” has been added.

Lines 126–175 : nothing in this description makes it clear that columns containing multiple layers are actually included in the analyses. The fact that all columns are partitioned into one of the three categories (i.e., clear, thin cloud, and opaque cloud) should be made clear from the very beginning, and not postponed until lines 176–179.

- **Change made:**
  ➢ In Sect. 2.1 (1st §): “The GCM-Oriented CALIPSO Cloud Product (GOCCP)-OPAQ (GOCCP v3.0; Guzman et al., 2017) segregates each atmospheric single column sounded by the CALIOP lidar as one of the 3 following single column types” has been replaced by “The GCM-Oriented CALIPSO Cloud Product (GOCCP)-OPAQ (GOCCP v3.0; Guzman et al., 2017) has 40 vertical levels with 480 m vertical resolution. Every CALIOP single shot profile — including multi-layer profiles — is classified into one of three types”.

Line 171 : in the vast majority of CALIPSO literature (including Garnier et al., 2015, which is cited here), the symbol for optical depth is τ. δ is used for depolarization ratios.

- **Response:** We agree with the reviewer.
- **Change made:**
  ➢ Throughout the paper: “δ” has been replaced by “τ”.

Lines 378–383 : here and elsewhere, I find the authors’ notation to be very complex and cumbersome, which makes the text difficult to read and hard to understand.

- **Response:** We agree with the reviewer that our notation can be sometimes cumbersome. However, we choose this very explicit notation in order to avoid misleading interpretation as, throughout the paper, calculations are made at different spatial resolution (lidar single shot, CERES footprint, and gridded).

Lines 530–531 : to my eye, the midlatitude emissivities are not “mostly centered around 0.25”

- **Response:** We agree with the reviewer that this statement is not very accurate and has been removed.
- **Change made:**

- In Sect. 6.3 (3rd §): "Given that $\varepsilon_{Thin}^{|}$ is mostly centered around 0.25 (Fig. 4d) it should not bring a substantial error, and" has been replaced by "However,".

Line 554 : according to my (admittedly limited) understanding of the way the GOCCP cloud detection scheme works, a more realistic assessment would have been obtained by using on bin lower rather than one bin higher.

- **Response:** We choose to take one bin higher for the sensitivity test on $Z_{Opaque}^{|}$ in order to be able to apply this in the same way for every opaque cloud profile. Indeed, a non-negligible amount of opaque cloud profiles have their $Z_{Opaque}^{|}$ at the lowest GOCCP level (240 m above sea level), and taking the equivalent of a bin lower would have given negative opacity altitudes (–240 m). This problem is avoided taking one bin higher instead and the sensitivity test should not be sensitive to this choice since the relation between $OLR_{Opaque}^{|}$ and $T_{Opaque}^{|}$ is linear.
- **Change made:**
  - In Sect. 6.5 (first §): "(as moving $Z_{Opaque}^{|}$ one bin down would have led to negative values for some $Z_{Opaque}^{|}$)" has been added.

Lines 641–642 : the suggestion that "the laser beam is not able go through the entire cloud if its vertical geometrical thickness is greater than 5 km" is demonstrably false. For example, see https://www-calipso.larc.nasa.gov/products/lidar/browse_images/show_detail.php?s=production&v=V4-10&browse_date=2010-01-01&orbit_time=12-47-14&page=3&granule_name=CAL_LID_L1-Standard-V4-10.2010-01-01T12-47-14ZN.hdf
The region between ~1.6° S and ~5.4° S contains numerous examples of transparent cirrus that are more than 6 km thick.

- **Response:** We agree with the reviewer.
- **Change made:**
  - In Appendix B (2nd §): "[…] the laser beam is not able go through the entire cloud if its vertical geometrical thickness is greater than 5 km […]" has been removed.

Point-by-point response to the reviews

Anonymous Referee #2

In this paper the authors devise a technique for relating – with a fairly high amount of accuracy – outgoing long wave radiation (OLR) at the top of the atmosphere (TOA) to several quantities that can be acquired from space-borne lidar (i.e., CALIOP on board Calipso). These quantities are the the radiative temperature and spatial coverage of opaque clouds and the radiative temperature, spatial coverage, and LW emissivity of thin clouds. Opaque clouds are defined as those for which the lidar beam becomes fully attenuated within the cloud, and typically have LW optical depths exceeding 1.5-2.5. Thin clouds, with LW optical depths less than this threshold, are semi-transparent and do not fully attenuate the lidar beam. The authors derive a simple semi-empirical relationship in which OLR increases by 2 W/m2 for every 1 K increase in opaque cloud radiating temperature. For thin clouds, this 2:1 relationship is scaled by the cloud LW emissivity. OLR inferred from the lidar-derived quantities compares well with that measured directly by CERES, at a variety of spatial scales.

I found the technique described in the paper to be a clever use of the unique measurements provided by active sensors in space. Despite the presence of errors (notably for thin clouds), the OLR can be largely reproduced from 5 basic measurements, which makes it a powerful tool for relating cloud property changes to OLR. I recommend publication pending revisions based on the my concerns that are detailed below.

Major Comments:

1) My main concern with this work is that the authors may be slightly overstating the value of such an analysis, especially in regard to how it is contrasted with passive sensors. Passive sensors are rightfully criticized for often giving incorrect information about cloud vertical distribution, which active sensors retrieve with much higher accuracy. However, passive sensors are (essentially) directly retrieving the quantity that the authors need to derive here: the emission temperature of clouds. Passive retrievals may not place the cloud top at the correct physical altitude like a lidar does, but they do place it at the effective radiating temperature, which is what matters for the OLR and any TOA LW anomalies. This is basically what makes studies that relate TOA radiation to passive-derived cloud fraction histograms like Hartmann et al. (1992), Zelinka et al DOI: 10.1175/JCLI-D-11-00248.1 (2012) and Yue et al DOI: 10.1175/JCLI-D-15-0257.1, (2016) possible. The authors are sort of reverse- engineering this problem: They have highly accurate measurements of backscatter by cloud particles as a function of altitude, which they then use in a clever way to derive the effective radiating temperature, which is what you would already have if you started with passive measurements. It is not obvious to me that this is superior. I think the paper requires a clear discussion of why one would prefer this technique over one relying directly on passive measurements, and/or a discussion of how they both could complement each other. Simply asserting that active sensors retrieve the vertical profile of condensate more accurately is not compelling in this particular context.

- **Response:** We agree with the reviewer that a clear discussion of why one would prefer this technique over one relying on passive measurements is required. Thank you for your comment.
- **Change made:**
  - In Sect. 3.1 (last §): "These cloud radiative temperatures are fundamental to study the LW CRE and are different from the effective radiating temperatures measured by passive instruments which are influenced by radiation coming from below the cloud. In the case of Opaque cloud which completely absorbs upward LW radiative flux propagating from below, the effective radiating temperature measured by passive instruments should agree with the cloud radiative temperature. However, this assumes to know that the cloud is Opaque, but cloud emissivity from passive measurements is also sensitive to hypothesis made on the clear sky and surface property. Unlike passive measurements, lidar measurements robustly separate Opaque clouds and Thin clouds from the presence or not of a surface echo (Guzman et al., 2017)." has been added.

One advantage I can think of relative to existing kernel techniques is that it does indeed seem desirable to have a small set of measurements that one can get both from observations (Calipso) and models (albeit, those running the Calipso simulator) that can give a highly accurate proxy for OLR, in keeping with the analogy to APRP in the SW. This is in contrast to relying on 7x7 histogram of cloud types from ISCCP and a kernel to match.

- **Response:** Thank you for this comment.
- **Change made:**
  - In Introduction (8th §): "We propose to build on these studies by adding the space-borne lidar information." has been replaced by "We propose to build on these studies by adding spaceborne lidar information to obtain a simplified radiative transfer model in the LW domain that can give a highly

accurate proxy for OLR with a small set of parameters available from both observations (space-lidar) and models (space-lidar simulator). This approach is in contrast to reliance on 7×7 histograms (altitude×optical depth) of cloud types from ISCCP and use of a matching radiative kernel.".

Perhaps another advantage has to do with the more practical issue of observing cloud changes over a long period of time. Few people trust ISCCP trends because of various issues that arise with splicing many individual satellites together that are poorly inter-calibrated and have non-climate related trends from satellite orbit changes, view angle changes, etc. (Norris and Evan DOI: 10.1175/JTECH-D-14-00058.1 2015). Presumably some of these issues are less relevant for lidars? If so, it would be important to distinguish these sorts of problems from those arising from the retrieval philosophy (e.g., if ISCCP was a perfect system without any artifacts, would the active approach still be superior?)

- **Response:** Thank you for this comment.
- **Change made:**
  - In Introduction (8th §): "Moreover, a highly stable long-time observational record is essential to study clouds and climate feedback (Wielicki et al., 2013), and current passive instruments have shown limited calibration stability over decadal time scales (e.g. Evan et al., 2007; Norris and Evan, 2015; Shea et al., 2017)." has been added.

2) On lines 362-365, the authors state "Monitoring T_Opaque on longterm should provide important information which should help to better understand the LW cloud feedback mechanism. Moreover, because the relationship is linear, it simplifies the derivatives in mathematical expressions of feedback and will allow to construct a useful framework to study LW cloud feedback in simulations of climate models." Feedbacks are conventionally defined as the change in a given quantity holding all else fixed. In the case of altitude feedback, this would be the change in cloud altitude only, with everything including the temperature profile fixed. Mathematically, this is equivalent to comparing a control OLR with a hypothetical one computed with the cloud at a higher altitude and therefore at a lower emission temperature. Of course we know that in reality the cloud top temperature is expected to stay nearly constant with surface warming as the cloud top altitude rises with the isotherms (i.e., FAT hypothesis of Hartmann and Larson 2002). Changes in T_Opaque will depend on both the change in cloud altitude and the change in temperature profile, and constant T_Opaque may mean perfectly complementary changes in both the altitude and the temperature profile, as one expects from FAT. If one uses your relationship between OLR and T_Opaque in computing feedbacks, then the mathematical formulation of the feedbacks will need to be changed to accommodate this. Specifically, I think one would need to compare the fixed T_Opqaue (FAT) case against a hypothetical baseline situation in which all things change except for the Z_Opaque, such that T_Opaque warms as much as a fixed altitude. While this is do-able, I disagree with the statement above that this simplifies the mathematics of feedbacks.

- **Response:** We agree with the reviewer that it does not simplify the mathematics of feedbacks as the equation is currently as a function of T_{Opaque}. We will adapt this equation for a future study using climate model outputs with lidar simulator so that the equation will be as a function of the altitude of T_{Opaque} ($Z_{T_{Opaque}}$) considering a linear atmospheric temperature lapse rate. In that way, a change in $Z_{T_{Opaque}}$, holding all else fixed, changes CRE_{Opaque} by a quantity which, divided by the global mean raise in surface temperature, is directly the cloud altitude feedback. This will so simplify the mathematics of feedbacks.

- **Change made:**
  - In Sect. 4.2 (2nd §): "Moreover, because the relationship is linear, it simplifies the derivatives in mathematical expressions of feedback and will allow to construct a useful framework to study LW cloud feedback in simulations of climate models." has been removed.

3) The English is very poor throughout the manuscript. There were far too many errors for me to list all of them (grammar, spelling, awkward phrasings, words that are plural that should not be, incorrect comma usage, etc.). In some places the writing was poor enough that the meaning of the sentence was unclear. This paper should be copyedited by a native English speaker before the reviewers see it again. In contrast, the figures were very clear, well-designed, and well-executed.

- **Response:** A native English speaker copy-edited the paper.

Minor Comments: In addition to the numerous English errors, I note the following:

Title: I would suggest deleting "the" before Outgoing and also rephrasing to ". . .where a space borne-lidar. . ."

- **Change made:**

- Title: "Link between the Outgoing Longwave Radiation and the altitude where the space-borne lidar beam is fully attenuated" has been replaced by "The link between Outgoing Longwave Radiation and the altitude where a spaceborne lidar beam is fully attenuated ".

Throughout: "cloud altitude longwave" seems awkward. Please rephrase to "longwave cloud altitude"

- **Change made:**
  - Throughout the paper: "cloud altitude longwave" has been replaced by "longwave cloud altitude".

Abstract: This ends very abruptly. It needs a better closing sentence.

- **Change made:**
  - In Abstract: "The link between outgoing longwave radiation and the altitude where a spaceborne lidar beam is fully attenuated provides a simple formulation of the cloud radiative effect in the longwave domain and so helps to understand the longwave cloud altitude feedback mechanism." has been put as closing sentence.

Lines 29-34: An uninformed reader of this paragraph will assume that the only reason there is uncertainty in how clouds will respond to warming is because models simulate biased clouds in the mean state. Surely this is not the only reason for low confidence in cloud feedbacks. There are a variety of recent review articles out on cloud feedbacks that may be helpful on this point.

- **Response:** We agree with the reviewer. Thank you for this comment.
- **Change made:**
  - In Introduction (1^{st} §): "One reason for this uncertainty is that […]" has been added.

Lines 52-54: This statement needs to be rephrased. Emergent constraints are not feedback mechanisms.

- **Response:** We agree with the reviewer.
- **Change made:**
  - In Introduction (3^{rd} §): "Such records do not exist yet. Klein and Hall (2015) suggested that some cloud feedback mechanisms, namely the "emergent constraints", could be tested with shorter records in comparing the simulated and the observed current climate interannual variabilities" has been replaced by "Such records do not exist yet, but existing records might help our understanding (Klein and Hall, 2015).".

Lines 64-65: I disagree that there is no link between observed cloud variables and LW CRE. See, for example, the section on LW cloud altitude feedback in Ceppi et al doi: 10.1002/wcc.465 (2017), which points out that high cloud amount and emissivity, along with the temperature structure of the upper troposphere, govern the strength of this feedback. All of these are observable.

- **Response:** We wanted to focus on the fact that, so far, there was no simple mathematical expression to directly link, at different scales, cloud properties to OLR.
- **Change made:**
  - In Introduction (4^{th} §): "Nevertheless, the cloud altitude LW feedback mechanism and its amplitude still struggle to be verified in observations. There is still no observational confirmation for the altitude LW cloud feedback mechanism because 1) there is no simple direct and robust formulation linking the observed fundamental cloud variables and the LW CRE at the TOA […]" has been replaced by "Nevertheless, the LW cloud altitude feedback mechanism and its magnitude still remain to be confidently verified with observations, because 1) there is no simple, robust, and comprehensive mathematical formulation linking the observed fundamental cloud variables and the LW CRE at the TOA […]".

Lines 85-87: Cloud fraction histograms from passive sensors generally report cloud fraction on 7 cloud top pressure bins; the high, mid, and low aggregating is usually done later to simplify.

- **Response:** We agree with the reviewer.
- **Change made:**
  - In Introduction (7^{th} §): "[…] and only retrieve the cloud top pressure and estimates of high-level, mid-level, and low-level cloud covers. These last estimates have been coupled with ranges of cloud optical depth to define different cloud types (Hartmann et al., 1992) associated to different values of CRE**.**" has been replaced by "[…] and instead retrieve single-layer effective cloud heights, often summarized as cloud fraction in seven cloud top pressure bins. Hartmann et al. (1992) used these pressure bins

coupled with ranges of cloud optical depth to define different cloud types associated to different values of CRE.".

Lines 88-89: Suggest also citing Zhou et al DOI: 10.1175/JCLI-D-12-00547.1 (2013) and Yue et al 10.1002/2016JD025174 (2017), who have done this globally

- **Response:** Thank you for this suggestion.
- **Change made:**
  - In Introduction (7th §): "Zhou et al., 2013" and "Yue et al., 2017" have been added.

Lines 90-91: These studies should be more clearly distinguished from the ones preceding it in the sentence: they have focused on trends, not interannual variability.

- **Response:** We agree with the reviewer.
- **Change made:**
  - In Introduction (7th §): "[…], as well as the International Satellite Cloud Climatology Project (ISCCP) and the Pathfinder Atmospheres Extended (PATMOS-x) (Marvel et al., 2015; Norris et al., 2016) in order to identify LW CRE changes associated to cloud properties changes." has been replaced by "[…]. Recently, Marvel et al. (2015) and Norris et al. (2016) analyzed data from the International Satellite Cloud Climatology Project (ISCCP) and the Pathfinder Atmospheres Extended (PATMOS-x) datasets in terms of these cloud types to search for trends in LW CRE which would be associated with changes in cloud properties.".

Line 97: Mace et al (2011) DOI: 10.1175/2010JCLI3517.1 should be cited here

- **Response:** We agree with the reviewer.
- **Change made:**
  - In Introduction (8th §): "Mace et al., 2011" has been added.

Lines 168-170: I can't understand this. Please rephrase.

- **Change made:**
  - In Sect. 2.1 (3rd §): "Thin cloud emissivity $\varepsilon_{Thin}^{|}$ of a *Thin cloud single column* is inferred from the mean attenuated scattering ratio of levels flagged as "Clear" below the cloud, that we note $\langle SR' \rangle_{below}$ and which approximately corresponds to the apparent two-way transmittance through the cloud. Indeed, considering a fixed multiple scattering factor $\eta = 0.6$, we retrieve the Thin cloud visible optical depth δ_{Thin}^{VIS} (Garnier et al., 2015)." has been replaced by "Thin cloud emissivity $\varepsilon_{Thin}^{|}$ of a *Thin cloud single column* is inferred from the attenuated scattering ratio of clear sky layers measured by the lidar below the cloud. This is approximately equal to the apparent two-way transmittance through the cloud which, considering a fixed multiple scattering factor $\eta = 0.6$, allows retrieval of the Thin cloud visible optical depth τ_{Thin}^{VIS} (Garnier et al., 2015). As cloud particles are much larger than the wavelengths of visible and infrared light, and assuming there is no absorption by cloud particles in the visible domain, the Thin cloud LW optical depth τ_{Thin}^{LW} is approximately half of τ_{Thin}^{VIS} (Garnier et al., 2015).".

Line 183: should be "sea ice"

- **Change made:**
  - In Sect. 2.1 (last §): "iced sea" has been replaced by "sea ice".

Line 185: Should be "Flux observations collocated with lidar cloud observations"

- **Change made:**
  - In Sect. 2.2 (title): "Fluxes observations collocated with lidar clouds observations" has been replaced by "Flux observations collocated with lidar cloud observations".

Line 216: Should "as" be "that"?

- **Response:** Yes, indeed. Thank you.
- **Change made:**
  - In Sect. 3 (1st §): "such as" has been replaced by "such that".

Figure 4: Is it possible to compare these cloud emission temperatures with those from passive sensors? They should be in agreement, right?

- **Response:** Passive sensors do not allow a clear separation of Opaque clouds and Thin clouds as done with the lidar. Moreover, it does not find the same cloud occurrence. Cloud emissivity retrieval depends on hypothesis on clear sky and surface properties. Comparison with classical product derived from passive sensor is not obvious. An equivalent comparison was done by Stubenrauch et al. (2010) with collocated measurements from CALIOP and the passive sounder AIRS: they compared the height of the cloud emission temperatures determined by AIRS with the "apparent middle" of the cloud sounded by CALIOP, which is actually our definition of where the emission temperature of the cloud is. They show very good agreement.

Line 273: "T_opaque among opaque clouds" is redundant. This sort of statement occurs throughout the document.

- **Response:** We agree this precision makes the reading difficult.
- **Change made:**
  - Throughout the paper: "among Opaque clouds" and "among Thin clouds" have been removed from the main text but left into figure captions and the 1st § of Sect. 3.2 to avoid misunderstanding.

Line 282: meaning of "mid-effect" is unclear

- **Change made:**
  - In Sect. 3.2 (2nd §): "These Opaque clouds will have a mid-effect on the local OLR," has been replaced by "The local radiative effect of these Opaque clouds is weaker than the effect if they were in tropical ascending regions.".

Line 288: "pick" should be "peak"

- **Response:** Thank you.
- **Change made:**
  - In Sect. 3.2 (3rd §): "pick" has been replaced by "peak".

Line 303: rephrase

- **Change made:**
  - In Sect. 3.2 (last §): "[…] emissivities of Thin clouds are usually small, and clouds with small emissivities have less impact on the OLR. This, once again, goes in the sense that the role that play Thin clouds on the total CRE should be significantly smaller than that of Opaque clouds." has been replaced by "[…] emissivities of Thin clouds are usually small, so they have little impact on the OLR and hence their contribution to CRE should be significantly smaller than that of Opaque clouds.".

Lines 422-423: Rephrase.

- **Change made:**
  - In Sect. 5.2 (1st §): "Interestingly, an inversion of cover predominance and colder temperature between Opaque and Thin clouds occurs around 30° latitude. " has been replaced by "There are always more Opaque clouds than Thin clouds in the extratropics (beyond 30° latitude) and they are colder than the Thin clouds. It is the opposite in the tropical belt: there are always more Thin clouds than Opaque clouds, and those are slightly warmer.".

Figure 8: Is the shading 2-sigma? Max to min?

- **Change made:**
  - In figure caption of Fig. 8: "(max to min)" has been added.
- **Additional change:**
  - Fig. 8 has been redrawn because an error in our script was discovered. During computation of annual means of T_{Opaque}, T_{Thin}, and ε_{Thin} on 2°x2° boxes (before averaging zonally), means were not weighted by monthly mean cover, on 2°x2° boxes, of opaque and thin clouds. It is now fixed. Changes are quite small and do not affect the conclusions.

Line 433: "under the tropics" – rephrase

- **Change made:**
  - In Sect. 5.2 (2nd §): "under the tropics" has been replaced by "in the tropics".

Line 453: I don't know what this statement means.

- **Response:** .
- **Change made:**
  - In Sect. 5.2 (last §): "Also, since the expression used for Thin clouds seems to give coherent results for $CRE_{Thin}^{\boxplus\,(LID)}$, it could also be used in a future work to quantify the role of a change in $C_{Thin}^{\boxplus}$, $T_{Thin}^{\boxplus}$, and $\varepsilon_{Thin}^{\boxplus}$ in the variations of $CRE_{Thin}^{\boxplus\,(LID)}$." has been replaced by "However, since the OLR expression above Thin clouds is almost as good as for the Opaque clouds, it could also be used in a future work to quantify the impact of changes in $C_{Thin}^{\boxplus}$, $T_{Thin}^{\boxplus}$, and $\varepsilon_{Thin}^{\boxplus}$ on the variations of $CRE_{Thin}^{\boxplus\,(LID)}$.".

Lines 488-493: The authors seem to be implying that omega is the only variable on which the cloud properties and CRE depend, and that therefore knowing how omega change will tell one how cloud properties and CRE will change. This is incorrect, as has been discussed many times over, most notably by Bony et al DOI 10.1007/s00382-003- 0369-6 (2004) where this type of analysis originally appeared. While omega changes may strongly determine regional changes in cloud properties, when averaged over the entire tropics, it is the thermodynamic sensitivity of cloud propertiesÂa˘ within omega bins that emerges as the dominant driver of cloud changes.

- **Response:** We agree with the reviewer.
- **Change made:**
  - In Sect. 5.3 (last §): "Because cloud properties seem to be invariants for dynamical regimes, a change in the tropics of the large-scale circulation should provide a change in the CRE predictable and linked to the spatial distribution (both covers and altitudes) of Opaque clouds and Thin clouds sounded by CALIOP. For example, under global warming, climate models suggest a narrowing of the ascending branch of the Hadley cell (e.g. Su et al., 2014), which means less convective regions and more subsiding regions and which should result in a decrease of the CRE predictable knowing the changes of ω_{500} all over the tropics." has been replaced by "Because cloud properties seem to be invariants for dynamical regimes between 20 hPa·day^{-1} and -100 hPa·day^{-1}, a change in the tropics of the large-scale circulation should lead to a predictable change in the CRE in regions that stay in this range of dynamical regimes, linked to the spatial distribution (both covers and altitudes) of Opaque clouds and Thin clouds sounded by CALIOP. For example, general circulation models suggest that a warmer climate will see a narrowing of the ascending branch of the Hadley cell (e.g. Su et al., 2014), which means less convective regions and more subsiding regions. This should result in a predictable decrease of the CRE, knowing the changes of ω_{500} for some part of the tropics.".

Section 6.1: It is unclear whether this is actually an error source. The authors raise the issue then immediately downplay it. Is it a source of error? Have you actually performed a sensitivity study to determine with these assumptions matter?

- **Response:** It is a source of error. The worst case for this is the multi-layer scenario when an optically thin cloud overlap an optically opaque cloud. This is now discussed in the new subsection 6.2. We could certainly have slightly more precise results using a centroid temperature for every case but it will add complexity to our expressions. However, the aim of our study is to find a simple expression of the CRE by determining its main cloud variable driver, not to reach the maximum of accuracy in CRE estimation.
- **Change made:**
  - In Sect. 6: Sect. 6.2 Multi-layer cloud and broken cloud situations has been added.
  - In Appendix:
    - Fig. A4 has been added. It shows the decomposition of Fig. 6 in "single-layer cloud" and "multi-layer cloud" situations. The main text refers to Fig. A4 in Sect. 6.2.
    - Fig. A5 has been added. It shows improvement on OLR_{Opaque} when considering multi-layer cloud in the computation of T_{Opaque}. The main text refers to Fig. A5 in Sect. 6.2.

Section 6.4: the impacts of these assumptions are being assessed on the global mean OLR, but I wonder whether they also influence the slope of OLR on T_Opaque.

- **Response:** As Z_{Opaque} is increased in every profile with the same amount (+480 m), and because atmospheric temperature profile is linearly dependent on the altitude, the slope of OLR_{Opaque} on T_{Opaque} is not influenced.

Point-by-point response to the reviews

Anonymous Referee #3

General

The authors present a methodology to estimate the outgoing longwave radiation (OLR) at the global scale from cloud products derived with the help of long-term space-borne measurements with the lidar CALIOP onboard CALIPSO. The major information comes from the opacity altitude of the atmosphere, i.e. the altitude at which the laser beam is fully attenuated due to clouds, and the geometrical cloud top height, which together allow the estimation of the radiative temperature of the cloud. It is shown that the latter one is linearly related to the OLR. Non-opaque (thin) clouds are treated in terms of top and base heights together with their emissivity, which is estimated from the lidar attenuated scattering ratio below the cloud under consideration of a constant multiple-scattering factor. For opaque clouds, a very good correlation between the derived OLR and the one measured by CERES is found, whereas a systematic deviation is seen for thin clouds. Despite some possible explanations the reason for the deviation in the case of thin clouds does not finally become clear.

In general, the paper presents an interesting approach to study longwave radiation effects of clouds at the global scale. The paper deserves publication, but has the potential to be improved both in terms of scientific contents as well as style of presentation. I recommend publication after consideration of the comments below.

Major

My major concerns are related to the rather simplified approach of using only two cloud scenarios, namely single-layer thin and opaque clouds. I would at least expect an extended sensitivity study regarding more realistic scenes in the very beginning. Justifying the approach before the presentation and discussion of results would be much more satisfying for the reader than the currently provided discussion of limitations in Sec. 6 (where several questions are tackled which the reader has already in mind when reading the major part of the paper). In particular, the following cases need to be considered in the evaluation and discussion of obtained results throughout the paper, starting already in Sec. 2.1 and Fig. 1.

- **Response:**
  - We agree with the reviewer that the proposed cases need to be discussed. We have dedicated a subsection in Sect. 6 for this. Specifications are given below.
  - We first tried to discuss all these aspects throughout the paper. However, this approach drowns the main message of the paper in digression. This is why we have decided to summarize them in Sect. 6.
- **Change made:**
  - In Sect. 6: Sect. 6.2 Multi-layer cloud and broken cloud situations has been added.

1) Multi-layer clouds: The discussion related to multi-layer clouds is not sufficient. The authors have added a very short paragraph in Sec. 2.1 (lines 176-179) during the technical revision of the paper. However, this explanation deals with thin clouds only. The more common feature is the appearance of thin, high cirrus clouds over mid-level or low-level opaque clouds. It is well known that retrievals from passive sensors locate the radiative cloud top height (or radiative temperature) in between the cloud layers in such cases, and that the location will depend on the optical thickness of the upper "thin" cloud. This fact is obviously not covered by the presented approach, since it considers only the geometrical properties of cloud top height and opacity altitude for the calculation of the radiative temperature. Although some discussion is provided in Sec. 6.2, no substantial investigation of the related consequences for the approach is given.

- **Response:** Thank you for this comment. An extensive investigation of multi-layer clouds is now given in Sect. 6.2.
- **Change made:**
  - In Appendix:
    - Fig. A4 has been added. It shows the decomposition of Fig. 6 in "single-layer cloud" and "multi-layer cloud" situations. The main text refers to Fig. A4 in Sect. 6.2 (1st §).
    - Fig. A5 has been added. It shows improvement on OLR_{Opaque} when considering multi-layer cloud in the computation of T_{Opaque}. The main text refers to Fig. A5 in Sect. 6.2 (1st §).

2) Broken clouds: The authors find a high amount of "thin clouds" in the lower troposphere at temperatures above 0 ◦C, i.e. liquid clouds (Fig. 4). Usually, liquid clouds are not penetrated by lidar, even if they are geometrically thin (thickness of a few hundred meters). Those occasions of "thin clouds" might often be related to broken opaque

clouds partly hit and partly missed by the lidar beam, thus leading to signals from the cloud and from the atmosphere and surface below the cloud in the same profile, so that the cloud appears to be transparent. The effect may be due to broken clouds within a single laser footprint, but can also result from averaging of laser shots over cloudy and clear atmospheric volumes before further retrievals are applied. From the description in Sec. 2.1, it does not become clear how averaging of lidar profiles is done, what exactly is meant with "each atmospheric single column" (line 127), which basic products (single shot, 1-km averages, 5-km averages) are used, and how the averaging to the 2◦x2◦ grid is performed. It should be studied which differences in the results are expected when sub-scale broken opaque clouds instead of thin clouds appear. It would be interesting to see whether the worse correlation between calculated and measured OLR found for thin clouds could be explained in this way. In this context, also the discussion in Sec. 6.2 is insufficient.

- **Response:** We agree with the reviewer that broken opaque clouds can be classified as thin clouds. However, in the GOCCP product, we do not average lidar profiles horizontally, so we only use single shot (90 m diameter footprint), which minimize this misclassification. Moreover, we plotted same as Fig. 6b only for Thin clouds with $T_{Thin} > 0\,°C$ (see Fig. A6): it shows excellent agreement between observed and lidar-derived OLR, and so does not explain the worse correlation between calculated and measured OLR as these clouds show excellent agreement.
- **Change made:**
  - In Sect. 2.1 (1st §): "The GCM-Oriented CALIPSO Cloud Product (GOCCP)-OPAQ (GOCCP v3.0; Guzman et al., 2017) segregates each atmospheric single column sounded by the CALIOP lidar as one of the 3 following single column types" has been replaced by "The GCM-Oriented CALIPSO Cloud Product (GOCCP)-OPAQ (GOCCP v3.0; Guzman et al., 2017) has 40 vertical levels with 480 m vertical resolution. Every CALIOP single shot profile — including multi-layer profiles — is classified into one of three types".
  - In Appendix:
    - Fig. A6 has been added. It shows Fig. 6b but only with $T^{\varnothing}_{Thin} > 0\,°C$. The main text refers to Fig. A6 in Sect. 6.2 (2nd §).

Minor

Abstract: The abstract doesn't say anything about the retrievals for thin clouds.

- **Change made:**
  - In Abstract: "Similarly, the longwave cloud radiative effect of optically thin clouds can be derived from their top and base altitudes and an estimate of their emissivity." has been added.

Line 185, should be: "Flux observations collocated with lidar cloud observations"

- **Change made:**
  - In Sect. 2.2 (title): "Fluxes observations collocated with lidar clouds observations" has been replaced by "Flux observations collocated with lidar cloud observations".

Line 290, regarding the "second mode": What does "more diffuse" mean? What about altocumulus, altostratus clouds?

- **Response:** We agree the reviewer it could also be due to altocumulus or altostratus clouds.
- **Change made:**
  - In Sect. 3.2 (3rd §): "The second mode could be due to more diffuse or developing convective clouds." has been replaced by "The middle mode, near 5 km, might be due to developing convective clouds or middle altitude clouds.".

Line 300, "cloud emissivity of the cloud": correct to either "cloud emissivity" or "emissivity of the cloud".

- **Response:** Thank you.
- **Change made:**
  - In Sect. 3.2 (last §): "cloud emissivity of the cloud" has been replaced by "cloud emissivity".

Lines 331-332, "in spite of significant differences in the atmospheric temperature and humidity profiles": What does "significant" mean? How are these differences considered/validated in the calculations?

- **Response:** The sentence was indeed not very clear, it has been modified.
- **Change made:**

- In Sect. 4.1 (2nd §): "Linear regressions done on other regions with different atmospheric conditions give a similar coefficient. This means that, in spite of the significant differences in the atmospheric temperature and humidity profiles, $OLR^{|}_{Opaque}$ depends essentially only on $T^{|}_{Opaque}$." has been replaced by "Conducting the same linear regression on very different atmospheric conditions (from tropical to polar) gives similar coefficients. This means that $OLR^{|}_{Opaque}$ depends mainly on $T^{|}_{Opaque}$.".

Line 372, "The evaluation . . . is only using observation from January 2008": This explanation should be given in the beginning of the discussion of Fig. 6.

- **Response:** .
- **Change made:**
  - In Sect. 4.2 (2nd §): "Figure 6 compares lidar-derived and observed OLR during January 2008." has been added.
  - In Sect. 4.2 (last §): "The evaluation showed in Fig. 6 is only using observation from January 2008." has been removed.

Lines 405-415: Explain the units to be applied in the equations.

- **Change made:**
  - In Sect. 5.1: "[…] where $CRE^{⊞\,(LID)}_{Opaque}$ and $OLR^{⊞}_{Clear}$ are expressed in W·m-2 and $T^{⊞}_{Opaque}$ in K." and "[…] where $CRE^{⊞\,(LID)}_{Thin}$ and $OLR^{⊞}_{Clear}$ are expressed in W·m-2 and $T^{⊞}_{Thin}$ in K." have been added after Eqs. (7) and (8).

Lines 556 and 561, "decreases...from...", "reduces...from...": The meaning of the sentences with the word "from" is unclear.

- **Change made:**
  - In Sect. 6.4: "from" has been replaced by "by".

There a many language/grammar/punctuation errors, which cannot be listed in detail here. The manuscript needs careful copy editing.

- **Response:** A native English speaker copy-edited the paper.

The ~~L~~link between ~~the~~ Outgoing Longwave Radiation and the altitude where ~~the~~ a space~~-~~borne lidar beam is fully attenuated

Thibault Vaillant de Guélis[1], Hélène Chepfer[1], Vincent Noel[2], Rodrigo Guzman[3], Philippe Dubuisson[4], David M. Winker[5], Seiji Kato[5]

[1]LMD/IPSL, Université Pierre et Marie Curie, Paris, France
[2]Laboratoire d'Aérologie, CNRS, Toulouse, France
[3]LMD/IPSL, CNRS, École polytechnique, Palaiseau, France
[4]Laboratoire d'Optique Atmosphérique, Université Lille, Lille, France
[5]NASA Langley Research Center, Hampton, Virginia, USA

Correspondence to: Thibault Vaillant de Guélis (thibault.vaillant-de-guelis@lmd.polytechnique.fr)

Abstract. According to climate model~~s'~~ simulations, the changing ~~cloud~~ altitude of mid and high clouds ~~change~~ is the dominant contributor ~~of~~ to the positive ~~ensemble~~ global mean longwave cloud feedback. Nevertheless, the mechanism of this ~~cloud altitude~~ longwave cloud altitude feedback ~~mechanism~~ and its ~~amplitude~~ magnitude ~~struggle~~ have not yet ~~to be~~been verified ~~in~~ by observations. A~~n a~~ccurate, stable~~ in time~~, and ~~potentially~~ long-term observations of a ~~cloud property summarizing~~metric characterizing ~~the~~ cloud vertical distribution and ~~driving~~ related to the longwave cloud radiative effect is needed to ~~hope to~~ achieve a better understanding of the mechanism of ~~cloud altitude~~ longwave cloud altitude feedback ~~mechanism~~. This study ~~proposes~~ shows ~~the~~ that direct ~~lidar~~ measurement of the altitude of ~~atmosphere~~ atmospheric lidar opacity ~~altitude~~ is a good candidate ~~to derive~~for the ~~needed~~ necessary ~~observed~~ observational ~~cloud property~~metric. The opacity~~is~~ altitude is the level at which a space~~-~~borne lidar beam is fully attenuated when probing an ~~optically~~ opaque cloud. By combining this altitude with ~~the~~ direct lidar measurement of the cloud top altitude, we derive the effective radiative temperature of opaque clouds ~~that~~ which linearly drives~~,~~ (as we will show)~~,~~ the outgoing longwave radiation. ~~This linear relationship provides a simple formulation of the cloud radiative effect in the longwave domain for opaque clouds and so, helps to understand the cloud altitude longwave feedback mechanism.~~ We find that~~,~~ ~~in presence of~~for an opaque cloud, a cloud temperature change of 1 K modifies its cloud radiative effect by 2 W·m^{-2}. Similarly, the longwave cloud radiative effect of optically thin clouds can be derived from their top and base altitudes and an estimate of their emissivity. We show with radiative transfer simulations that ~~this linear~~these relationships hold~~s~~ true at single atmospheric column scale~~ with radiative transfer simulations~~, at the ~~instantaneous radiometer footprint~~ scale of the Clouds and the Earth's Radiant Energy System (CERES) instantaneous footprint, and at monthly mean 2°×2° ~~gridded~~ scale. Opaque clouds cover 35 % of the ice-free ocean and contribute to 73 % of the global mean cloud radiative effect. Thin cloud~~s~~ coverage is 36 % and contributes ~~to~~ 27 % of the global mean cloud radiative effect. ~~This linear relationship~~The link between outgoing longwave radiation and the altitude where a spaceborne lidar beam is fully attenuated provides~~s~~ a simple formulation of the cloud radiative effect in the longwave domain ~~for opaque clouds~~ and so~~,~~ helps to understand the longwave cloud altitude ~~longwave~~ feedback mechanism.

1 Introduction

Cloud feedbacks ~~mechanisms remain~~ reamin the main source of uncertainty ~~for current~~in predictions of ~~the~~ climate sensitivity (e.g. Dufresne and Bony, 2008; Vial et al., 2013; Webb et al., 2013; Caldwell et al., 2016). One reason for this uncertainty is that c~~C~~louds simulated by climate models in the current climate, exhibit large biases compared to observations (e.g. Zhang et al., 2005; Haynes et al., 2007; Chepfer et al., 2008; Williams and Webb, 2009; Marchand and Ackerman, 2010; Cesana and Chepfer, 2012; Kay et al., 2012; Nam et al., 2012; Cesana and Chepfer, 2013; Klein et al., 2013)~~, leading~~ leading to low confidence in the cloud feedbacks predicted by ~~climate~~ the models.

~~In order t~~To understand ~~the~~ feedback mechanisms, it is useful to identify the fundamental variables ~~that~~ driveing the climate radiative response, and then to decompose the overall radiative response as the sum of the individual ~~radiative~~ responses due to changes in each of these variables. This classical feedback analysis has been ~~largely~~ frequently applied to outputs from numerical climate system simulations in order to estimate the effects of changes in water vapor, temperature lapse rate, clouds and surface albedo on the overall climate radiative response (e.g. Cess et al., 1990; Le Treut et al., 1994; Watterson et al., 1999; Colman, 2003; Bony et al., 2006; Bates, 2007; Soden et al., 2008; Boucher et al., 2013; Sherwood et al., 2015; Rieger et al., 2016). Focusing only on the cloud feedback mechanisms, ~~such approach (~~Zelinka et al.~~,~~ (2012a) and others used this approach ~~has been used~~ to isolate the role of each of the fundamental cloud variables that contribute to the cloud radiative response: ~~the~~ cloud cover, ~~the~~ cloud optical depth or ~~condensed~~ water phase (liquid ~~and~~ or ice), and ~~the~~ cloud altitude (or cloud temperature). The shortwave (SW) cloud feedback is primarily driven by changes in ~~the~~ cloud cover and ~~the~~ cloud optical depth, whereas the longwave (LW) cloud feedback is driven by changes in ~~the~~ cloud cover, ~~the~~ cloud optical depth and ~~the~~ cloud vertical distribution (e.g. Klein and Jakob, 1999; Zelinka et al., ~~2012a,~~ 2012b, 2013, 2016).

Using observations to ~~V~~verify~~ing~~ the cloud feedback mechanisms ~~that have been predicted by~~simulated in climate models ~~simulations using observations~~ requires two steps: ~~1)~~ First, establish a ~~direct and~~ robust link between the ~~the~~ observed fundamental cloud variables and the ~~the~~ cloud radiative effect (CRE) at the top of the atmosphere (TOA)~~;~~, so that a~~ny~~ change in a ~~the~~ fundamental cloud variable~~s~~ can be unambiguously ~~translated within~~ related to a change in the CRE at the TOA~~;~~. ~~2)~~ Second, establish an observational record of these ~~cloud~~ fundamental cloud variables that is long enough, stable enough, and accurate enough to detect the cloud changes due to greenhouse gases forcing (Wielicki et al., 2013). Such records do not exist yet~~. Despite this last limitation, Klein and Hall (2015) suggested that some~~ , but existing records might help our understanding ~~cloud feedback mechanisms~~(Klein and Hall, 2015)~~, namely the "emergent constraints", could be tested with shorter records in comparing the simulated and the observed current climate interannual variabilities~~.

Th~~e current~~ is paper focuses on the LW cloud feedback. Current climate models consistently predict that ~~the~~ cloud altitude change is the dominant contributor to the LW cloud feedback (Zelinka et al., 2016) ~~in agreement~~consistent with many previous ~~works~~ studies (e.g. Schneider, 1972; Cess, 1975; Hansen et al., 1984; Wetherald and Manabe, 1988; Cess et al., 1996; Hartmann and Larson, 2002). ~~If the~~While models agree on the sign and the physical mechanism of the LW cloud altitude feedback, they predict different ~~amplitudes~~magnitude. Simulations from the Coupled Model Intercomparison Project Phase 5 (CMIP5) ~~climate model simulations~~ suggest that upper tropospheric ~~the~~ clouds ~~altitude~~ w~~ould~~ill rise ~~up~~ by 0.7 to 1.7 km, ~~in the upper troposphere in all regions~~at all latitudes, in a warmer climate (+4 K)~~,~~. This is a ~~which is a~~ significant change compared to the currently observed variability and means cloud altitude~~, and thus,~~ could be a more robustly observable signature of climate change than the CRE (Chepfer et al., 2014). Nevertheless, the LW cloud altitude ~~LW~~ feedback mechanism and its ~~amplitude~~ magnitude still ~~struggle~~ remain to be confidently verified ~~in~~with observations~~.~~, ~~There is still no observational confirmation for the altitude LW cloud feedback mechanism~~ because 1) there is no simple, ~~direct and~~ robust, and comprehensive mathematical formulation linking the observed fundamental cloud variables and the LW CRE at the TOA and 2) there ~~is~~ are no sufficiently accurate and stable observations of the vertical distribution of clouds over several decades.

~~Thus, a~~A preliminary step toward observational constraints ~~progress~~ on ~~the~~ LW cloud feedback ~~is~~ would be to establish a ~~direct and~~ robust link between the LW CRE at the TOA and a small number of fundamental cloud properties that can be both accurately observed and ~~which can also be~~ simulated in climate models. In the SW, Taylor et al. (2007) defined such a simplified radiative transfer model by robustly expressing the SW CRE as a function of the cloud cover and the cloud optical depth. This linear relationship has been ~~largely~~ widely used for decomposing ~~the~~ SW cloud feedbacks into contributions ~~due to~~from changes in cloud cover ~~change~~ and optical depth ~~change~~. ~~Contrary to~~Unlike the SW CRE, the LW CRE ~~does not only depend on the cloud cover and the cloud optical depth, but also~~depends on a third variable, ~~the~~ cloud vertical distribution, in addition to cloud cover and optical depth. ~~As stated in Taylor et al. (2007) and in the attempt made by Yokohata et al. (2005),~~This makes establishing a simple radiative transfer model that robustly expresses the ~~LW~~ CRE as a function of a limited number of properties ~~(which can be reliably observed and which can also be simulated in climate models), is~~ more challenging in the LW than in the SW, as Taylor et al. (2007) and Yokohata et al. (2005) recognized. ~~because the LW involves three variables instead of two: the cloud cover, the cloud optical depth and the cloud vertical distribution.~~

Detailed information from active sensors has already been fed into comprehensive~~Complete~~ radiative transfer simulations ~~allow~~ to accurately compute the TOA and surface LW CRE ~~for~~ in ~~a~~ well-defined atmospher~~e~~ic conditions ~~(clear sky and clouds): detailed information on the atmospheric columns collected by active sensors have been used to estimate TOA CRE and surface CRE~~ (e.g. Zhang et al., 2004; L'Ecuyer et al., 2008; Kato et al., 2011; Rose et al., 2013). ~~In contrast, the definition of~~Defining a simple ~~and robust~~ linear formulation ~~between~~ linking the LW CRE at the TOA ~~and~~ to a limited number of cloud variables~~, that~~ would be more directly useful for decomposing ~~climate~~ cloud climate feedbacks ~~decomposition~~. This formulation, however, cannot ~~use~~ utilize the detail~~s~~ed ~~of the entire~~ cloud vertical distribution~~: first, one needs to~~ but must be ~~summarize the entire cloud vertical profile within a few~~based on specific cloud levels that drive~~s~~ the LW CRE at the TOA~~, and second, this~~. Further, these specific cloud levels ~~need to~~must be accurately ~~observed~~ observable at global scale from satellites.

Most of the cloud climatologies derived from space observations rely on passive satellites, which do not retrieve the ~~actual~~ detailed cloud vertical distribution, and ~~only retrieve the cloud top pressure and estimates of high-level, mid-level, and low-level cloud covers~~instead retrieve single-layer effective cloud heights, often summarized as cloud fraction in seven cloud top pressure bins. ~~These last estimates have been~~ Hartmann et al. (1992) used these pressure bins coupled with ranges of cloud optical depth to define different cloud types ~~(Hartmann et al., 1992)~~ associated to different values of CRE. These cloud types have been used to analyze the interannual cloud record collected by the Moderate Resolution Imaging Spectroradiometer (MODIS) (e.g. Zelinka and Hartmann, 2011; Zhou et al., 2013; Yue et al., 2017).~~,~~ Recently, Marvel et al. (2015) and Norris et al. (2016) analyzed data from ~~as well as~~ the International Satellite Cloud Climatology Project (ISCCP) and the Pathfinder Atmospheres Extended (PATMOS-x) datasets ~~(Marvel et al., 2015; Norris et al., 2016)~~ in terms of these cloud types ~~order~~ to ~~identify~~search for trends in LW CRE ~~changes~~which would be associated ~~to~~ with changes in cloud properties ~~changes~~.

Today, ten years of satellite-borne active sensor data collected by the Cloud-Aerosol LIdar with Orthogonal Polarization (CALIOP) from the Cloud-Aerosol Lidar and Infrared Pathfinder Satellite Observations (CALIPSO; Winker et al., 2010) and the Cloud Profiling Radar (CPR) from CloudSat (Stephens et al., 2002) are available to provide a detailed and accurate view of cloud vertical distribution. ~~But r~~Recently, Stephens et al. (submitted) used combined passive ~~observations~~ and active sensor~~s~~ observations (2B-FLXHR-LIDAR product; Henderson et al., 2013) ~~collected by the Cloud-Aerosol LIdar with Orthogonal Polarization (CALIOP) from the Cloud-Aerosol Lidar and Infrared Pathfinder Satellite Observations (CALIPSO) and the Cloud Profiling Radar (CPR) from CloudSat (Stephens et al., 2002)~~ to re-build ~~similar~~ cloud types ~~as in~~similar to Hartmann et al. (1992). Stephens et al (submitted) found differences in attribution of CRE to cloud type compared to Hartmann et al. (1992)~~and Hartmann et al. (1992)~~, largely due to ambiguities of passive cloud top height retrievals in the presence of optically thin and multi-layer clouds found very different results because passive sensors cannot retrieve reliable cloud altitude contrarily to active sensors (e.g. Sherwood et al., 2004; Holz et al., 2008; Mace et al., 2011; Michele et al., 2013; Stubenrauch et al., 2013). Today, ten years of satellite-borne active sensors data provide a detailed and accurate view of the cloud vertical distribution, whichData from CALIOP and CloudSat can be used to build, for the first time, a simplified radiative transfer model that robustly expresses the LW CRE as a function of the cloud cover, the optical depth (or emissivity) and the cloud altitude, and that can be tested against observations. To do so, iIn thise current paper, we summarize the entire cloud vertical profiles of clouds observed by active sensors with using three specific cloud levels that drive the LW CRE at the TOA and that can be accurately observed by space-borne lidar: the cloud top altitude, the cloud base altitude, and the altitude of opacity, at which where the laser beam getslidar signal becomes fully attenuated when it passes throughwithin an Opaque cloud. This altitude of opacity together withand the Opaque cloud cover, are both observed by space-borne lidar, and are strongly correlated to the LW CRE (Guzman et al., 2017) because emissions of from layers located below the altitude of opacity have little influence on the outgoing LW radiation (OLR). Previous studies (Ramanathan, 1977; Wang et al., 2002), suggested that the link between the Opaque cloud temperature and the OLR is linear, which would be mathematically very convenient for the study of cloud feedbacks (derivatives), but these studies are limited to radiative transfer simulations only. We propose to build on these studies by adding the space-borne lidar information to obtain a simplified radiative transfer model in the LW domain that can give a highly accurate proxy for OLR with a small set of parameters available from both observations (space-lidar) and models (space-lidar simulator). This approach is in contrast to reliance on 7×7 histograms (altitude×optical depth) of cloud types from ISCCP and use of a matching radiative kernel. Moreover, a highly stable long-time observational record is essential to study clouds and climate feedback (Wielicki et al., 2013), and current passive instruments have shown limited calibration stability over decadal time scales (e.g. Evan et al., 2007; Norris and Evan, 2015; Shea et al., 2017).

In Section 2 we present the data and tools methods used in this study. In Section 3 we define the radiative temperatures of Opaque clouds and Thin clouds derived from combined lidar cloud altitude observations and reanalysis, and present the observed distributionsdocument them over the mid-latitudes region and the ascending and subsiding regime areas in the tropics. In Section 4 we use radiative transfer simulations to establish a simple expression of the OLR as a function of lidar cloud observations for Opaque cloud single columns, and for Thin cloud (non-opaque) single columns, using clear sky data by addingfrom the Clouds and the Earth's Radiant Energy System (CERES) clear sky satellite observationsinstrument. Then, wWe verify this relationship using CERES and CALIPSO observations, first collocatedagainst observations at the instantaneous 20 km scale, using high spatial resolution collocated satellite-borne broadband radiometer (CERES) and lidar data (CALIPSO), and atthen monthly- mean averaged on 2° latitude × 2° longitude gridded scales. In Section 5 we estimate the independent contributions to the LW CRE of optically Opaque clouds and optically Thin clouds to the CRE. We then focus on the Tropics and examine Opaque and Thin cloud CREs partitioned into regions of subsidence and deep convectivione regions. Section 6 discusses the limits of the linear expression we propose, and concluding remarks are summarized in Section 7.

2 Data and ~~Tools~~Method

2.1 Opaque and Thin cloud~~s~~ observations by space~~-~~borne lidar

Eight years (2008–2015) of CALIPSO observations are used in this study. The GCM-Oriented CALIPSO Cloud Product (GOCCP)-OPAQ (GOCCP v3.0; Guzman et al., 2017) has 40 vertical levels with 480 m vertical resolution. ~~segregates~~ Every ~~each atmospheric single column sounded by the~~ CALIOP ~~lidar~~ single shot profile — including multi-layer profiles — is classified ~~as one of the 3 following single column~~into one of three types (Fig. 1):

- ~~The~~ *Clear sky single column* (brown, center) is entirely free of clouds~~. In other words,~~: none of the 40 levels ~~of 480 m vertical resolution~~ composing the atmospheric single column ~~is~~ are flagged as "Cloud" (cloud detection information in Chepfer et al., 2010).
- ~~The~~ *Opaque cloud single column* (orange, right) contains a cloud in~~to~~ which the ~~laser beam of the~~ lidar ~~ends~~ is fully attenuated, at an altitude termed $Z^{|}_{Opaque}$. ~~$Z^{|}_{Opaque}$ (as well as any $X^{|}$ variable used later on in the paper) refers to a *single column*, i.e. a 1D atmospheric column from surface to the TOA where each altitude layer is homogeneously filled with molecules and/or clouds, as mentioned by the exponent symbol "|". Such single column is directly identified by the presence of a level flagged as "z_opaque".~~ Full attenuation of the ~~lidar~~ signal is reached ~~for~~ at a visible optical depth~~, integrated from the top of the atmosphere (TOA),~~ of about 3 to 5 integrated from the TOA (Vaughan et al., 2009). This corresponds to a cloud LW emissivity of 0.8 to 0.9, if we consider that cloud particles do not absorb visible wavelengths and that ~~diffusion~~ scattering can be neglected in the LW domain. In GOCCP, such an opaque single column is identified by one level flagged as "z_opaque". Like other variables identified by the superscript "|" in the rest of this paper, $Z^{|}_{Opaque}$ refers to a *single column*, i.e. a 1D atmospheric column from the surface to the TOA where each altitude layer is uniformly filled with molecules and/or clouds. $Z^{|}_{Opaque}$ depends on the horizontal and vertical averaging used in the retrieval algorithm. It is also affected during daytime by noise from the solar background. At 480 m vertical resolution, it depends weakly on the characteristics of the lidar.
- ~~The~~ *Thin cloud single column* (brown and blue, left), contains ~~a~~ one or more semi-transparent cloud~~s~~s. In GOCCP, ~~S~~such a single column is identified by ~~the presence of~~ at least one level flagged as "Cloud" ~~without a~~but no level flagged as "z_opaque".

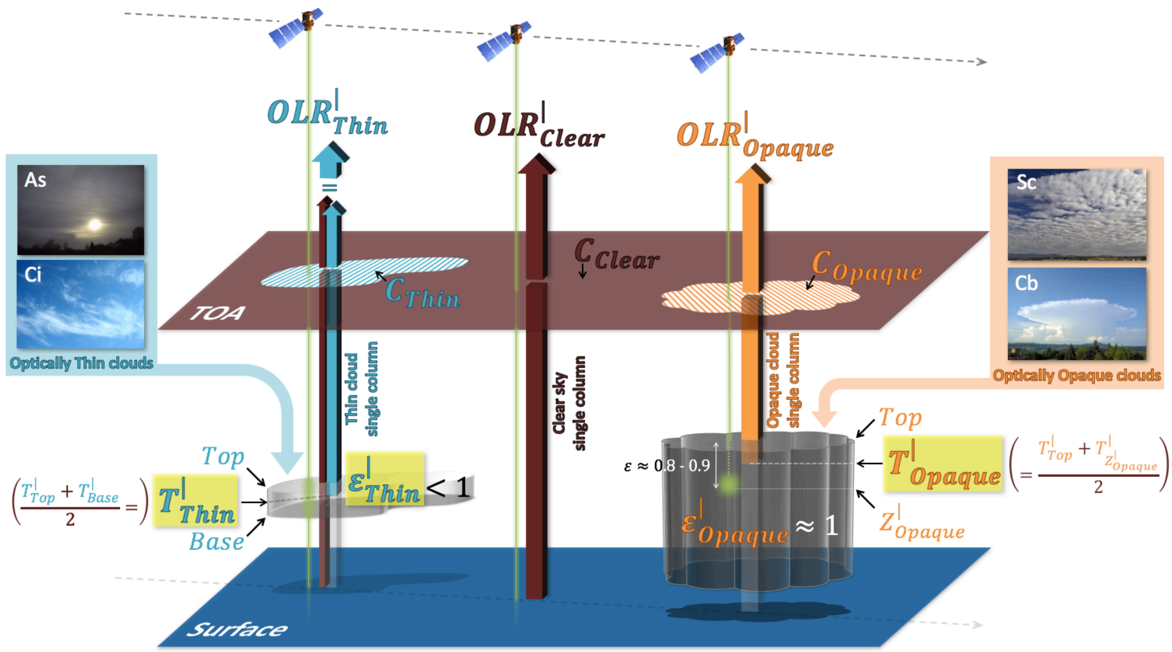

FIG. 1. Partitioning of the atmosphere into 3 single column types thanks to the CALIOP lidar: (left) Thin cloud single column, when a cloud is detected in the lidar signal and the laser beam ~~achieve to wholly go through the cloud until~~reaches the surface, (middle) Clear sky single column, when no cloud is detected, and (right) Opaque cloud single column, when a cloud is detected and the laser beam ~~ends~~ becomes fully attenuated ~~into the cloud~~ at a level called $Z^{|}_{Opaque}$. C, T and ε ~~respectively~~ account for cover, temperature and emissivity. ~~The v~~Variables highlighted in yellow are the key cloud properties, extracted from ~~the~~ GOCCP-OPAQ ~~product~~, that drive OLR over Thin cloud and Opaque cloud single columns. The total gridded OLR will be computed from the 3 single column OLRs weighted by their respective cover: C_{Thin}, C_{Clear}, C_{Opaque}.

Figure 2 shows the global cover~~ages~~ of these 3 single column types ~~, using~~on 2°×2° grids. ~~The g~~Global mean Opaque cloud~~s~~ cover $C^{\boxplus}_{Opaque}$ is 35 %, Thin clouds cover $C^{\boxplus}_{Thin}$ is 36 % and the Clear sky cover $C^{\boxplus}_{Clear}$ is 29 %. $C^{\boxplus}_{Opaque}$, $C^{\boxplus}_{Thin}$ and $C^{\boxplus}_{Clear}$ ~~(as well as any $X^{\boxplus}$ variable used later on in the paper)~~ refer to 2°×2° grid box, like any variable identified by the superscript "⊞" in the rest of the paper ~~as mentioned by the exponent symbol "⊞"~~. Opaque cloud~~s~~ cover is very high at mid-latitudes and, in the tropics, high occurrences clearly reveal regions of deep convection (warm pool, ITCZ) and stratocumulus regions at the east part of oceans. Thin cloud~~s~~ cover is very homogeneous over all oceans, with ~~some~~ slight maxima in some regions, ~~namely~~ near the warm pool. These results are discussed ~~in detail~~ in Guzman et al. (2017).

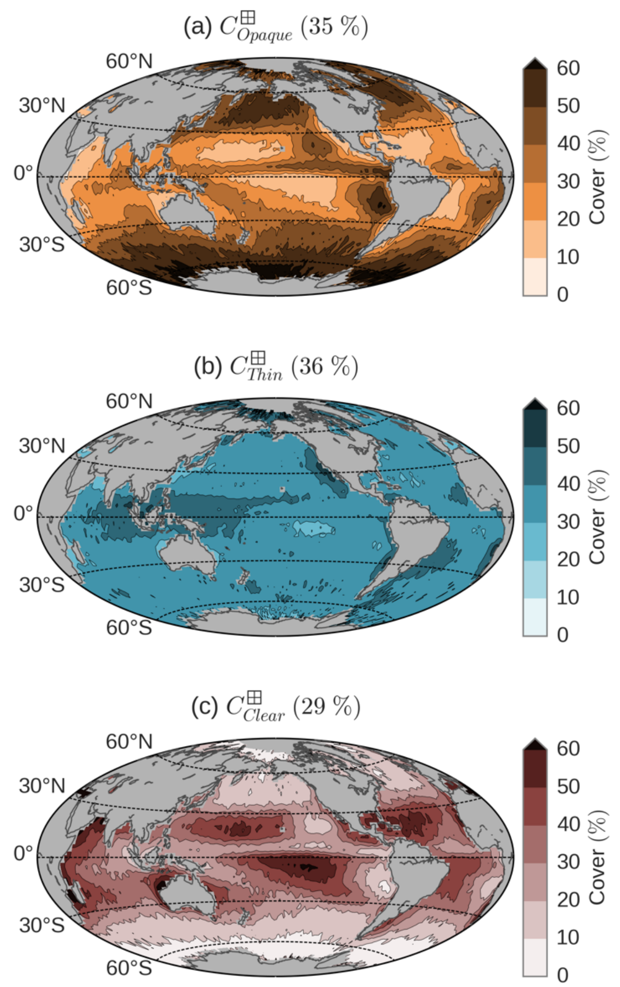

FIG. 2. Maps of (a) Opaque cloud cover (b) Thin cloud cover and (c) Clear sky cover. Only nighttime over ice-free oceans for the 2008–2015 period is considered. Global mean values are given in parentheses.

Our study builds on the work of Guzman et al. (2017) by ~~using~~ considering $Z^{|}_{Opaque}$ in terms of temperature~~s~~ rather than ~~instead of~~ altitude~~s~~, and by estimating an additional variable, the Thin cloud emissivity:

- Temperatures $T_{Z^{|}_{Opaque}}$, $T^{|}_{Top}$ and $T^{|}_{Base}$ are respectively those at the altitudes of the level flagged as "z_opaque" ($Z^{|}_{Opaque}$) and of the highest ($Z^{|}_{Top}$) and lowest ($Z^{|}_{Base}$) levels flagged as "Cloud", using ~~the~~ temperature profiles ~~of~~ from the NASA Global Modeling and Assimilation Office (GMAO) reanalysis (Suarez et al., 2005) provided in CALIOP Level 1 data and also reported in GOCCP v3.0 data.
- Thin cloud emissivity $\varepsilon^{|}_{Thin}$ of a *Thin cloud single column* is inferred from the ~~mean~~ attenuated scattering ratio of ~~levels flagged as "Clear" below the cloud, that we note $\langle SR' \rangle_{below}$ and~~ clear sky layers measured by the lidar below the cloud. This is ~~which~~ approximately ~~corresponds~~ equal to the apparent two-way transmittance through the cloud~~.~~ which ~~Indeed~~, considering a fixed multiple scattering factor $\eta = 0.6$, ~~we~~ allows ~~retrieve~~ retrieval of the Thin cloud visible optical depth $\delta\tau^{VIS}_{Thin}$ (Garnier et al., 2015). ~~Then, a~~As ~~the~~ cloud particles are much larger than the wavelengths of visible and infrared ~~wavelengths~~light, and ~~considering~~ assuming there is no absorption by cloud particles ~~is occurring~~ in the visible domain, the Thin cloud LW optical depth $\delta\tau^{LW}_{Thin}$ is approximately half of $\delta\tau^{VIS}_{Thin}$ (Garnier et al., 2015). Finally, we retrieve the Thin cloud emissivity ~~with~~ as $\varepsilon^{|}_{Thin} = 1 - e^{-\delta\tau^{LW}_{Thin}}$. ~~Opaque cloud~~

~~e~~Emissivity of Opaque clouds cannot be inferred and we ~~do the approximation that~~assume they are approximately ~~it is close to a~~ black ~~body~~bodies, ~~so~~ i.e. $\varepsilon^{|}_{Opaque} \approx 1$.

Our approach takes into account the possibility of multi-layer clouds within ~~S~~single columns: ~~with multi-layers of clouds are also consider in this study, i.e.~~ $T^{|}_{Top}$ and $Z^{|}_{Top}$ refer to the highest ~~"Cloud" flagged~~ level of the highest cloud in the column and $T^{|}_{Base}$ and $Z^{|}_{Base}$ to the lowest ~~"Cloud" flagged~~ level of the lowest cloud in the column. ~~Also, i~~In this case, $\varepsilon^{|}_{Thin}$ is computed from the summed optical depth of all cloud layers ~~present~~ in the column.

~~In order t~~To avoid ~~all possible uncertainties due to~~effects of solar background noise, results presented in this paper are only for nighttime conditions. Furthermore, we ~~restricted this study to~~only consider observations over oceans to avoid uncertainties due to the ground temperature diurnal cycle over land. ~~And, i~~In order ~~to~~ not to be influenced by major surface changes ~~of surface physical properties~~ across ~~the~~ seasons, we also removed from this study all observations over ~~iced~~ sea ice, based on sea ice fraction from the European Centre for Medium-Range Weather Forecasts (ECMWF) ERA-Interim reanalysis (Berrisford et al., 2011).

2.2 Flux~~es~~ observations collocated with lidar cloud~~s~~ observations

The CERES radiometer, on-board the Aqua satellite, measures the OLR at the ~~same~~ location where the CALIOP lidar, on board the CALIPSO satellite, will ~~shoot~~ fire 2 minutes and 45 seconds ~~afterwards~~later. ~~So, t~~The instantaneous Single Scanner Footprint (SSF) of the CERES swath crossing the CALIPSO ground-track gives the OLR over atmospheric single columns sounded by the lidar. ~~Because a~~The CERES footprint has a ~~diameter of~~ ~20 km diameter, ~~whereas~~ while the CALIOP lidar samples every 333 m along-track with a ~~footprint of~~ 70 m diameter footprint, ~~several~~ meaning the lidar can sample up to 60 atmospheric single columns ~~sounded by the lidar (up to 60) are located~~ within a single CERES footprint. To collocate the GOCCP-OPAQ instant data and the CERES SSF measurements, we use the CALIPSO, CloudSat, CERES, and MODIS Merged Product (C3M; Kato et al., 2011) which flags the instantaneous CERES SSF footprints where ~~of~~ the CERES swath ~~crossing~~ crosses the CALIPSO ground-track. ~~Finally, f~~For each of these flagged CERES SSF footprints, we matched, from geolocation information, all the GOCCP-OPAQ single columns falling into the CERES footprint. We consider that an atmospheric column with CERES footprint base is an Opaque (Thin) cloud column if all matched single columns are declared as Opaque (Thin) cloud single column. We then use these Opaque and Thin cloud columns to validate the lidar-derived OLR.

From the C3M product, we also use the estimated Clear sky OLR of the instantaneous CERES SSF ~~of~~ where the CERES swath ~~crossing~~ crosses the CALIPSO ground-track. This estimated Clear sky OLR is computed from radiative transfer simulations using the ~~synergy~~ synergistic information of the different instruments flying in the Afternoon Train (A-Train) satellite constellation. As C3M ~~is only released through~~ only covers the period when both CALIPSO and CloudSat are both fully operational (until April 2011)~~, during the time period when both CALIPSO and CloudSat are healthy,~~ we also use the Clear sky OLR from 1°×1° gridded data monthly mean CERES Energy Balanced and Filled (EBAF) Edition 2.8 1°×1° product (Loeb et al., 2009), that we average over 2°×2° grid boxes.

2.3 Radiative transfer computations

For all the radiative transfer computations needed in this study, we use the GAME radiative transfer code (Dubuisson et al., 2004) combined with mean sea surface temperature (SST) and atmospheric profiles of temperature, humidity and ozone extracted from the ERA-Interim reanalysis. GAME ~~is an accurate radiative transfer code to~~ calculates the radiative flux and radiances over the total solar and infrared spectrum. The radiative transfer equation is solved using DISORT (Stamnes et al., 1988) and gaseous absorption is calculated from the k-distribution method. ~~This~~ The code accounts for ~~aerosol and clouds~~ scattering and absorption by aerosol and clouds as well as interactions with gaseous absorption.

GAME ~~radiative transfer code~~ does not take into account cloud 3D effects, and is based on the plane-parallel approximation. In this study, we use GAME to compute integrated OLR between 5 and 100 μm.

3 Radiative temperatures of Opaque ~~clouds~~ and Thin clouds derived from lidar cloud observations and reanalysis

We define ~~here an approximation of~~in this section the ~~Opaque and Thin cloud~~ radiative temperatures of Opaque and Thin clouds ~~which~~ that can be derived from lidar measurements. The cloud radiative temperature corresponds to the equivalent radiative temperature of the cloud $T_{rad}^{|}$ such ~~as~~ that the upward top of the cloud LW radiative flux emitted by the~~a~~ cloud ~~of~~ with emissivity $\varepsilon^{|}$~~, at the top of the cloud,~~ is $F_{Cloud}^{\uparrow LW|}(Cloud\ Top)=\varepsilon^{|}\sigma\left(T_{rad}^{|}\right)^{4}$, where σ denotes the Stefan–Boltzmann constant. We present distributions of these cloud radiative temperatures derived from lidar measurements over the mid-latitudes ~~region~~ and the tropics.

3.1 Definition and approximations of the cloud radiative temperature

Considering an optically uniform cloud with a cloud total LW optical depth $\delta\tau_{Cloud}^{LW|}$, and assuming a linearly ~~increase~~ increasing ~~of the~~ temperature from the cloud top to the cloud base, we can compute the upward LW radiative flux at the cloud top emitted by the cloud ~~at the top of the cloud~~ $F_{Cloud}^{\uparrow LW|}(Cloud\ Top)$ ~~can be computed from~~using the radiative transfer equation (RTE) (see appendix A). ~~Then, s~~Solving the equation $F_{Cloud}^{\uparrow LW|}(Cloud\ Top)=\varepsilon^{|}\sigma\left(T_{rad}^{|}\right)^{4}=\left(1-e^{-\delta\tau_{Cloud}^{LW|}}\right)\sigma\left(T_{rad}^{|}\right)^{4}$, we can infer the value of the equivalent radiative cloud temperature $T_{rad}^{|}$. Figure 3 shows $T_{rad}^{|}$ ~~deduced~~ computed from RTE (green) as a function of $\delta\tau_{Cloud}^{LW|}$. As $\delta\tau_{Cloud}^{LW|}$ increases, $T_{rad}^{|}$ ~~is found~~decreases and approaches the cloud top temperature ~~closer to the cloud top and so the cloud radiative temperature decreases~~.

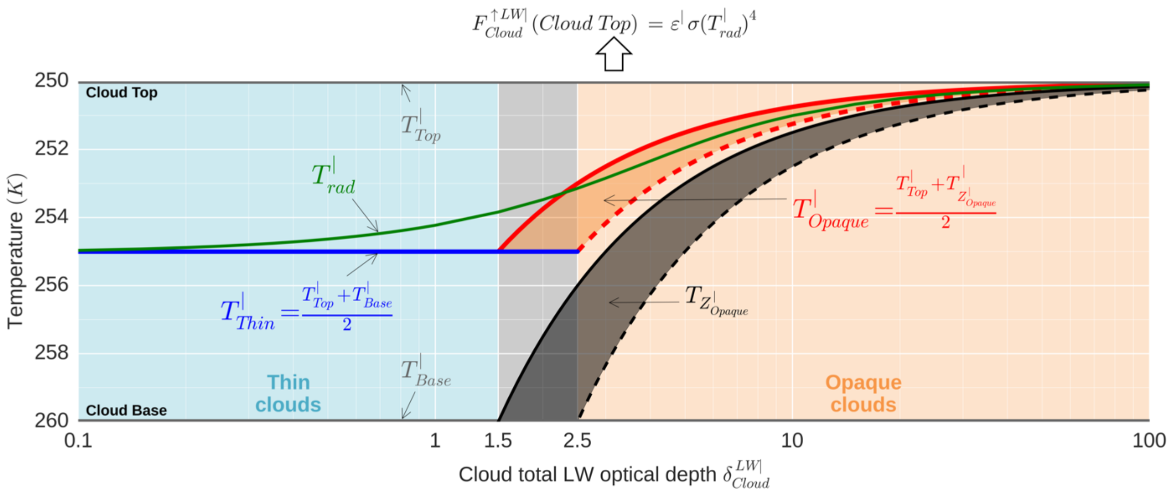

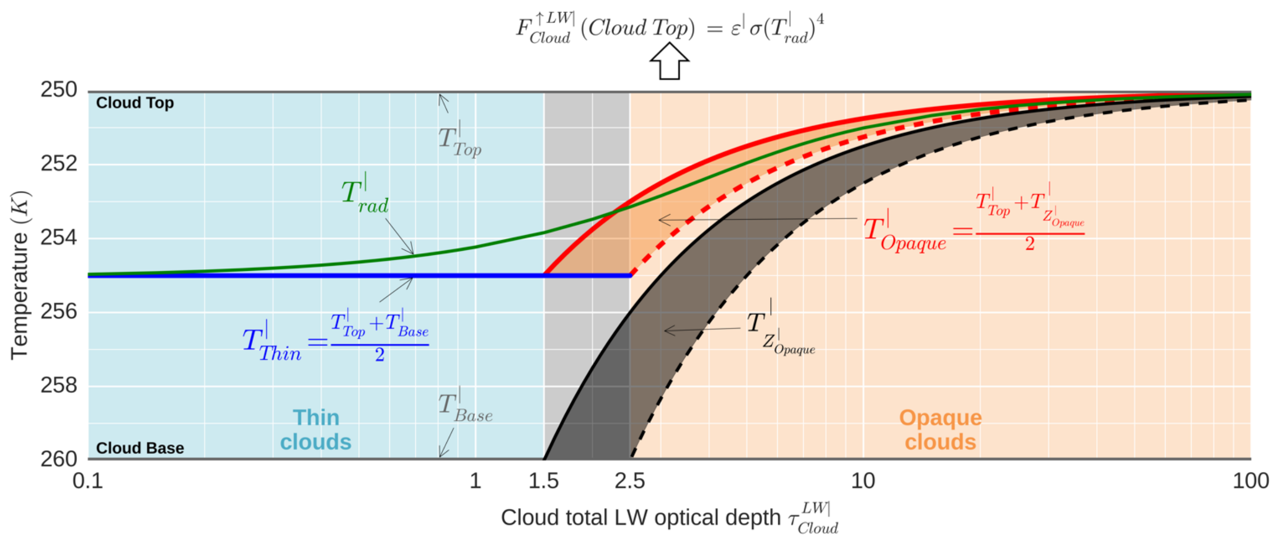

FIG. 3. Comparison of (green) the cloud radiative temperature $T_{rad}^{|}$ inferred from the RTE (see appendix A) with the lidar-definitions of (blue) the Thin cloud radiative temperature $T_{Thin}^{|}$ and (red) the Opaque cloud radiative temperature $T_{Opaque}^{|}$, as a function of the cloud total LW optical depth $\delta\tau_{Cloud}^{LW|}$. Here, on an example with a fixed cloud top temperature $T_{Top}^{|}$ at 250 K and a fixed cloud base temperature $T_{Base}^{|}$ at 260 K.

$T_{rad}^{|}$ is obtained by computing the LW flux emitted by the cloud at the top ~~of the cloud~~ $F_{Cloud}^{\uparrow LW|}(Cloud\ Top)$ from the RTE and ~~then~~ solving $F_{Cloud}^{\uparrow LW|}(Cloud\ Top) = \varepsilon^{|}\sigma\left(T_{rad}^{|}\right)^4$.

~~Clouds are declared as (o~~Orange area~~)~~ defines Opaque clouds~~,~~ ~~if they present an opacity level altitude $Z_{Opaque}^{|}$. This occurs~~which in lidar observations ~~for~~ have $\delta\tau_{Cloud}^{LW|}$ greater than a limit situated between 1.5 to 2.5. Below this limit clouds are declared as ~~(blue area)~~ Thin clouds (blue area). Clouds with $\delta\tau_{Cloud}^{LW|}$ between 1.5 and 2.5 could be ~~(gray area)~~ either Opaque or Thin clouds (gray area)~~depending on the limit~~.

We ~~will now~~ approximate $T_{rad}^{|}$ for Opaque clouds and Thin clouds using straightforward formulations ~~which could~~that can be derived from lidar cloud observations and reanalysis. ~~In an~~For the Opaque cloud ~~single column~~case (Fig. 1, right), the optically ~~very~~ thick cloud ~~prevents~~ completely absorbs upward LW radiative flux propagating from below ~~to propagate upwards~~. ~~Thus~~In this case, atmospheric layers below $Z_{Opaque}^{|}$ have little influence on ~~the OLR over an Opaque cloud single column~~ $OLR_{Opaque}^{|}$. ~~Here~~Therefore, ~~we propose that~~ $OLR_{Opaque}^{|}$ is mainly driven by an *Opaque cloud radiative temperature* defined as:

$$T_{Opaque}^{|} = \frac{T_{Top}^{|}+T_{Z_{Opaque}}^{|}}{2}. \quad (1)$$

~~In~~ For ~~a~~the Thin cloud ~~single column~~case (Fig. 1, left), the cloud~~y part is optically semi-transparent and lets through~~is translucent so that a part of the upward LW radiative flux ~~coming from~~emitted by the surface and cloud-free atmospheric layers ~~and surface~~ underneath the cloud is transmitted through the cloud. ~~Then, the OLR over a Thin cloud single~~In this case ~~column,~~ $OLR_{Thin}^{|}$ depends ~~on one hand~~ on the surface temperature~~, the surface~~ and surface emissivity, the temperature ~~profile,~~ and ~~the~~ humidity profiles below the cloud, ~~and on the other hand on~~ the cloud emissivity $\varepsilon_{Thin}^{|}$~~,~~ and the *Thin cloud radiative temperature* defined as:

$$T_{Thin}^{|} = \frac{T_{Top}^{|}+T_{Base}^{|}}{2}. \quad (2)$$

~~Comparisons of~~ $T_{Thin}^{|}$~~, the cloud radiative temperature of Thin clouds~~ ($\delta\tau_{Cloud}^{LW|} < 1.5$, blue area in Fig. 3)~~,~~ and $T_{Opaque}^{|}$~~, the cloud radiative temperature of Opaque clouds~~ ($\delta\tau_{Cloud}^{LW|} > 2.5$, orange area)~~,~~ agree well with $T_{rad}^{|}$ (deduced from

RTE, (green) show good agreement in Fig. 3. Clouds with 1.5 < $\delta\tau^{LW|}_{Cloud}$ < 2.5 (gray area) can be either Thin or Opaque clouds depending on the integrated LW optical depth at which $Z^{|}_{Opaque}$ will occur. Here, computations were performed for aIn computing LW radiative flux, we assume the fixed cloud top temperature $T^{|}_{Top}$ at of 250 K and a fixed cloud base temperature $T^{|}_{Base}$ at of 260 K. $T^{|}_{Opaque}$ will depends on the integrated LW optical depth $\tau^{LW|}$ from cloud top $\delta^{LW|}$ to where $Z^{|}_{Opaque}$ will occur, which. Since the equivalent visible optical depth $\tau^{VIS|}$ to $Z^{|}_{Opaque}$ is between 3 and 5 (Vaughan et al., 2009), and $\tau^{LW|} = \frac{1}{2}\tau^{VIS|}$ (Chepfer et al., 2014), $\tau^{LW|}$ is known to be situated between 1.5 and 2.5, provided a range of: $\delta^{LW|} = \frac{1}{2}\delta^{VIS|}$ (Chepfer et al., 2014), with $\delta^{VIS|}$ between 3 and 5 (Vaughan et al., 2009). Then, according to possible values of $T^{|}_{Z^{|}_{Opaque}}$ $Z^{|}_{Opaque}$ possible values given this approximation (black shadow area), and then, a range of possible values of $T^{|}_{Opaque}$ range is deduced (red shadow area).

Computations with other pairs of $T^{|}_{Top}$ and $T^{|}_{Base}$ temperatures (not shown) reveal that the relative vertical position into the cloud of $T^{|}_{rad}$ does not depend much of the cloud top and cloud base temperatures. In other words, with other pairs of $T^{|}_{Top}$ and $T^{|}_{Base}$ temperatures, we obtainwould produce almost the same figure as Fig. 3, only with the y-axis temperature values changed. This means that the difference between $T^{|}_{rad}$ and $T^{|}_{Thin}$ or between $T^{|}_{rad}$ and $T^{|}_{Opaque}$ becomes larger as the difference between $T^{|}_{Top}$ and $T^{|}_{Base}$ increases. Naturally, in realityGenerally, the error made by using specific values of $T^{|}_{Thin}$ and $T^{|}_{Opaque}$ as approximations ofin computing $T^{|}_{rad}$ will also depends on other cloud properties used in the computation, such as cloud inhomogeneity and cloud microphysics. However, this simple theoretical calculation allows us to assertshows that $T^{|}_{Thin}$ and $T^{|}_{Opaque}$ as we defined above are good approximations of the cloud radiative temperature of the Thin and Opaque clouds, with less than a. Considering a cloud with $\tau^{LW|}_{Cloud}$ > 5 and 10 K between its base and top temperatures, this approximation leads to an error of the radiative temperature less than 2 K error for a Thin cloud with a 10 K difference between its cloud base and cloud top temperatures, and less less than than a 1 K error for an Opaque cloud with $\delta^{LW|}_{Cloud}$ > 5 and with a 10 K difference between its cloud base and cloud top temperatures.

These cloud radiative temperatures are fundamental to study the LW CRE and are different from the effective radiating temperatures measured by passive instruments which are influenced by radiation coming from below the cloud. In the case of Opaque cloud which completely absorbs upward LW radiative flux propagating from below, the effective radiating temperature measured by passive instruments should agree with the cloud radiative temperature. However, this assumes to know that the cloud is Opaque, but cloud emissivity from passive measurements is also sensitive to hypothesis made on the clear sky and surface property. Unlike passive measurements, lidar measurements robustly separate Opaque clouds and Thin clouds from the presence or not of a surface echo (Guzman et al., 2017).

3.2 $T^{|}_{Opaque}$ and $T^{|}_{Thin}$ retrieved from CALIOP observations during 2008–2015

For each cloudy single column sounded observed by CALIOP, we derive $T^{|}_{Opaque}$ from $T^{|}_{Top}$ and $T^{|}_{Z^{|}_{Opaque}}$ using Eq. (1)., We alsoand we derive $T^{|}_{Thin}$ from $T^{|}_{Top}$ and $T^{|}_{Base}$ using Eq. (2). Then, wWe then computed the probability density function (PDF) of $T^{|}_{Opaque}$ among Opaque clouds and $T^{|}_{Thin}$ among Thin clouds for 3 different regions: the tropical ascendinging regions region between ±30° latitude with monthly mean 500-hPa pressure vertical velocity ω_{500} < 0 hPa·day^{-1}, the tropical subsidingence regions region between ±30° latitude with monthly mean ω_{500} > 0 hPa·day^{-1} and the mid-latitudes (North and South) region between 65° S and 30° S and between 30° N and 65° N put together. To compute these PDFs, e.g. the PDF of $T^{|}_{Opaque}$ among Opaque clouds, we firstly compute a the PDF of $T^{|}_{Opaque}$ among using all single columns on each 2°×2° grid box for the 2008–2015 period. Then, we compute the PDF with area-weighted average~~d PDF of~~ ~~a~~by region, weighting each 2°×2° grid box PDF by the ratio of the number of Opaque single columns over the number of all single columns. We do this latter weighting in order to take into account ~~the~~ sampling differences ~~in each~~among 2°×2° grid boxes.

Figure 4a shows the distributions of $T^{|}_{Opaque}$ ~~among Opaque clouds~~. In ~~the~~ tropical subsid~~ing~~ence regions ~~region~~ (green), 71 % of $T^{|}_{Opaque}$ are ~~found~~ between 0 °C and 25 °C with a maximum at 15 °C. Because the~~y~~se clouds are almost as warm as the surface, they do not strongly affect the OLR compared to clear~~-~~ sky conditions. These clouds are the marine boundary layer clouds ~~of~~ present over the descending branches of the Hadley cells. In ~~the~~ tropical ascend~~ing~~ing regions ~~region~~ (red), $T^{|}_{Opaque}$ ~~has~~ follows a bimodal distribution with few ~~warm~~ clouds warmer than ~~between~~ 0 °C ~~and 25 °C~~ (21 %) and most clouds ~~temperatures spread~~ between 0 °C and -80 °C (79 %). These ~~latter~~ cold Opaque clouds ~~will~~ have locally a very strong impact on the OLR since ~~their temperatures are up to~~they can be 100 K ~~lower~~ colder than the surface skin temperature. However, ~~the~~ tropical ascend~~ing~~ing regions ~~region only~~ represent~~s~~ about only 1/5 of the ocean ~~surface~~ between 65° S and 65° N, making their global ~~effect~~ contribution ~~at global scale~~ less striking. In the mid-latitudes ~~region~~ (purple), $T^{|}_{Opaque}$ are ~~unsurprisingly located at temperatures less extreme than in tropical regions with temperatures ranging from~~concentrated in a narrower range (20 °C to -60 °C), ~~and are rather evenly distributed~~with temperatures mostly between 10 °C and -30 °C. Th~~es~~e local radiative effect of these Opaque clouds ~~will have a mid-effect on the local OLR~~is weaker than the effect if they were in tropical ascending regions.~~, but the m~~Mid-latitudes ~~region represent~~ are, however, a large area (43 % of the ocean surface between 65° S and 65° N) ~~and their~~and the cover ~~over~~ of Opaque clouds ~~these regions~~ is large (Fig. 2a). So, ~~they will certainly also play an important role on~~their contribution to the global CRE is expected to be large.

The ~~Opaque cloud~~ radiative temperature of Opaque clouds $T^{|}_{Opaque}$ is based on the key new lidar information $Z^{|}_{Opaque}$ (Eq. (1)). Figure 4b shows that $Z^{|}_{Opaque}$ is ~~mostly~~ low ~~in~~ for all regions, ~~at around~~near 1 km altitude~~, in the boundary layer clouds~~, especially ~~for the~~in subsid~~ing~~ence regions ~~region~~. ~~Some non-negligible amount of~~ $Z^{|}_{Opaque}$ are sometimes ~~found~~ between 2 km and 8 km in the mid-latitudes storm track regions. In ~~the~~ tropical ascend~~ing~~ing regions ~~region~~, the PDF is tri-modal with a ~~first~~ lowest ~~pick~~ peak around 1 km associated with boundary layer clouds, and a ~~second~~ highest peak ~~around 5 km and a third~~ around 12 km associated with deep convection systems~~, suggesting the presence of Opaque clouds in the boundary layer and at very high altitudes due to deep convection for the first and last mode~~. The ~~second~~ middle mode, near 5 km, ~~could~~ might be due to ~~more diffuse or~~ developing convective clouds or middle altitude clouds. Since $T^{|}_{Opaque}$ also depends on $Z^{|}_{Top}$, distributions of the distance between cloud top and $Z^{|}_{Opaque}$ ~~among Opaque clouds~~ are given in Fig. A1a (appendix B).

~~As in Fig. 4a but for Thin clouds, Fig. 4c also shows, in the tropical subsiding region, a large majority of $T^{\dagger}_{Thin}$ higher than 0 °C (65 %).~~ The radiative temperature of Thin clouds $T^{|}_{Thin}$ is mostly warmer than 0°C in tropical subsidence regions (Fig. 4c). $T^{|}_{Thin}$ colder than -40 °C ~~are~~ occurs more frequently than ~~for~~ $T^{|}_{Opaque}$ colder than -40 °C, suggesting high-altitude optically thin cirrus from detrainments of anvil clouds being generated in adjacent convective regions. In ~~the~~ tropical ascend~~ing~~ing regions ~~region~~, the "warm" mode of the bimodal distributions of $T^{|}_{Thin}$ is ~~bigger~~ more populated and warmer than that of $T^{|}_{Opaque}$. The main mode of $T^{|}_{Thin}$ in the mid-latitudes ~~region~~, is also warmer than that of $T^{|}_{Opaque}$. Warmer cloud temperatures, implying smaller CREs, reinforces the importance of the role of the Opaque clouds versus ~~the~~ Thin clouds in the total CRE. Distributions of the distance between ~~cloud~~ top and ~~cloud~~ base for Thin clouds ~~among Thin clouds~~ are given in Fig. A1b (appendix B).

Because the radiative impact of ~~the~~ Thin clouds will also depend on ~~the~~ cloud emissivity ~~of the cloud~~, we also compute~~d~~ the distributions of $\varepsilon^{|}_{Thin}$ ~~among Thin clouds.~~ (Fig~~ure~~ 4d) ~~shows these distributions~~. For all regions, the maximum ~~is~~ occurs ~~located~~ around 0.25~~. So,~~: emissivities of Thin clouds are usually small, ~~and clouds with small emissivities~~so they have ~~less~~ little impact on the OLR~~. This, once again, goes in the sense that the role that play Thin clouds on the total~~ and hence their contribution to CRE should be significantly smaller than that of Opaque clouds.

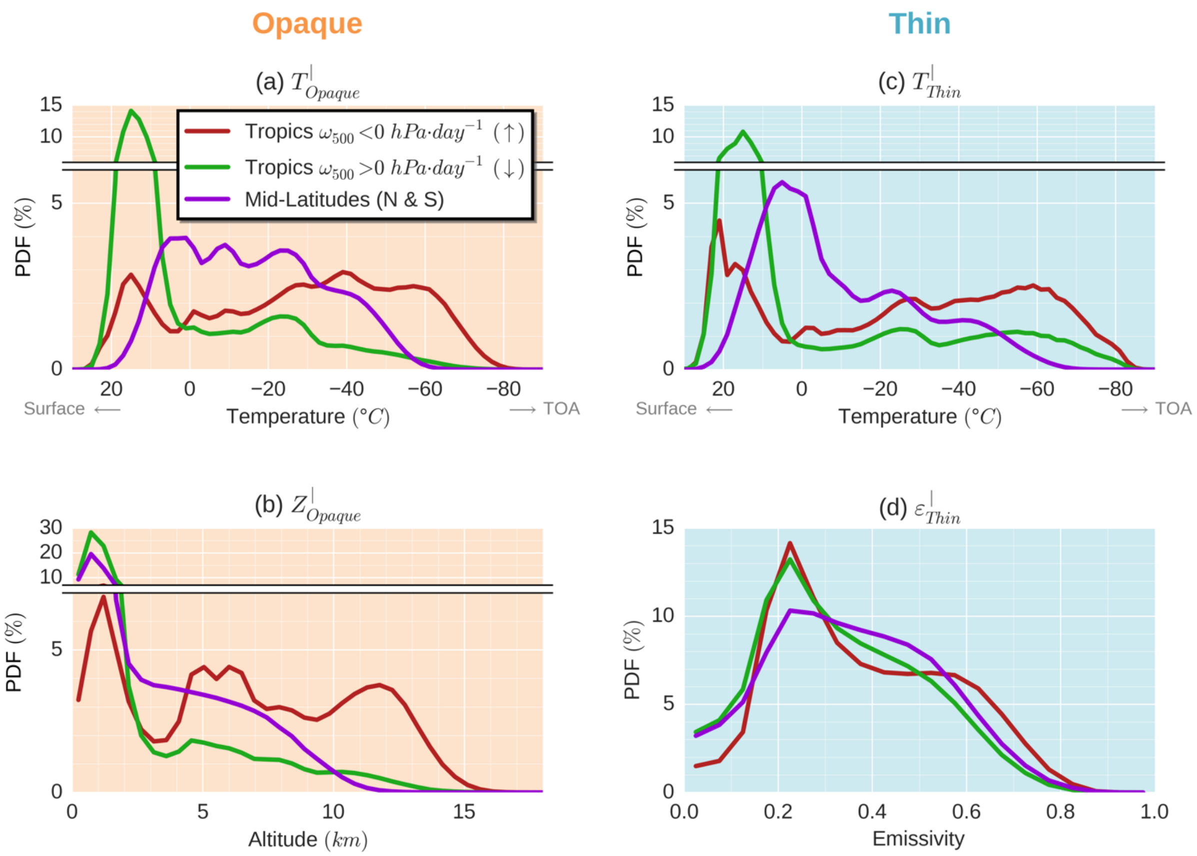

FIG. 4. Observed distributions of (a) $T^{|}_{Opaque}$ among Opaque clouds, (b) $Z^{|}_{Opaque}$ among Opaque clouds, (c) $T^{|}_{Thin}$ among Thin clouds and (d) $\varepsilon^{|}_{Thin}$ among Thin clouds in three regions: (red) the tropical ascendance [30° S–30° N] ~~ascending regime areas~~ (monthly mean $\omega_{500} < 0$ hPa·day^{-1}), (green) the tropical ~~[30° S–30° N]~~ subsid~~ing~~ence ~~regime areas~~ [30° S–30° N] (monthly mean $\omega_{500} > 0$ hPa·day^{-1}) and (purple) the mid-latitudes [30°–65°]. These regions represent respectively 22 %, 35 % and 43 % of ~~their total area~~the ±65° ocean surface. Only nighttime over ice-free oceans for the 2008–2015 period is considered.

4. Outgoing longwave radiation derived from lidar cloud observations

In this section, we express the OLR as a function of cloud properties derived from lidar observations ($T^{|}_{Opaque}$, $T^{|}_{Thin}$, and $\varepsilon^{|}_{Thin}$). ~~Then, w~~We ~~verify~~ evaluate this relationship ~~against~~ with observations at an instantaneous 20 km footprint scale, using high spatial resolution collocated satellite-borne broadband radiometer and lidar data.~~, and~~ We also evaluate the relationship at a monthly mean 2° latitude × 2° longitude gridded scale.

4.1 Linear relationship deduced from radiative transfer simulations over a single cloudy column

The goal of this sub-section is to establish a simple and robust relationship between 1) the OLR over an Opaque cloud single column $OLR^{|}_{Opaque}$ and the radiative temperature $T^{|}_{Opaque}$ and, 2) the OLR over a Thin cloud single column $OLR^{|}_{Thin}$ and the radiative temperature $T^{|}_{Thin}$ and the Thin cloud emissivity $\varepsilon^{|}_{Thin}$.

1) For an Opaque cloud single column, we computed $OLR^{|}_{Opaque}$, using direct radiative transfer computations, for various atmospheres containing an Opaque cloud ~~with~~ with ~~different~~ variable altitudes~~s~~ and vertical extent. The clouds~~,~~ is represented by a cloud layer with emissivity equal to 1 at $Z^{|}_{Opaque}$ topped with optically uniform cloud layers with vertically integrated visible optical depth equal to 3.2, which corresponds to $\varepsilon \approx 0.8$. Dots in Fig.~~ure~~ 5a shows~~s on dots~~ the obtained $OLR^{|}_{Opaque}$ as function of $T^{|}_{Opaque}$ for tropical atmosphere conditions. Linear regression (solid line) leads to:

$$OLR^{|\,(LID)}_{Opaque} = 2.0T^{|}_{Opaque} - 310. \quad (3)$$

where $OLR^{|\,(LID)}_{Opaque}$ is expressed in W·m^{-2} and $T^{|}_{Opaque}$ in K. So, when $T^{|}_{Opaque}$ decreases ~~of~~ by 1 K (e.g. if the Opaque cloud rises up) then the OLR decreases by 2 W·m^{-2}. This linear relationship, ~~firstly found~~initially pointed out by Ramanathan (1977), has a slope which is consistent with previous work that found 2.24 W·m^{-2}/K (Wang et al. (2002) using the radiative transfer model of Fu and Liou (1992, 1993) and the analysis of Kiehl (1994)). Conducting the same ~~L~~linear regression~~s done~~ on ~~other regions with~~ very different atmospheric conditions (from tropical to polar) gives ~~a~~ similar coefficients. This means that~~, in spite of the significant differences in the atmospheric temperature and humidity profiles,~~ $OLR^{|}_{Opaque}$ depends ~~essentially only~~mainly on $T^{|}_{Opaque}$. This remarkable result demonstrates that a cloud property ~~which~~ driv~~es~~ing the OLR can be derived from spaceborne lidar measurement. ~~Figure 5a also shows the black body emission (dashed line).~~ Differences between the computed OLR and the black body emission (dashed line in Fig. 5a) represent the extinction effect of the atmospheric layers ~~located~~ above the cloud.

2) For a Thin cloud single column, we can consider that $OLR^{|}_{Thin}$ is composed of two parts (Fig. 1). ~~A~~ The first part, coming from the LW flux emitted by the cloud, ~~which~~ can be expressed in the same way as Eq. (3) using $T^{|}_{Thin}$ instead of $T^{|}_{Opaque}$, and weighted by the Thin cloud emissivity $\varepsilon^{|}_{Thin}$. The second part is equal to the OLR over a Clear sky single column $OLR^{|}_{Clear}$ (the same single column without the cloud) multiplied by the cloud transmissivity $(1-\varepsilon^{|}_{Thin})$:

$$OLR^{|\,(LID)}_{Thin} = \varepsilon^{|}_{Thin}\left(2.0T^{|}_{Thin} - 310\right) + \left(1-\varepsilon^{|}_{Thin}\right)OLR^{|}_{Clear}. \quad (4)$$

where $OLR^{|\,(LID)}_{Thin}$ and $OLR^{|}_{Clear}$ are expressed in W·m^{-2} and $T^{|}_{Thin}$ in K. In order to evaluate this expression and to examine the dependence of $OLR^{|}_{Thin}$ to $T^{|}_{Thin}$ and $\varepsilon^{|}_{Thin}$, we computed $OLR^{|}_{Thin}$, using direct radiative transfer computations, for various atmospheres containing a Thin cloud (represented by optically uniform cloud layers with integrated emissivities equal to $\varepsilon^{|}_{Thin}$) with different altitudes, vertical extents and emissivities. Dots in Fig.~~ure~~ 5b shows~~s on dots~~ the resulting $OLR^{|}_{Thin}$ as a function of $T^{|}_{Thin}$ for 4 different values of $\varepsilon^{|}_{Thin}$, ~~for~~ in tropical atmosphere conditions. We compare these results with the linear expression of Eq. (4) (solid lines), in which $OLR^{|}_{Clear}$ is ~~obtained by~~ comput~~ing~~ed ~~the OLR~~ for a single column without cloud. The theoretical formulation agrees quite well with the different simulations. ~~It may be noted,~~

~~however, that t~~This formulation seems to overestimate $OLR^{|}_{Thin}$ (up to +10 W·m^{-2}) ~~for~~ in many cases. Reasons for it are discussed in Section 6.

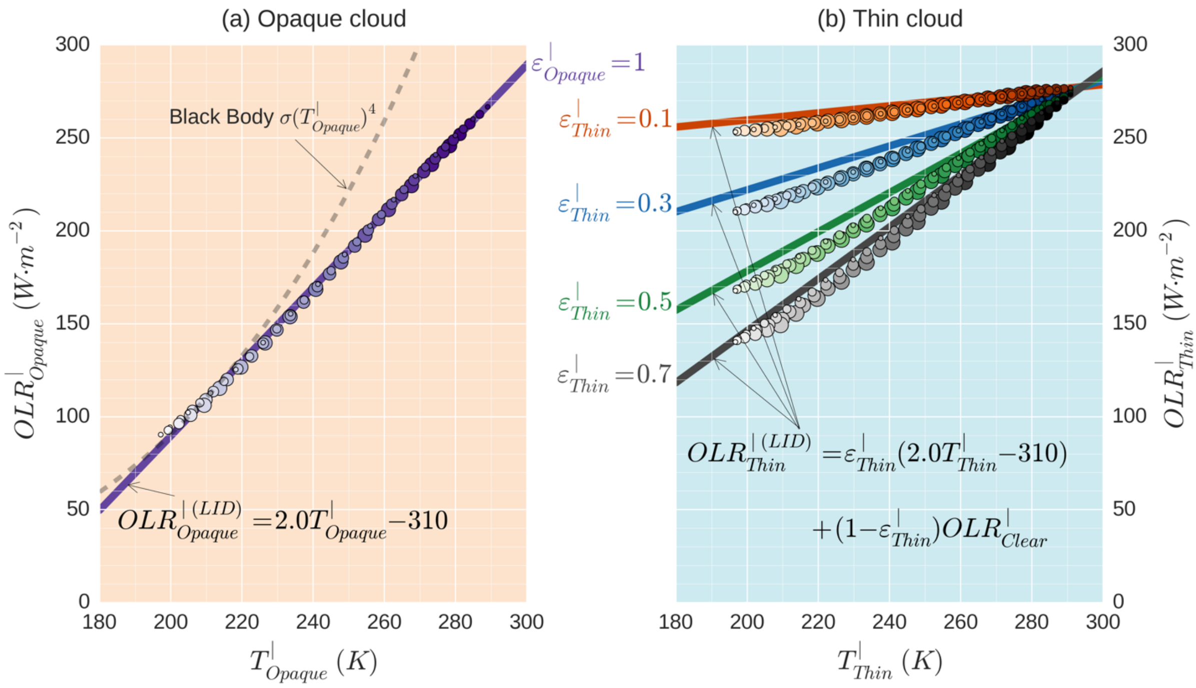

FIG. 5. Relationship between the OLR and the cloud radiative temperature from radiative transfer computations: (a) over an Opaque cloud single column and (b) over a Thin cloud single column. Direct radiative transfer computations are shown in dots. Solid lines represent the linear relationships inferred from a regression on dots in the Opaque case and applied to the Thin clouds case according to Eq. (4). For a fixed value of cloud emissivity (dots colors; 1 [purples] for Opaque clouds and 0.1 [reds], 0.3 [blues], 0.5 [greens], 0.7 [greys] for Thin clouds), the linear relationship does not depend on the cloud altitudes (dots light intensity; 0 km [dark] – 16 km [bright]) or ~~the~~ geometrical thicknesses (dots size; 1 km [small] – 5 km [large]). Results shown here use the 2008-year mean thermodynamic atmospheric variables over the tropicals ~~region~~ [30° S–30° N] from ERA-I reanalysis.

4.2 Evaluation of the linear relationship using observations at instantaneous CERES footprint scale

We evaluate the robustness of the OLR expressions (Eqs. (3) and (4)) at the resolution of a CERES footprint (~20 km) using CERES measurements, and cloud properties derived from collocated CALIOP observations $T^{\oslash}_{Opaque}$, $T^{\oslash}_{Thin}$ and $\varepsilon^{\oslash}_{Thin}$. For this purpose, we apply Eqs. (3) and (4) using $T^{\oslash}_{Opaque}$, $T^{\oslash}_{Thin}$, $\varepsilon^{\oslash}_{Thin}$ and the estimated OLR over the scene ~~removing~~ without the clouds ~~given by C3M~~ $OLR^{\oslash}_{Clear}$ given by C3M. $T^{\oslash}_{Opaque}$, $T^{\oslash}_{Thin}$, $\varepsilon^{\oslash}_{Thin}$ refer to an atmospheric column with a CERES footprint base~~, as mentioned~~ (identified by the ~~exponent symbol~~superscript "∅")~~,~~ and are obtained by averaging ~~respectively~~ all $T^{|}_{Opaque}$, $T^{|}_{Thin}$ and $\varepsilon^{|}_{Thin}$ ~~falling into~~within the CERES footprint. $OLR^{\oslash}_{Clear}$, $OLR^{\oslash}_{Opaque}$ and $OLR^{\oslash}_{Thin}$ refer to atmospheric columns with a CERES footprint base.

Figure 6 compares lidar-derived and observed OLR during January 2008. Figure 6a compares the $OLR^{\oslash\,(CERES)}_{Opaque}$ measured by CERES ~~only~~ over footprints entirely covered by an Opaque cloud, with the $OLR^{\oslash\,(LID)}_{Opaque}$ computed from $T^{\oslash}_{Opaque}$ using Eq. (3). We see a very strong correlation between observed and computed OLR (R = 0.95). ~~Therefore, t~~This confirms that the OLR over an Opaque cloud is linearly dependent o~~n~~f $T^{\oslash}_{Opaque}$~~. So, from lidar measurement~~, and that it is possible to derive a cloud property which is proportional to the OLR from lidar measurement. Monitoring $T^{|}_{Opaque}$ on long-term should provide important information ~~which should help~~useful to better understand the LW cloud feedback mechanism. ~~Moreover,~~

~~because the relationship is linear, it simplifies the derivatives in mathematical expressions of feedback and will allow to construct a useful framework to study LW cloud feedback in simulations of climate models.~~

Figure 6b is the same as Fig. 6a but only ~~for~~ CERES footprints entirely covered by a Thin cloud are used. ~~So~~ $OLR_{Thin}^{\oslash\,(LID)}$, ~~is~~ computed from $T_{Thin}^{\oslash}$, $\varepsilon_{Thin}^{\oslash}$ and $OLR_{Clear}^{\oslash}$ using Eq. (4), ~~$OLR_{Thin}^{\oslash\,(LID)}$ compared to observations (~~ correlates well with $OLR_{Thin}^{\oslash\,(CERES)}$ ~~) also shows quite good correlation~~ (R = 0.89)~~,~~ but the regression line slightly differs from the identity line. Possible reasons for disagreements between ~~observed $OLR_{Thin}^{\oslash\,(LID)}$ and computed $OLR_{Thin}^{\oslash\,(CERES)}$~~ both values are discussed in Section 6. These same results are also ~~drawn~~ shown as a function of $T_{Thin}^{\oslash}$ and $\varepsilon_{Thin}^{\oslash}$ in Fig. A2 for a fixed value of $OLR_{Clear}^{\oslash}$ (we selected measurements where $OLR_{Clear}^{\oslash} \in [275, 285]$ W·m^{-2}) in order to show the effect of those two cloud properties on $OLR_{Thin}^{\oslash\,(CERES)}$.

~~The evaluation showed in Fig. 6 is only using observation from January 2008.~~ The same evaluation performed with July 2008 data (not shown) gives similar results, with R = 0.96 for Opaque clouds and R = 0.90 for Thin clouds.

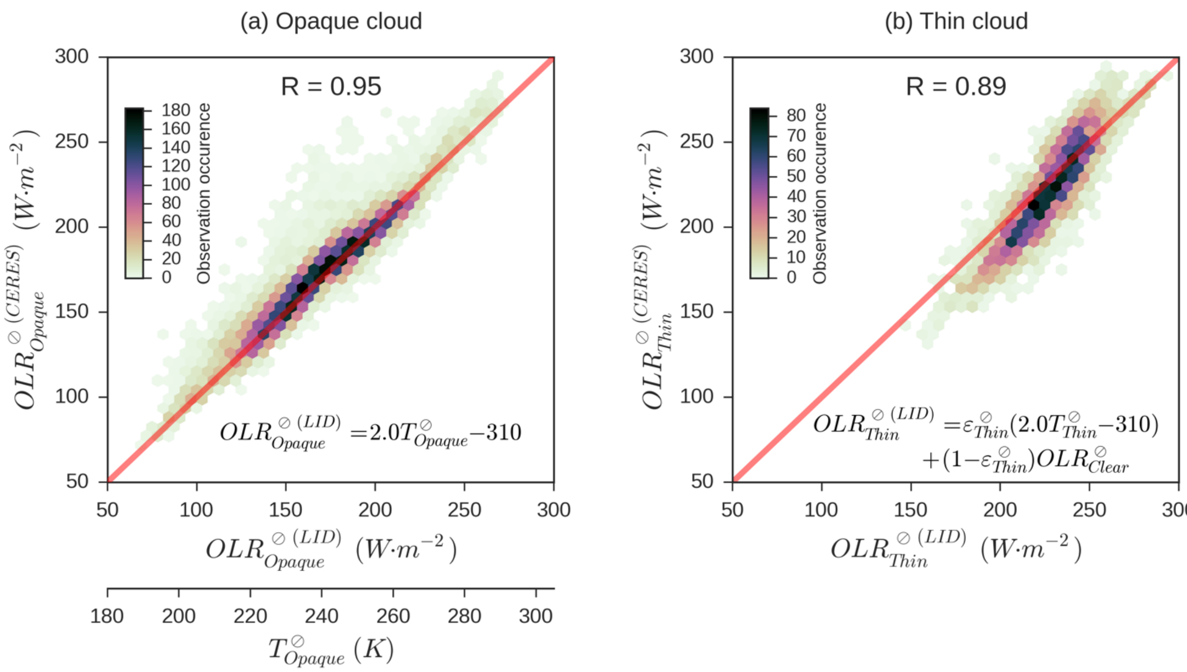

Fig. 6. Comparison between observed and lidar-derived OLR at CERES footprint scale: (a) over Opaque cloud single columns and (b) over Thin cloud single columns. Results obtained from CERES (y-axis) and CALIOP (x-axis) collocated measurements. $OLR_{Opaque}^{\oslash\,(LID)}$ and $OLR_{Thin}^{\oslash\,(LID)}$ are computed using Eqs. (4) and (5). Only nighttime conditions over ice-free oceans for January 2008 ~~is~~ are considered. *R* is the correlation coefficient.

4.3 Evaluation of the linear relationship using observations at monthly mean 2°×2° gridded scale

We first compute the monthly mean gridded total OLR from gridded lidar cloud properties:

$$OLR_{Total}^{\boxplus\,(LID)} = C_{Clear}^{\boxplus} OLR_{Clear}^{\boxplus} + C_{Opaque}^{\boxplus} OLR_{Opaque}^{\boxplus\,(LID)} + C_{Thin}^{\boxplus} OLR_{Thin}^{\boxplus\,(LID)}, \quad (5)$$

where $C_{Clear}^{\boxplus}$, $C_{Opaque}^{\boxplus}$ and $C_{Thin}^{\boxplus}$ are the monthly mean covers (Figs. 1,2): the ratio between the number of a specific kind of single column ~~over~~ to the total number of single columns that fall into the grid box during a month. $OLR_{Opaque}^{\boxplus\,(LID)}$ is computed from $T_{Opaque}^{\boxplus}$ using Eq. (3), and $OLR_{Thin}^{\boxplus\,(LID)}$ is computed from $T_{Thin}^{\boxplus}$, $\varepsilon_{Thin}^{\boxplus}$ and $OLR_{Clear}^{\boxplus}$ using Eq. (4). $T_{Opaque}^{\boxplus}$, $T_{Thin}^{\boxplus}$ and $\varepsilon_{Thin}^{\boxplus}$ are obtained by averaging respectively all $T_{Opaque}^{|}$, $T_{Thin}^{|}$ and $\varepsilon_{Thin}^{|}$ ~~falling into~~ within the 2°×2° box.

We then evaluate the lidar-derived $OLR_{Total}^{\boxplus\,(LID)}$ against the CERES measurements $OLR_{Total}^{\boxplus\,(CERES)}$. To do so, we computed the 2008–2010 mean $OLR_{Total}^{\boxplus\,(LID)}$ from Eq. (5) using $OLR_{Clear}^{\boxplus}$ from C3M and compared it with the one measured by CERES-Aqua. Figure 7 shows the comparison between the computed $OLR_{Total}^{\boxplus\,(LID)}$ (Fig. 7a) and the measured $OLR_{Total}^{\boxplus\,(CERES)}$ (Fig. 7b). We first ly observenote the noteworthy agreement of OLR patterns. Figure 7c shows the difference between those two maps. The global mean difference is -0.1 W·m^{-2}, meaning: $OLR_{Total}^{\boxplus\,(LID)}$ very slightly underestimate the observed $OLR_{Total}^{\boxplus\,(CERES)}$. The zonal mean differences (not shown) are quite small andmostly lower than 2 W·m^{-2}, never exceeding 5 W·m^{-2} and are mostly lower than 2 W·m^{-2}. Locally, we note a lack of OLR over the warm pool, the Intertropical Convergence Zone (ITCZ) and the stratocumulus regions off the West coast of continents (up to 6–8 W·m^{-2}) and an excess of OLR over latitudes beyond 50° N or 40° S (up to 4–6 W·m^{-2}). As C3M only covers through April 2011, but we aim to use this framework on long time-series observations, we replace $OLR_{Clear}^{\boxplus}$ from C3M by $OLR_{Clear}^{\boxplus}$ from CERES-EBAF in the following rest of this paper. Comparison between observed and lidar-derived OLR using $OLR_{Clear}^{\boxplus}$ from CERES-EBAF instead of $OLR_{Clear}^{\boxplus}$ from C3M is showed in Fig. A3. Using $OLR_{Clear}^{\boxplus}$ from C3M instead of CERES-EBAF increases the global mean $OLR_{Total}^{\boxplus\,(LID)}$ by 0.6 W·m^{-2}. (Fig. A3), for Rreasons for this increase are discussed in Section 6.

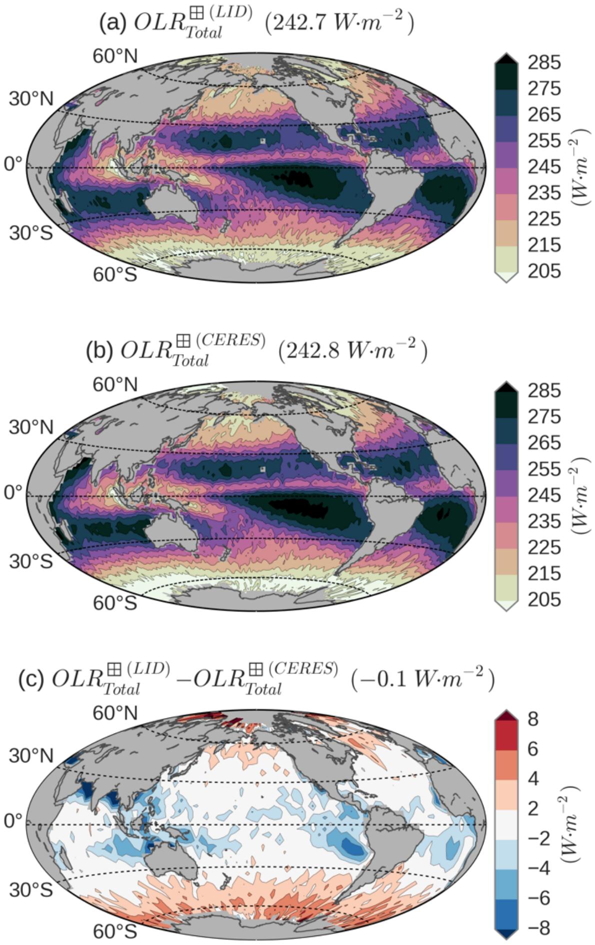

FIG. 7. Comparison between observed and lidar-derived OLR at 2°×2° gridded scale: (a) derived from CALIOP observations and (b) measured by CERES-Aqua. (c) = (a) - (b). Only ~~from~~ nighttime conditions over ice-free oceans for the 2008–2010 period ~~is~~ are considered. Global mean values are given in parentheses.

5 Contributions of Opaque clouds and Thin clouds to the cloud radiative effect

In the previous section, we found a ~~clear~~ linear relationship ~~for Opaque clouds~~ between OLR_{Opaque} and T_{Opaque} at different scales. The relationship for Thin clouds, though quite simple, is not linear and agrees less with observations than for Opaque clouds. In this section, we evaluate the contributions of Opaque clouds and Thin clouds to the total CRE.

5.1 Partitioning cloud radiative effect into Opaque CRE and Thin CRE

Using Eq. (5), we ~~are able to~~can decompose the total CRE at the TOA, computed from lidar observations, in ~~its~~ Opaque and Thin clouds contributions:

$$CRE_{Total}^{\boxplus\,(LID)} = OLR_{Clear}^{\boxplus} - OLR_{Total}^{\boxplus\,(LID)}$$

$$= \underbrace{C_{Opaque}^{\boxplus}\left(OLR_{Clear}^{\boxplus} - OLR_{Opaque}^{\boxplus\,(LID)}\right)}_{CRE_{Opaque}^{\boxplus\,(LID)}} + \underbrace{C_{Thin}^{\boxplus}\left(OLR_{Clear}^{\boxplus} - OLR_{Thin}^{\boxplus\,(LID)}\right)}_{CRE_{Thin}^{\boxplus\,(LID)}} . \quad (6)$$

Thereby, using Eq. (3), we can express $CRE_{Opaque}^{\boxplus\,(LID)}$ as a function of $C_{Opaque}^{\boxplus}$, $T_{Opaque}^{\boxplus}$ and $OLR_{Clear}^{\boxplus}$:

$$CRE_{Opaque}^{\boxplus\,(LID)} = C_{Opaque}^{\boxplus}\left(OLR_{Clear}^{\boxplus} - 2.0T_{Opaque}^{\boxplus} + 310\right) \quad (7)$$

where $CRE_{Opaque}^{\boxplus\,(LID)}$ and $OLR_{Clear}^{\boxplus}$ are expressed in W·m^{-2} and $T_{Opaque}^{\boxplus}$ in K.

Using Eq. (4), we can express $CRE_{Thin}^{\boxplus\,(LID)}$ as a function of $C_{Thin}^{\boxplus}$, $T_{Thin}^{\boxplus}$, $\varepsilon_{Thin}^{\boxplus}$ and $OLR_{Clear}^{\boxplus}$:

$$CRE_{Thin}^{\boxplus\,(LID)} = C_{Thin}^{\boxplus}\varepsilon_{Thin}^{\boxplus}\left(OLR_{Clear}^{\boxplus} - 2.0T_{Thin}^{\boxplus} + 310\right) \quad (8)$$

where $CRE_{Thin}^{\boxplus\,(LID)}$ and $OLR_{Clear}^{\boxplus}$ are expressed in W·m^{-2} and $T_{Thin}^{\boxplus}$ in K.

5.2 Global means of the Opaque cloud CRE and the Thin cloud CRE

Figure 8 shows the zonal mean observations of the 5 cloud properties ($C_{Opaque}^{\boxplus}$, $T_{Opaque}^{\boxplus}$, $C_{Thin}^{\boxplus}$, $T_{Thin}^{\boxplus}$ and $\varepsilon_{Thin}^{\boxplus}$). ~~In~~ Over the subsidence branches of the Hadley cell, around 20° S and 20° N, $C_{Opaque}^{\boxplus}$ is minimum (Fig. 8a), $T_{Opaque}^{\boxplus}$ and $T_{Thin}^{\boxplus}$ are warm (Fig 8b, temperatures in y-axis oriented downward) and $\varepsilon_{Thin}^{\boxplus}$ is minimum (Fig. 8c). So, we do not expect a ~~very~~ large contribution to the CRE from these regions. In contrast, the Intertropical Convergence Zone (ITCZ) corresponds to local maxima of Opaque and Thin cloud covers, extremely cold $T_{Opaque}^{\boxplus}$ and $T_{Thin}^{\boxplus}$ and a maximum of $\varepsilon_{Thin}^{\boxplus}$. ~~Very~~ A large CRE ~~will arise~~is, therefore, expected from ~~there~~this region. ~~Interestingly, an inversion of cover predominance and colder temperature between Opaque and Thin clouds occurs around 30° latitude~~ There are always more Opaque clouds than Thin clouds in the extratropics (beyond 30° latitude) and they are colder than the Thin clouds. It is the opposite in the tropical belt: there are always more Thin clouds than Opaque clouds, and those are slightly warmer. This suggests that the relative contribution of the Thin clouds to the CRE is larger in the tropic~~sal belt~~ than in the rest of the globe. This should not be very dependent on ~~the~~ a specific year since the interannual variations of these 5 cloud properties (represented by the shaded areas) are very small compared to the zonal differences.

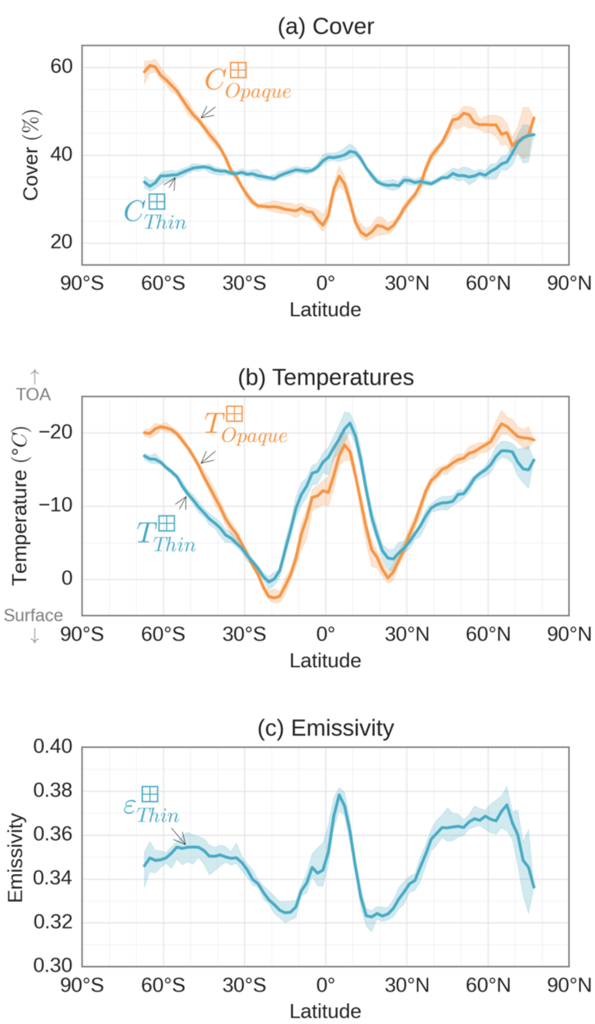

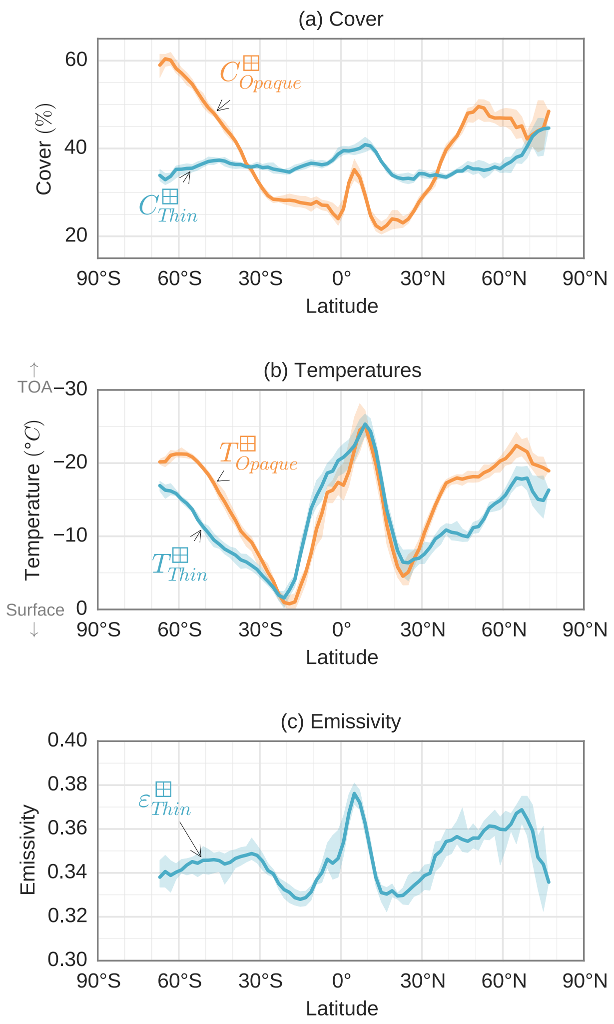

FIG. 8. Zonal mean observations: (a) $C^{\boxplus}_{Opaque}$ and $C^{\boxplus}_{Thin}$, (b) $T^{\boxplus}_{Opaque}$ among Opaque clouds and $T^{\boxplus}_{Thin}$ among Thin clouds and (c) $\varepsilon^{\boxplus}_{Thin}$ among Thin clouds. Only nighttime conditions over ice-free oceans for the 2008–2015 period ~~is~~ are considered. Shaded areas represent the envelope (max to min) including interannual variations.

Figure 9 shows that Opaque clouds contribute the most (73 %) to the total CRE. We can also note that the zonal variations of $CRE^{\boxplus\,(LID)}_{Opaque}$, and so approximately the variations of $CRE^{\boxplus\,(LID)}_{Total}$ (black line), can be explained by the zonal variations of $T^{\boxplus}_{Opaque}$ and $C^{\boxplus}_{Opaque}$ (Fig. 8a,b). For example, the absolute maximum CRE at 5° N (~44 W·m^{-2}) is associated with a large cover and cold temperature of Opaque clouds. As suggested ~~hereinbefore~~earlier, ~~we see that~~ the relative contribution of Thin clouds ($CRE^{\boxplus\,(LID)}_{Thin}/CRE^{\boxplus\,(LID)}_{Total}$, Fig. 9b) is larger ~~under~~ in the tropics, approximately ~~2 times~~twice larger below 30° (up to 40 %) than beyond those latitudes.

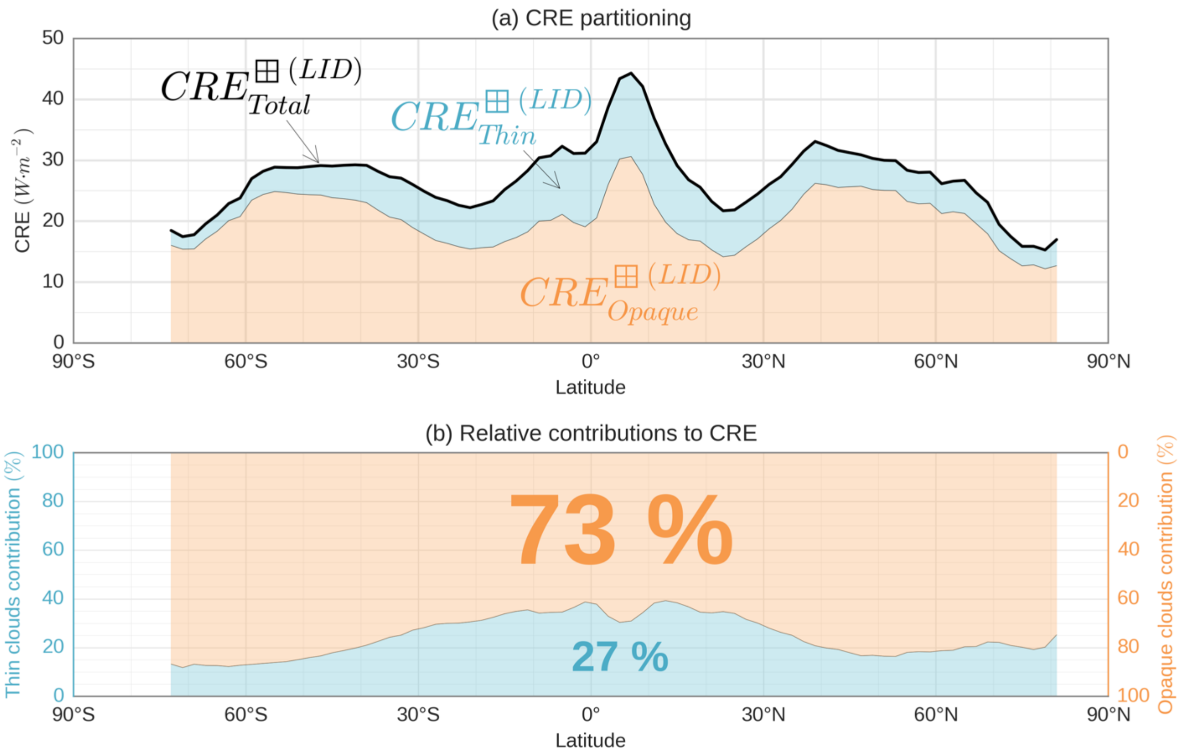

FIG. 9. (a) Partitioning of total CRE into Opaque CRE and Thin CRE. (b) Ratios of the Opaque and ~~(~~Thin~~)~~ CRE to the total CRE. Only nighttime conditions over ice-free oceans for the 2008–2015 period ~~is~~ are considered.

Figure 10 shows the same CRE partitioning on maps. The ~~likeness~~ similarity of patterns between total CRE (Fig. 10a) and the Opaque clouds CRE contribution (Fig. 10b) is ~~prominent~~obvious, ~~strengthening~~ showing again ~~the importance of the~~that Opaque clouds ~~in~~ mostly drive the CRE. ~~We can also note that~~The contribution of Thin clouds to the CRE ~~contribution~~ (Fig. 10c) ~~have~~ is quite large ~~values~~ between 20° S and 20° N in the Indian Ocean and the West Pacific Ocean, especially all around Indonesia, where $C^{\boxplus}_{Thin}$ (Fig. 2b) is maximum and $T^{\boxplus}_{Thin}$ minimum (not shown).

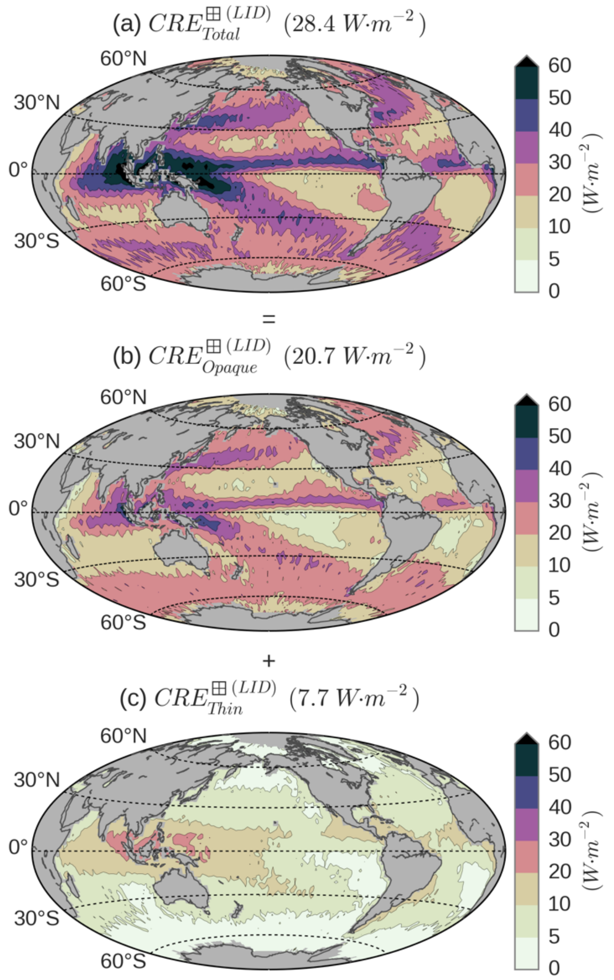

FIG. 10. Maps of (a) the total CRE (b) the Opaque CRE and (c) the Thin CRE. Only nighttime conditions over ice-free oceans for the 2008–2015 period ~~is~~ are considered. Global mean values are given in parentheses.

Globally, the predominance of $CRE^{\boxplus\,(LID)}_{Opaque}$ is obvious since it represents nearly ~~the~~ three ~~fourth~~ quarters of the total $CRE^{\boxplus\,(LID)}_{Total}$. Thereby, the cloud property $T^{\boxplus}_{Opaque}$ inferred from lidar observations and linearly linked to $OLR^{\boxplus}_{Opaque}$ should be a very good candidate to constrain LW cloud feedbacks since Thin clouds only account for 27 % of $CRE^{\boxplus\,(LID)}_{Total}$. ~~Also~~However, since the OLR expression ~~used for~~ above Thin clouds ~~seems to give coherent results for $CRE^{\boxplus\,(LID)}_{Thin}$~~ is almost as good as for Opaque clouds, it could also be used in a future work to quantify the ~~role~~ impact of ~~a~~ changes in $C^{\boxplus}_{Thin}$, $T^{\boxplus}_{Thin}$, and $\varepsilon^{\boxplus}_{Thin}$ ~~in~~ on the variations of $CRE^{\boxplus\,(LID)}_{Thin}$.

5.3 Tropical Opaque cloud CRE and Thin cloud CRE in dynamical regimes

Figure 11 shows the cloud properties as a function of dynamical regime in the tropics (whose PDF according to the 500-hPa pressure velocity is given Fig. 11h). In ~~the~~ tropical convecti~~ve~~on ~~regimes~~ ($\omega_{500} < 0$ hPa·day^{-1}), $C^{\boxplus}_{Opaque}$ is strongly driven by the velocity of ascending air (25 % to 45 % increase from 0 hPa·day^{-1} to -100 hPa·day^{-1}) ~~by the velocity of ascending air~~, whereas $C^{\boxplus}_{Thin}$ seems to be poorly dependent ~~of~~ on it, with an almost constant cover around 40 %. In subsidence ~~regions~~, the mean $C^{\boxplus}_{Opaque}$ is also increasing when the air descending velocity is larger but with a wide range of variation from month to month (Fig. 11a). More strikingly, $T^{\boxplus}_{Opaque}$ and $T^{\boxplus}_{Thin}$ (Fig. 11b) vary linearly with ω_{500}, with a small variability from month to month. $T^{\boxplus}_{Opaque}$ and $T^{\boxplus}_{Thin}$ linearly decrease from 20 hPa·day^{-1} to -100 hPa·day^{-1} from approximately 5 °C to -35 °C and are constant between 20 hPa·day^{-1} and 70 hPa·day^{-1} at 5 °C. This suggests that, locally, $T^{\boxplus}_{Opaque}$ and $T^{\boxplus}_{Thin}$ are invariant~~s~~ in each dynamical regime. Radiative cloud temperatures $T^{\boxplus}_{Opaque}$ and $T^{\boxplus}_{Thin}$ presented in Fig. 11b were built respectively from temperatures at altitudes $Z^{|}_{Opaque}$ and $Z^{|}_{Top}$, and from temperatures at altitudes $Z^{|}_{Base}$ and $Z^{|}_{Top}$ (see Section 3.1). The linear decrease from 20 hPa·day^{-1} to -100 hPa·day^{-1} of $T^{\boxplus}_{Opaque}$ and $T^{\boxplus}_{Thin}$ is due to the cumulative effects of a rising of the altitude of "apparent cloud base" ($Z^{|}_{Opaque}$ for Opaque clouds and $Z^{|}_{Base}$ for Thin clouds; see monthly mean 2°×2° gridded $Z^{\boxplus}_{Opaque}$ and $Z^{\boxplus}_{Thin}$ on Fig. 11c) and an elongation of the cloud vertical distribution which gives even higher $Z^{|}_{Top}$ (see monthly mean 2°×2° gridded distance of "apparent cloud base" $Z^{\boxplus}_{Top} - Z^{\boxplus}_{Opaque}$ and $Z^{\boxplus}_{Top} - Z^{\boxplus}_{Base}$ on Fig. 11d). Figure 11e shows the distribution in dynamical regimes of ε_{Thin}. It increases from 0.31 to 0.42 between 20 hPa·day^{-1} and -100 hPa·day^{-1}, being almost invariant from month to month, and it is around 0.32 in average in subsidence ~~region~~.

An interesting point ~~which~~ that appears in these figures is, in the tropics, the very small variability in the relationship between cloud properties and ω_{500} in dynamical regimes between 20 hPa·day^{-1} and -100 hPa·day^{-1}: standard deviation is around 2.5 % for $C^{\boxplus}_{Opaque}$, less than 2 % for $C^{\boxplus}_{Thin}$, around 2.5 K for $T^{\boxplus}_{Opaque}$, less than 3 K for $T^{\boxplus}_{Thin}$, approximately 0.01 for ε_{Thin}, around 350 m for $Z^{\boxplus}_{Opaque}$ and $Z^{\boxplus}_{Base}$, 300 m for $Z^{\boxplus}_{Top} - Z^{\boxplus}_{Opaque}$ and 200 m for $Z^{\boxplus}_{Top} - Z^{\boxplus}_{Base}$. So, a change in the large-scale dynamic regimes produces a change in the cloud properties and CRE that seem predictable. For example, if ~~an intensification of the upward air motions velocity change~~ ω_{500} on a region changes from -40 hPa·day^{-1} to -80 hPa·day^{-1}, $C^{\boxplus}_{Opaque}$ ~~would~~ will increase by 8 % ($C^{\boxplus}_{Thin}$ will remain more or less constant), $T^{\boxplus}_{Opaque}$ will decrease by 10 K and $T^{\boxplus}_{Thin}$ by 7 K, and ε_{Thin} will increase by 0.03. These cloud changes would increase the CRE by 17 W·m^{-2}, including 14 W·m^{-2} from Opaque clouds (Fig. 11f). Because $C^{\boxplus}_{Thin}$ will remain more or less constant whereas $C^{\boxplus}_{Opaque}$ will increase with a decrease of ω_{500} in ascend~~ing~~ance ~~regime~~, the relative contribution of Opaque clouds to the total CRE will be ~~more and more important as~~ increase with convection ~~increases~~. This is why we see in Fig. 11g a decrease of the Thin clouds relative contribution from 20 hPa·day^{-1} to -100 hPa·day^{-1}.

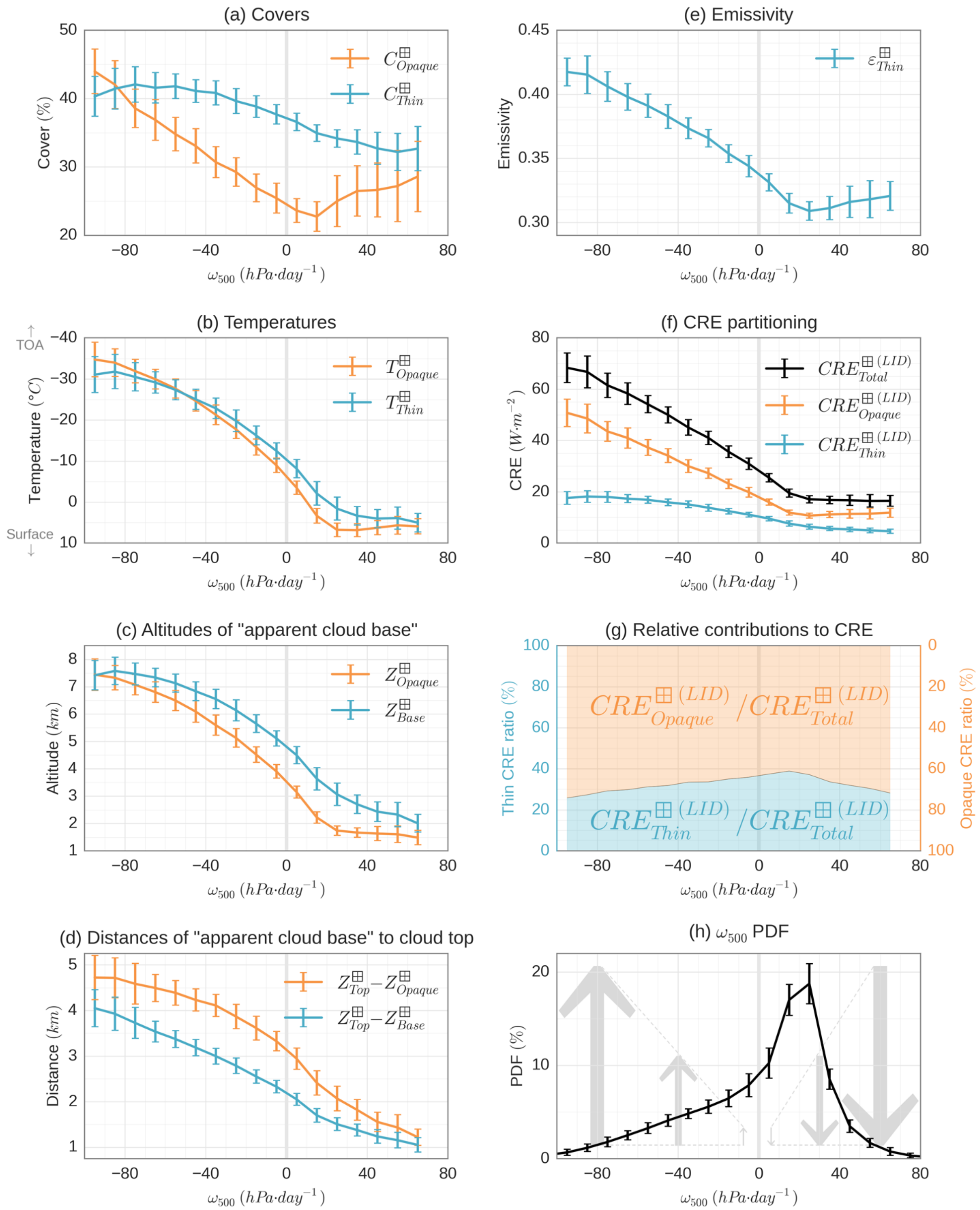

FIG. 11. Tropical mean cloud properties and radiative effects as a function of the 500-hPa pressure velocity: (a) $C_{Opaque}^{\boxplus}$ and $C_{Thin}^{\boxplus}$, (b) $T_{Opaque}^{\boxplus}$ among Opaque clouds and $T_{Thin}^{\boxplus}$ among Thin clouds, (c) $Z_{Opaque}^{\boxplus}$ among Opaque clouds and $Z_{Base}^{\boxplus}$ among Thin clouds, (d) $Z_{Top}^{\boxplus} - Z_{Opaque}^{\boxplus}$ among Opaque clouds and $Z_{Top}^{\boxplus} - Z_{Base}^{\boxplus}$ among Thin clouds, (e) $\varepsilon_{Thin}^{\boxplus}$ among Thin clouds, (f) total CRE, Opaque CRE and Thin CRE and (g) relative contribution of Opaque CRE and Thin CRE. (h) Distribution of the 500-hPa pressure velocity. Results obtained from monthly mean 2°×2° gridded variables. Only nighttime conditions over ice-free oceans for the 2008–2015 period in [30°S–30°N] ~~is~~ are considered. The error bars show the ± standard deviation of the 96-monthly means.

Because cloud properties seem to be invariants for dynamical regimes between 20 $hPa\cdot day^{-1}$ and -100 $hPa\cdot day^{-1}$, a change in the tropics of the large-scale circulation should ~~provide~~ lead to a predictable change in the CRE in regions that stay in this range of dynamical regimes, ~~predictable and~~ linked to the spatial distribution (both covers and altitudes) of Opaque clouds and Thin clouds sounded by CALIOP. For example, ~~under global warming, climate~~general circulation models suggest that a warmer climate will see a narrowing of the ascending branch of the Hadley cell (e.g. Su et al., 2014), which means less convective regions and more subsiding regions. This ~~and which~~ should result in a predictable decrease of the CRE, ~~predictable~~ knowing the changes of ω_{500} ~~all over~~for some part of the tropics.

6 Limitations of the OLR linear expression

In this study, from the direct measurement of the altitude of opacity for a ~~atmosphere opacity by~~ spaceborne lidar, termed $Z^{|}_{Opaque}$, we were able to infer the radiative temperature of Opaque clouds $T^{|}_{Opaque}$, which we found linearly ~~linked~~ related to the OLR. We propose $Z^{|}_{Opaque}$ as a good candidate to provide an observational constraint on the LW CRE~~. W~~ and we tested the linear relationship at different ~~space~~ scales from instantaneous to monthly means. ~~Hereinbelow~~In this section, we list possible ~~reasons for~~sources of uncertainty~~ies~~.

6.1 Cloud radiative temperatures $T^{|}_{Opaque}$ and $T^{|}_{Thin}$

The definitions of the c~~C~~loud radiative temperatures $T^{|}_{Opaque}$ and $T^{|}_{Thin}$ ~~definitions~~ (Section 3.1) only take into account the apparent cloud ~~extremities~~ edges seen by the lidar ($Z^{|}_{Top}$ and $Z^{|}_{Opaque}$ or $Z^{|}_{Base}$). A temperature defined by ~~the~~ a centroid altitude (Garnier et al., 2012) would ~~take into~~better account for the ~~entire~~ cloud vertical profile~~.~~, and ~~It~~ could give a better estimate ~~better~~ of the equivalent radiative temperature. However, our results show that the CRE is mainly driven by $Z^{|}_{Opaque}$ and $Z^{|}_{Top}$ ~~over~~ above Opaque clouds and $Z^{|}_{Base}$ and $Z^{|}_{Top}$ ~~over~~ above Thin clouds. Furthermore, observation~~al~~-based studies from the Atmospheric InfraRed Sounder (AIRS) and CALIOP showed that the radiative cloud height is located ~~at~~ near the "apparent middle" of the cloud (Stubenrauch et al., 2010). The authors defin~~ing~~e the "apparent middle" of the cloud as the middle between the cloud top ($Z^{|}_{Top}$) and the "apparent" cloud base see~~s~~n by the CALIOP lidar ($Z^{|}_{Base}$ for Thin clouds and $Z^{|}_{Opaque}$ for Opaque clouds), consistently with our own definitions (Eqs. (1) and (2)).

6.2 Multi-layer cloud and broken cloud situations

Plotting the results of Fig. 6 in single-cloud-layer situations (~~not shown~~Fig. A4c,d) ~~shows~~gives better correlation coefficients, with R = 0.99 for Opaque clouds and R = 0.92 for Thin clouds. ~~It reveals that~~This shows our linear expression ~~can be affected by additional uncertainties~~does not capture non-linearities which can occur in multi-layers situations (Fig. A4e,f). As an example, all the occurrences far ~~from and~~away above ~~over~~ the identity line in Fig. 6a are due to ~~cloud~~ multi-layer~~s~~ situations. For single columns with Opaque cloud~~ single columns~~, taking into account the optical depth of the thinner cloud which overlaps an Opaque cloud in the expression of $T^{|}_{Opaque}$ improves the results for the multi-layer scenario from R = 0.79 (Fig. A4e) to R = 0.86 (Fig. A5)~~ (R = 0.97)~~. However, this subtlety adds complexity to the comput~~e~~ation of $T^{|}_{Opaque}$~~,~~ and ~~only gives~~provides small improvements to a simple expression ~~with~~which already provides very satisfying results when considering all scenarios (R = 0.95 on Fig. 6a).

When clouds are broken, single lidar shots, having a 90 m diameter footprint, can fall on the edge of an Opaque cloud leading to signals from both cloud and the atmosphere and surface below the cloud in the same lidar profile. In this case an Opaque cloud can appear to be semi-transparent. Thus, the frequency of liquid clouds (T > 0°C) classified as Thin clouds (Fig. 4c) may be exaggerated as most liquid clouds are optically dense and not penetrated by lidar. This misclassification does not affect the computation of OLR, as $OLR^{\oslash}_{Thin}$ derived from lidar observations when $T^{\oslash}_{Thin} > 0$ °C show excellent agreement with measurements made by CERES (R = 0.94; Fig. A6).

6.~~2~~ 3 Evaluation of the OLR over Thin clouds

We saw that the theoretical linear expression of $OLR^{|}_{Thin}$ for a fixed $\varepsilon^{|}_{Thin}$ overestimates the simulated ~~one~~relationship, by up to +10 W·m^{-2} ~~for~~ in many cases (Section 4.1). This is partly due to ~~the fact that~~ the linear theoretical expression ~~does~~ not tak~~e~~ing into account the ~~diffusion~~ scattering of the LW radiation within the clouds. ~~It could partly~~This may partially explain why $OLR_{Thin}^{\emptyset\,(LID)}$ is larger than ~~compared to~~ the measured $OLR_{Thin}^{\emptyset\,(CERES)}$ (Fig. 6b). However, we do not think ~~it should really~~this should substantially affect the global scale partitioning of $CRE_{Total}^{\boxplus\,(LID)}$ between $CRE_{Opaque}^{\boxplus\,(LID)}$ and $CRE_{Thin}^{\boxplus\,(LID)}$~~,~~ because~~,~~ replacing $CRE_{Thin}^{\boxplus\,(LID)}$ by the difference $CRE_{Total}^{\boxplus\,(CERES)} - CRE_{Opaque}^{\boxplus\,(LID)}$~~, reveals that~~ only increases the contribution of Opaque clouds ~~contribute~~to the total CRE to 74 %, ~~to the total CRE~~ instead of 73 %.

~~Plotting results of Fig. 6 in single-cloud-layer situations (not shown) shows better correlation coefficients, with R = 0.99 for Opaque clouds and R = 0.92 for Thin clouds. It reveals that our linear expression can be affected by additional uncertainties in multilayers situations. As an example, all the occurrences far from and over the identity line in Fig. 6a are due to cloud multilayers. For Opaque cloud single columns, taking into account the optical depth of the thinner cloud which overlaps an Opaque cloud in the expression of $T_{Opaque}^{\dagger}$ improves the results (R = 0.97). However, this subtlety adds complexity to compute $T_{Opaque}^{\dagger}$, and only gives small improvements to a simple expression with already very satisfying results (R = 0.95 on Fig. 6a).~~

Also, the value of $\varepsilon_{Thin}^{\boxplus}$ used to construct $OLR_{Thin}^{\boxplus\,(LID)}$ does not account for Thin cloud single columns where no "Clear" bin is found below the cloud (these clouds are not present in the $\varepsilon_{Thin}^{|}$ PDFs of Fig. 4d). This happens when very low clouds are present in the lowest 480 m bin~~.~~, and ~~S~~so, emissivities of Thin clouds close to the surface are not taken into account in the averaged $\varepsilon_{Thin}^{\boxplus}$. But since all these "missed" cloud emissivities are from clouds near the surface, their temperature is certainly close to the surface temperature and their LW CRE should be small. So, this effect should have no significant impact on the presented results.

~~Moreover~~Further, applying $OLR_{Thin}^{|}$ Eq. (4) to 2°×2° gridded variables introduces errors since the equation is non-linear (the product of $T_{Thin}^{|}$ and $\varepsilon_{Thin}^{|}$) unlike Eq. (5) for the $OLR_{Opaque}^{|}$ ~~Eq. (5)~~ which is linearly dependent on $T_{Opaque}^{|}$. ~~Given that $\varepsilon_{Thin}^{\dagger}$ is mostly centered around 0.25 (Fig. 4d) it should not bring a substantial error, and~~ However, the comparison of the computed gridded $OLR_{Total}^{\boxplus\,(LID)}$ against the measured $OLR_{Total}^{\boxplus\,(CERES)}$ has shown very good agreement.

Finally, ~~due to the fact that~~since one of the objectives of the GOCCP product was ~~built in order~~ to avoid false cloud detections during both nighttime and daytime conditions, the signal threshold chosen for cloud detection is quite large, ~~implies~~ meaning that ~~GOCCP does not detect~~ high clouds with ~~an~~ optical depths smaller than about 0.07 are absent from GOCCP (Chepfer et al., 2010, 2013). These subvisible cirrus clouds are ~~not included~~therefore excluded from ~~in~~ this study, but as their emissivities are very small (smaller than about 0.03), they would~~ill~~ likely not ~~change the~~impact our results ~~of the paper~~.

6.~~3~~ 4 Gridded OLR

Concerning gridded OLR, ~~it should be noted that~~ we used monthly mean $OLR_{Clear}^{\boxplus}$ from CERES-EBAF in Eqs. (4-5) instead of instantaneous $OLR_{Clear}^{\boxplus}$ from C3M since this product is only available up to April 2011. Clear sky OLR from CERES-EBAF data is derived only from measurements over Clear sky atmospheric columns which are generally drier than the clear part of a cloudy atmospheric CERES column. ~~Then, b~~Because a drier atmospheric column leads to a stronger OLR (e.g. Spencer and Braswell, 1997; Dessler et al., 2008; Roca et al., 2012), $OLR_{Clear}^{\boxplus}$ from CERES-EBAF should overestimate~~s~~ $OLR_{Clear}^{\boxplus}$ from C3M ~~i~~on average. The diurnal cycle, which is taken into account in $OLR_{Clear}^{\boxplus}$ from CERES-EBAF but not in $OLR_{Clear}^{\boxplus}$ from C3M (since we only used nighttime observations) could also play a role in the difference. We found an increase of 0.6 W·m^{-2} for the global mean $OLR_{Total}^{\boxplus\,(LID)}$ computed with $OLR_{Clear}^{\boxplus}$ from CERES-EBAF compared to $OLR_{Total}^{\boxplus\,(LID)}$ computed with $OLR_{Clear}^{\boxplus}$ from C3M for the 2008–2010 period.

Differences between $OLR_{Total}^{\boxplus\,(LID)}$ and $OLR_{Total}^{\boxplus\,(CERES)}$ could also be related, to multi-layer clouds in atmospheric single columns, to cloud microphysic~~s~~al ~~cloud~~ properties, and to differences in local atmospheric properties. However, using this very simple expression ~~of~~ for the OLR give an excellent correlation (R = 0.95) between monthly mean $OLR_{Total}^{\boxplus\,(LID)}$ and $OLR_{Total}^{\boxplus\,(CERES)}$ and a good agreement of the linear regression with the identity line (appendix C, 2D distribution of monthly means 2°×2° gridded measured and computed OLR is given in Fig. ~~A4~~A6).

6.~~4~~ 5 Sensitivity to $Z_{Opaque}^{|}$ and to the multiple scattering factor

We also checked the sensitivity of $OLR_{Total}^{\boxplus\,(LID)}$ to the uncertainty in the altitude of full attenuation of the lidar signal. To do this, we ~~computed the $OLR_{Total}^{\boxplus\,(LID)}$ assuming~~conducted a test by moving $Z_{Opaque}^{|}$ one bin up (480 m) in all Opaque single columns ~~is located one bin (480 m) higher than $Z_{Opaque}^{|}$ given by GOCCP v3.0.~~ (as moving $Z_{Opaque}^{|}$ one bin down would have led to negative values for some $Z_{Opaque}^{|}$). This ~~leads to a modification of~~changes the Opaque cloud radiative temperature, ~~and then to a modification of~~ the $OLR_{Opaque}^{|\,(LID)}$, and so the $OLR_{Total}^{\boxplus\,(LID)}$. ~~Doing this~~Results show that after this change~~,~~ ~~decreases~~ the global mean $OLR_{Total}^{\boxplus\,(LID)}$ ~~from~~ is decreased by 0.9 W·m^{-2} (appendix D, Fig. ~~A5a~~A7a).

Finally, ~~the use of~~ a fixed multiple scattering factor η is used for the retrieval~~ing~~ of the Thin cloud emissivity, whereas ~~it depends~~there is evidence of a dependence on cloud temperature (Garnier et al., 2015). This~~,~~ could also play an important role in the differences between computed $OLR_{Thin}^{\varnothing\,(LID)}$ and measured $OLR_{Thin}^{\varnothing\,(CERES)}$. We tested the sensitivity of ~~a change~~variability in η on the computed $OLR_{Total}^{\boxplus\,(LID)}$, by modifying the value of η from 0.6 to 0.5. ~~It~~ This reduced~~s~~ the global mean $OLR_{Total}^{\boxplus\,(LID)}$ ~~from~~ by 1.1 W·m^{-2} (appendix D, Fig. ~~A5b~~A7b), which we consider negligible compared to the global mean value of $CRE_{Total}^{\boxplus\,(LID)}$ equal to 28.4 W·m^{-2}.

7 Conclusion

Simple radiative transfer models that estimate ~~the top of the atmosphere~~ outgoing radiation~~s~~ at the TOA ~~as a function of~~from a limited number of variables are useful ~~tools~~ to build a first-order decomposition of climate feedbacks. Such simple models exist in the SW domain, but not in the LW domain because ~~the~~ LW fluxes are sensitive to the cloud vertical distribution, making the definition of such a simple model more challenging~~ in the LW than in the SW~~. In this work, we propose a simple LW radiative model which ~~express~~ derives the LW CRE ~~as a function of~~from five variables: two ~~of them~~ describing~~e~~ ~~the~~ Opaque clouds (Opaque cloud cover~~,~~ and Opaque cloud radiative temperature) and three which ~~others~~ describe ~~the~~ semi-transparent clouds (Thin cloud cover, Thin cloud radiative temperature, and Thin cloud emissivity).

The originality of ~~the~~ our approach ~~proposed in this paper re~~lies ~~on~~ in how the cloud vertical distribution is described in this simple radiative transfer model. We have used three altitude levels ~~of altitude~~which can be precisely ~~documented~~ measured by ~~a~~ space~~-~~borne lidar to describe the cloud vertical distribution within the simple radiative model. Our approach contrasts with ~~the~~ techniques based on passive space~~-~~borne sensors ~~because those latter measure vertically integrated variables and~~that ~~do not provide direct~~ retrieve effective cloud heights rather than profile information on the cloud vertical distribution. Our approach also contrasts with techniques based on full-profile lidar/radar measurements ~~that use~~using 40 levels of altitude (or more) to describe ~~the~~ cloud vertical distribution in the troposphere. In this work, we have taken advantage of the precision and accuracy of ~~the~~ space~~-~~borne lidar to describe ~~the~~ cloud vertical structure, but have ~~we~~ retained only three levels of altitude~~ out of the 40 or more,~~ to describe the cloud vertical distribution. Considering ~~only~~ three levels of altitude ~~allows to~~allows us build a simple radiative model~~s~~, useful for first-order cloud feedback analysis, given that the more complex radiative transfer models using ~~40~~ all altitude levels cannot ~~hardly~~ be used for this purpose. We have selected t~~T~~he three levels of altitude ~~that we have selected are the ones which~~that influence ~~the most~~ the OLR the most: 1) ~~the~~ cloud top altitude $Z^{|}_{Top}$, 2) the level of full attenuation of the lidar laser beam $Z^{|}_{Opaque}$, in ~~a~~ single columns containing an Opaque cloud, and 3) ~~the~~ cloud base $Z^{|}_{Base}$, in ~~a~~ single columns containing ~~a~~ semi-transparent Thin cloud. These three ~~levels of~~ altitudes ~~have two advantages: they~~ are first~~-~~order drivers of the LW CRE, and ~~they~~ have been measured precisely and unambiguously over a decade with the CALIPSO space~~-~~borne lidar.

Using radiative transfer computations, we found that the OLR above an opaque cloud can be expressed linearly as a function of the "Opaque temperature": $OLR^{|(LID)}_{Opaque} = 2.0T^{|}_{Opaque} - 310$, where $T^{|}_{Opaque}$ is obtained from the combination of the cloud top altitude $Z^{|}_{Top}$, the level of full attenuation of the lidar laser beam $Z^{|}_{Opaque}$, and a temperature profile taken from a reanalysis product. ~~From t~~This simple relationship predicts~~, it results~~ that if the altitude an Opaque cloud ~~rises up, and~~increases so as to decrease~~s~~ its $T^{|}_{Opaque}$ by 1 K, then the OLR is decreased by 2 W·m^{-2}. Using this linear relationship together with CALIPSO and CERES observations, we estimated ~~the contribution of the Opaque clouds to the global mean LW CRE.~~that Opaque clouds, which cover 35 % of the ice-free ocean, contribute to 73 % of the global mean ~~cloud radiative effect~~CRE whereas Thin clouds, which cover 36 %, contribute to 27 %.

We checked the robustness of th~~e~~is linear relationship ~~given here above~~ against observations at two different space and time scales. ~~. First, we tested the~~Using instantaneous ~~time scale at small space scale (20 km) using~~collocated observations from the CALIPSO lidar ~~data collocated with~~and ~~-~~CERES broadband radiometer data at the sensor spatial scale (20 km)~~.~~, w~~W~~e found a correlation coefficient of 0.95 between the lidar derived $T^{\varnothing}_{Opaque}$ and the OLR measured by the broadband radiometer CERES. ~~Second, we tested the validity of the relationship using~~Averaging the same data monthly ~~mean data~~ within 2° latitude × 2° longitude grid boxes~~.~~, ~~There we found that the global annual mean OLR derived from the combination of the lidar data and the linear relationship,~~our derived OLR differs by 0.1 W·m^{-2} from the OLR measured by CERES.

To conclude, this paper proposes a simple approximate ~~formulation of~~solution to the complex problem of radiative transfer in the LW domain, ~~that~~ which could be used to explore first-order LW cloud feedbacks in both observations and climate model simulations. On the observational side, future work will ~~consist in~~ analyz~~ing~~e the inter-annual variability of the record collected by space~~-~~borne lidars and broadband radiometers: CALIPSO/CERES in the A-train (10+ years), followed ~~completed~~ by ~~EarthCare~~ EarthCARE (Illingworth et al., 2014) to be launched in ~~the coming years~~2018. On the climate model simulation side, this new framework will be included in the Cloud Feedback Model Intercomparison Project (CFMIP) Observation Simulator Package (COSP; Bodas-Salcedo et al., 2011) lidar simulator (Chepfer et al., 2008) and applied to climate model outputs in order to quantify the ~~role~~ contribution of each cloud property ~~in~~ to the simulated cloud feedbacks.

Appendix A: Radiative cloud temperature

Schematically, if we consider an optically uniform cloud, i.e. the LW optical depth $\delta\tau^{LW|}$ increases linearly through the cloud, with a cloud total LW optical depth $\delta\tau^{LW|}_{Cloud}$, we can compute the upward LW radiative flux emitted by the cloud at the top of the cloud ($\delta\tau^{LW|} = 0$). Neglecting the cloud particle reflectivity in the longwave domain, from the integral form of the Schwarzschild's equation, we can express the upward zenithal spectral radiance $I^{|}_{\upsilon}$ emitted by the cloud at the top of the cloud:

$$I^{|}_{\upsilon_{Cloud}}\left(\delta\tau^{LW|} = 0\right) = \int_0^{\delta\tau^{LW|}_{Cloud}} B_{\upsilon}\left(T\left(\delta\tau^{LW|}\right)\right) e^{-\delta\tau^{LW|}} d\delta\tau^{LW|} \qquad [\mathrm{W \cdot m^{-2} \cdot sr^{-1} \cdot m^{-1}}] \ (\mathrm{A1})$$

Considering a linear increase of the temperature with $\delta\tau^{LW|}$ from the cloud top to the cloud base ($T\left(\delta\tau^{LW|}\right) = k_1\delta\tau^{LW|} + k_2$) and integrating $I^{|}_{\upsilon_{Cloud}}$ throughout the whole LW spectrum (using Stefan-Boltzmann law $\int B_{\upsilon}\, d\upsilon = \sigma T^4/\pi$), we can write the LW radiance $I^{LW|}$ emitted by the cloud at the top of the cloud as:

$$I^{LW|}_{Cloud}\left(\delta\tau^{LW|} = 0\right) = \int_0^{\delta\tau^{LW|}_{Cloud}} \frac{\sigma}{\pi}\left(k_1\delta\tau^{LW|} + k_2\right)^4 e^{-\delta\tau^{LW|}} d\delta\tau^{LW|} \qquad [\mathrm{W \cdot m^{-2} \cdot sr^{-1}}]$$

(A2)

Assuming that the cloud emits as a Lambertian surface, the upward LW radiative flux $F^{\uparrow LW|}$ emitted by the cloud at the top of the cloud is given by:

$$F^{\uparrow LW|}_{Cloud}\left(\delta\tau^{LW|} = 0\right) = \int_0^{\delta\tau^{LW|}_{Cloud}} \sigma\left(k_1\delta\tau^{LW|} + k_2\right)^4 e^{-\delta\tau^{LW|}} d\delta\tau^{LW|} \qquad [\mathrm{W \cdot m^{-2}}]$$

(A3)

Then, for specific values of coefficient k_1 and k_2, which determine the gradient of temperature in the cloud and the cloud top temperature (and so the cloud base temperature knowing $\delta\tau^{LW|}_{Cloud}$), it is possible to compute $F^{\uparrow LW|}_{Cloud}\left(\delta\tau^{LW|} = 0\right)$ and then solve the equation $F^{\uparrow LW|}_{Cloud}\left(\delta\tau^{LW|} = 0\right) = \varepsilon^{|}\sigma\left(T^{|}_{rad}\right)^4 = \left(1 - e^{-\delta\tau^{LW|}_{Cloud}}\right)\sigma\left(T^{|}_{rad}\right)^4$ to find the corresponding equivalent cloud radiative temperature $T^{|}_{rad}$.

Appendix B: Vertical distributions of clouds directly observed by CALIOP

For 3 regions, as for Fig. 4, Fig. A1 shows distributions of the distance between cloud top and $Z^{|}_{Opaque}$ ~~among Opaque clouds~~ and the distance between cloud top and cloud base ~~among Thin clouds~~. In the 3 regions, when an Opaque cloud (Fig. A1a) is penetrated by the laser beam of the lidar, $Z^{|}_{Opaque}$ is mostly found in the 1st km below $Z^{|}_{Top}$ (30 % in the tropical convective region, 52 % in the mid-latitudes region and 75 % in the tropical subsiding region). The frequency distribution collapses after 1 km (note the logarithmic y-axis). The greater altitude differences between $Z^{|}_{Top}$ and $Z^{|}_{Opaque}$ can be due to a more vertically spread cloud or to multiple cloud layers. If we look at the dashed lines, which represent the part of the PDF considering only profiles without multilayers, we can see that the curves of the 3 regions fall to zero around 4–5 km. This means that all the part of PDFs over 5 km are due to ~~cloud~~ multi-layer~~s~~ clouds. ~~It also suggests that the laser beam never sounds deeper than 5 km within a cloud.~~

Regarding Thin clouds (Fig. A1b), we mostly found $Z^{|}_{Base}$ in the 1st km below $Z^{|}_{Top}$ (49 % in the tropical convective region, 68 % in the mid-latitudes region and 76 % in tropical subsiding region). The frequency distribution collapses after 1 km (again, note the logarithmic y-axis). The part of the PDF of profiles without multilayer (dashed lines), i.e. single columns which contain only one optically thin cloud layer and so directly represent the geometrical thickness of Thin clouds, fall to zero around 4–5 km. This means, as for Opaque clouds, that all the part of PDFs over 5 km are due to overlap of ~~multiple~~ multi-layer clouds~~-layers~~. ~~It therefore suggests, if we look at both Figs. A1a and A1b, that the laser beam is not able go through the entire cloud if its vertical geometrical thickness is greater than 5 km. In other words, a cloud with a vertical~~

~~geometrical thickness greater than 5 km is always declared as an Opaque cloud.~~ Furthermore, as PDFs collapse after 1 km in both figures A1a and A1b and for all regions, it ~~also~~ suggests that, ~~even if the maximum penetration depth is 5 km,~~ the laser beam is almost every time totally attenuated when exceeding 1 km thickness.

Appendix C: Verification of the lidar-derived gridded OLR against CERES observations

Figure ~~A4~~ A7 shows the correlation between the OLR computed from lidar observations ($OLR_{Total}^{\boxplus\,(LID)}$) and the OLR measured by the CERES radiometer on-board the Aqua satellite on which we extract only footprints collocated with the CALIPSO ground track ($OLR_{Total}^{\boxplus\,(CERES)}$) for nighttime and over ice-free oceans on 2°×2° monthly means for the 2008. We found an excellent correlation (R = 0.95) and the regression slope is near the one-to-one line which reinforces our confidence in this simple OLR expression to correctly estimate the observed OLR.

Appendix D: Sensitivity of the lidar-derived gridded OLR to $Z_{Opaque}^{|}$ and to the multiple scattering factor

Figure ~~A5a~~ A8a shows the difference between lidar-derived gridded $OLR_{Total}^{\boxplus\,(LID)}$ shown in Fig. 7a and the one which would be obtain if $Z_{Opaque}^{|}$ was found 480 m higher. To do this, we replaced the altitude $Z_{Opaque}^{|}$ of each Opaque cloud single column found with the lidar by the bin above, so the altitude of $Z_{Opaque}^{|}$ is systematically increased by 480 m. We then recomputed $OLR_{Total}^{\boxplus\,(LID)}$ in the exact same way as described in this paper. The effect of an increase in the altitude of $Z_{Opaque}^{|}$ is a global mean decrease in $OLR_{Total}^{\boxplus\,(LID)}$ by 0.9 W·m^{-2}. Areas where $OLR_{Total}^{\boxplus\,(LID)}$ is the most affected correspond to areas with large values of Opaque cloud cover (patterns for 2008–2015 period on Fig. 2a are quite similar to those for the year 2008) except for the stratocumulus regions off the West coasts of the African, the American and the Oceanian continents where $C_{Opaque}^{\boxplus}$ is large but where $OLR_{Total}^{\boxplus\,(LID)}$ change is not very pronounced. A higher $Z_{Opaque}^{|}$ increases the level of the radiative temperature of the Opaque clouds, so decreases this temperature and then weakens $OLR_{Total}^{\boxplus\,(LID)}$. Since $OLR_{Total}^{\boxplus\,(LID)}$ is not affected as much in the stratocumulus regions, this suggests that vertical temperature gradient where these clouds are founded must be weak.

Figure ~~A5b~~ A8b shows the difference between lidar-derived gridded $OLR_{Total}^{\boxplus\,(LID)}$ shown in Fig. 7a and the one which is obtain using a fixed multiple scattering factor $\eta = 0.5$ instead of $\eta = 0.6$. Decreasing η, increases the retrieved emissivity of the Thin clouds by 0.05. Consequently, areas where Thin cloud cover is large and where they are high and cold, so where they have a strong cloud radiative effect, are regions where $OLR_{Total}^{\boxplus\,(LID)}$ is the most affected by this change (in the multiple scattering factor), up to a decrease of 3.5 W·m^{-2} in the Indonesian region.

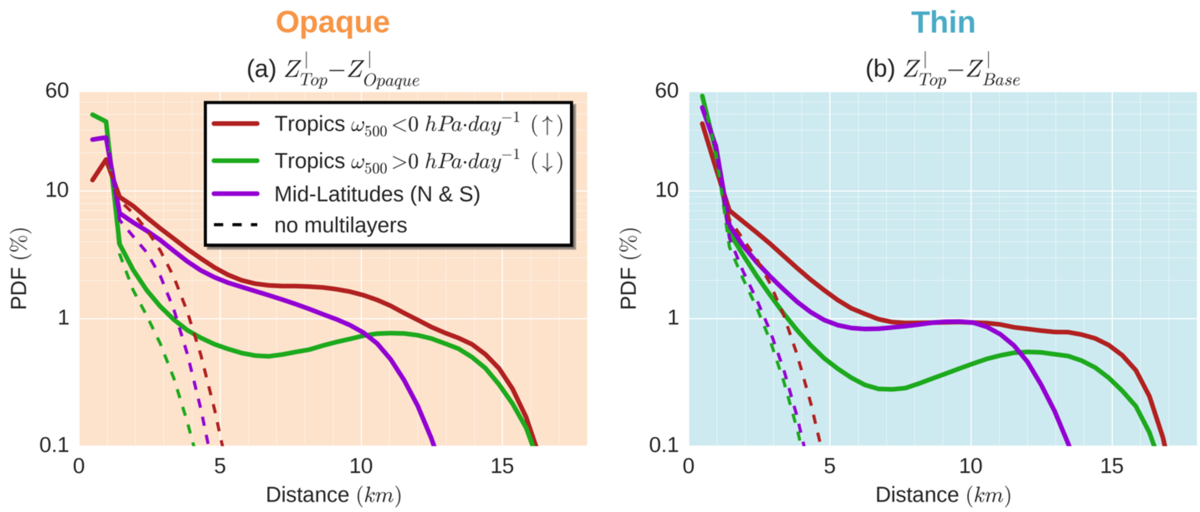

FIG. A1. Distributions of (a) the distance between cloud top and $Z^{|}_{Opaque}$ among Opaque clouds and (b) the distance between cloud top and cloud base among Thin clouds in three regions: same as Fig. 4. Dashed lines represent the distribution only among single columns where a unique cloud layer was found (no multiple cloud layers). Only nighttime conditions over ice-free oceans for the 2008–2015 period ~~is~~ are considered.

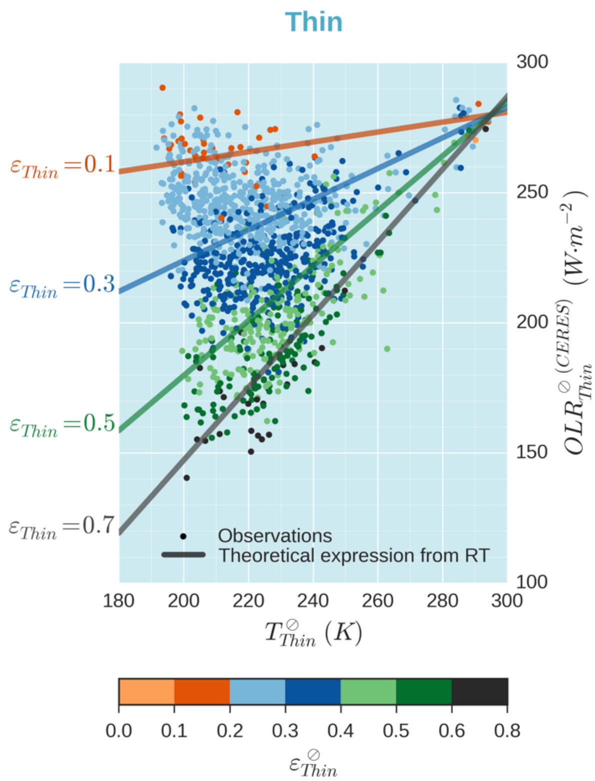

FIG. A2. Comparison between observed and lidar-derived OLR, at CERES footprint scale, as a function of $T^{\oslash}_{Thin}$ and $\varepsilon^{\oslash}_{Thin}$. Results obtained from CERES (dots) and CALIOP (lines) collocated measurements. Theoretical expressions are from Eq. (4). Same results as in Fig. 6b but only for measurements where $OLR^{\oslash}_{Clear}$ is close to 280 W·m^{-2} selected ($OLR^{\oslash}_{Clear} \in [275\text{–}285]$ W·m-2), in order to only see the contribution of $T^{\oslash}_{Thin}$ and $\varepsilon^{\oslash}_{Thin}$ on the OLR. Only nighttime conditions over ice-free oceans for January 2008 ~~is~~ are considered.

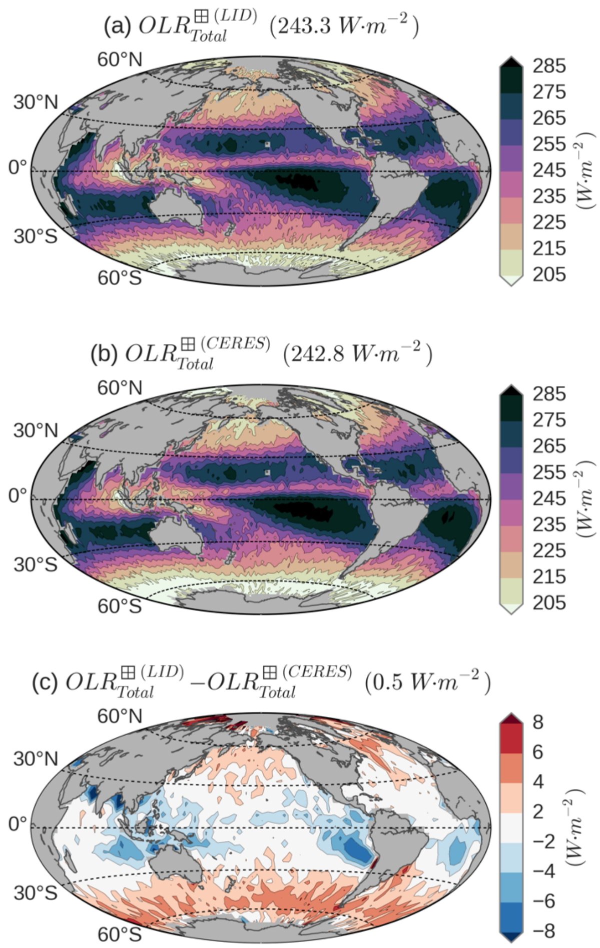

FIG. A3. Same as Fig. 7 but using $OLR_{Clear}^{\boxplus}$ from CERES-EBAF instead of $OLR_{Clear}^{\boxplus}$ from CERES-Aqua in the calculation of $OLR_{Total}^{\boxplus\,(LID)}$.

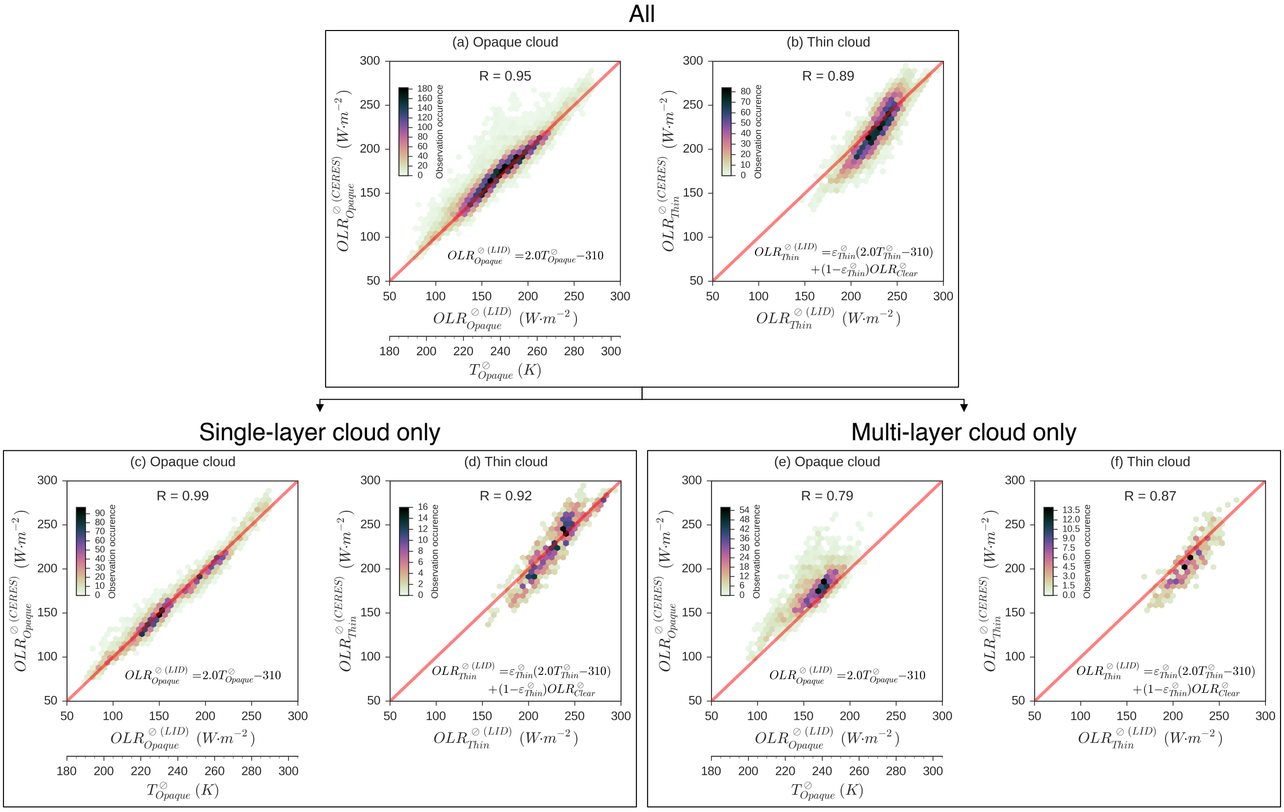

FIG. A4. (a) and (b) are the same as Fig. 6a and 6b. They are decomposed here into (c,d) single-layer cloud situations and (e,f) multi-layer cloud situations.

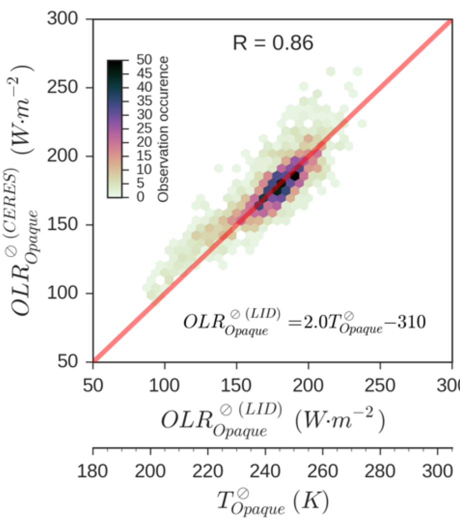

FIG. A5. As Fig. A4e but with multi-layer cloud considered in the computation of $T^{|}_{Opaque}$, considering that the cloud layers above the optically opaque cloud (below) have an equivalent emissivity $\varepsilon_{above} = 0.3$: $T^{|}_{Opaque} = (1-\varepsilon_{above})T^{|}_{below} + \varepsilon_{above}T^{|}_{above}$ where $T^{|}_{below} = \frac{T^{|}_{Top_{below}} + T^{|}_{z_{Opaque}}}{2}$ and $T^{|}_{above} = \frac{T^{|}_{Top_{above}} + T^{|}_{Base_{above}}}{2}$.

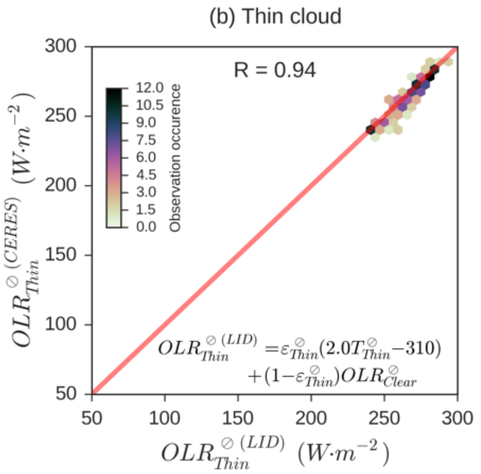

FIG. A6. As Fig. 6b but only with $T^{\oslash}_{Thin} > 0\ °C$ which could be liquid broken Opaque clouds misclassified as Thin clouds.

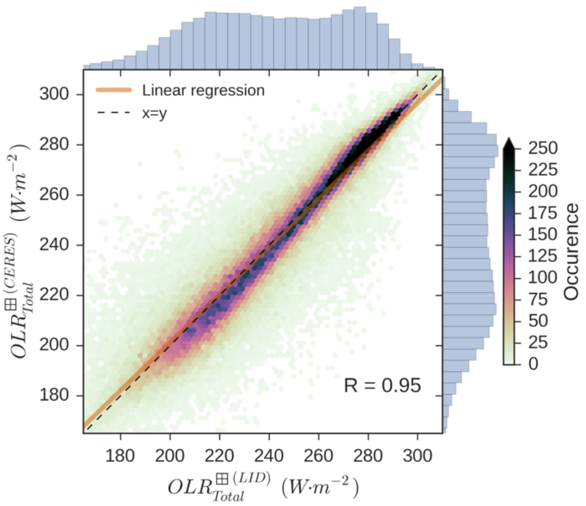

FIG. ~~A4~~A7. Comparison between observed and lidar-derived OLR at monthly mean 2°×2° gridded scale. Only nighttime conditions over ice-free oceans for the 2008-year period ~~is~~ are considered.

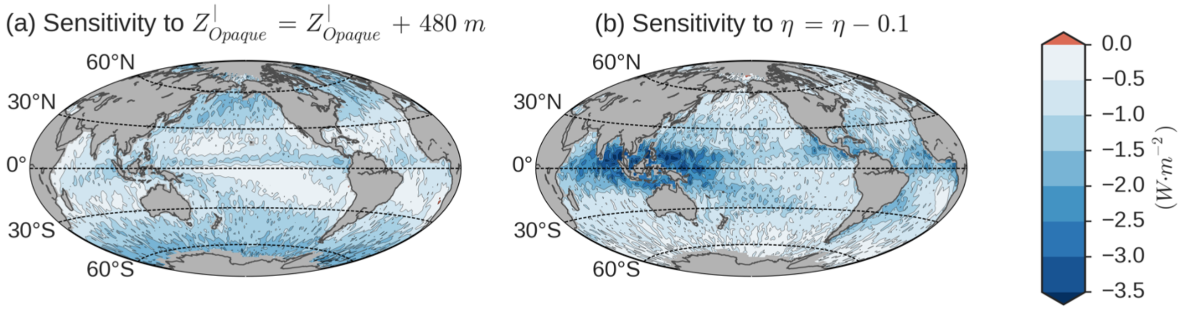

FIG. ~~A5~~A8. Sensitivity of the lidar-derived annual-mean gridded $OLR_{Total}^{\boxplus(LID)}$ to the altitude of full attenuation of the lidar into Opaque clouds $Z^{|}_{Opaque}$ and to the multiple scattering factor η: (a) difference between $OLR_{Total}^{\boxplus(LID)}$ of Fig. 7a and $OLR_{Total}^{\boxplus(LID)}$ which would be obtain if $Z^{|}_{Opaque}$ was found a 480 m-bin upper and (b) difference between $OLR_{Total}^{\boxplus(LID)}$ of Fig. 7a and $OLR_{Total}^{\boxplus(LID)}$ which is obtain using a fixed multiple scattering factor $\eta = 0.5$ instead of $\eta = 0.6$. Only nighttime conditions over ice-free oceans for the 2008 year ~~is~~ are considered.

References

Bates, J. R.: Some considerations of the concept of climate feedback, Q. J. R. Meteorol. Soc., 133, 545–560, doi:10.1002/qj.62, 2007.

Berrisford, P., Dee, D., Poli, P., Brugge, R., Fielding, K., Fuentes, M., Kallberg, P., Kobayashi, S., Uppala, S., and Simmons, A.: The ERA-Interim archive Version 2.0, ERA Report Series 1, ECMWF, Shinfield Park, Reading, UK, 2011.

Bodas-Salcedo, A., Webb, M. J., Bony, S., Chepfer, H., Dufresne, J. L., Klein, S. A., Zhang, Y., Marchand, R., Haynes, J. M., Pincus, R., and John, V. O.: COSP: Satellite simulation software for model assessment, Bull. Am. Meteorol. Soc., 92, 1023–1043, doi:10.1175/2011BAMS2856.1, 2011.

Bony, S., Colman, R., Kattsov, V. M., Allan, R. P., Bretherton, C. S., Dufresne, J.-L., Hall, A., Hallegatte, S., Holland, M. M., Ingram, W., Randall, D. A., Soden, B. J., Tselioudis, G., and Webb, M. J.: How Well Do We Understand and Evaluate Climate Change Feedback Processes?, J. Clim., 19, 3445–3482, doi:10.1175/JCLI3819.1, 2006.

Boucher, O., Randall, D., Artaxo, P., Bretherton, C., Feingold, G., Forster, P., Kerminen, V.-M., Kondo, Y., Liao, H., Lohmann, U., Rasch, P., Satheesh, S. K., Sherwood, S., Stevens, B., and Zhang, X. Y.: Clouds and aerosols, in: Climate Change 2013: The Physical Science Basis. Contribution of Working Group I to the Fifth Assessment Report of the Intergovernmental Panel on Climate Change, Cambridge University Press, United Kingdom and New York, USA, 571–657, doi:10.1017/CBO9781107415324.016, 2013.

Caldwell, P. M., Zelinka, M. D., Taylor, K. E., and Marvel, K.: Quantifying the Sources of Intermodel Spread in Equilibrium Climate Sensitivity, J. Clim., 29, 513–524, doi: 10.1175/JCLI-D-15-0352.1, 2016.

Cesana, G. and Chepfer, H.: How well do climate models simulate cloud vertical structure? A comparison between CALIPSO-GOCCP satellite observations and CMIP5 models, Geophys. Res. Lett., 39, L20803, doi:10.1029/2012GL053153, 2012.

Cesana, G. and Chepfer, H.: Evaluation of the cloud thermodynamic phase in a climate model using CALIPSO-GOCCP, J. Geophys. Res., 118, 7922–7937, doi:10.1002/jgrd.50376, 2013.

Cess, R. D.: Global climate change: an investigation of atmospheric feedback mechanisms, Tellus, 27, 193–198, doi: 10.3402/tellusa.v27i3.9901, 1975.

Cess, R. D., Potter, G. L., Blanchet, J. P., Boer, G. J., Del Genio, A. D., Déqué, M., Dymnikov, V., Galin, V., Gates, W. L., Ghan, S. J., Kiehl, J. T., Lacis, A. A., Le Treut, H., Li, Z.-X., Liang, X.-Z., McAvaney, B. J., Meleshko, V. P., Mitchell, J. F. B., Morcrette, J.-J., Randall, D. A., Rikus, L., Roeckner, E., Royer, J. F., Schlese, U., Sheinin, D. A., Slingo, A., Sokolov, A. P., Taylor, K. E., Washington, W. M., Wetherald, R. T., Yagai, I., and Zhang, M.-H.: Intercomparison and interpretation of climate feedback processes in 19 atmospheric general circulation models, J. Geophys. Res., 95, 16601–16615, doi:10.1029/JD095iD10p16601, 1990.

Cess, R. D., Zhang, M. H., Ingram, W. J., Potter, G. L., Alekseev, V., Barker, H. W., Cohen-Solal, E., Colman, R. A., Dazlich, D. A., Genio, A. D. D., Dix, M. R., Dymnikov, V., Esch, M., Fowler, L. D., Fraser, J. R., Galin, V., Gates, W. L., Hack, J. J., Kiehl, J. T., Le Treut, H., Lo, K. K.-W., McAvaney, B. J., Meleshko, V. P., Morcrette, J.-J., Randall, D. A., Roeckner, E., Royer, J.-F., Schlesinger, M. E., Sporyshev, P. V., Timbal, B., Volodin, E. M., Taylor, K. E., Wang, W., and Wetherald, R. T.: Cloud feedback in atmospheric general circulation models: An update, J. Geophys. Res., 101, 12791–12794, doi:10.1029/96JD00822, 1996.

Chepfer, H., Bony, S., Winker, D., Chiriaco, M., Dufresne, J.-L., and Sèze, G.: Use of CALIPSO lidar observations to evaluate the cloudiness simulated by a climate model, Geophys. Res. Lett., 35, L15704, doi:10.1029/2008GL034207, 2008.

Chepfer, H., Bony, S., Winker, D., Cesana, G., Dufresne, J. L., Minnis, P., Stubenrauch, C. J., and Zeng, S.: The GCM-Oriented CALIPSO Cloud Product (CALIPSO-GOCCP), J. Geophys. Res., 115, D00H16, doi:10.1029/2009JD012251, 2010.

Chepfer, H., Cesana, G., Winker, D., Getzewich, B., Vaughan, M., and Liu, Z.: Comparison of Two Different Cloud Climatologies Derived from CALIOP-Attenuated Backscattered Measurements (Level 1): The *CALIPSO*-ST and the *CALIPSO*-GOCCP, J. Atmos. Oceanic Technol., 30, 725–744, doi: 10.1175/JTECH-D-12-00057.1, 2013.

Chepfer, H., Noel, V., Winker, D., and Chiriaco, M.: Where and when will we observe cloud changes due to climate warming?, Geophys. Res. Lett., 41, 8387–8395, doi: 10.1002/2014GL061792, 2014.

Colman, R.: A comparison of climate feedbacks in general circulation models, Clim. Dyn., 20, 865–873, doi:10.1007/s00382-003-0310-z, 2003.

Dessler, A. E., Yang, P., Lee, J., Solbrig, J., Zhang, Z., and Minschwaner, K.: An analysis of the dependence of clear-sky top-of-atmosphere outgoing longwave radiation on atmospheric temperature and water vapor, J. Geophys. Res., 113, D17102, doi:10.1029/2008JD010137, 2008.

Dubuisson, P., Dessailly, D., Vesperini, M., and Frouin, R.: Water vapor retrieval over ocean using near-infrared radiometry, J. Geophys. Res., 109, D19106, doi:10.1029/2004JD004516, 2004.

Dufresne, J.-L. and Bony, S.: An Assessment of the Primary Sources of Spread of Global Warming Estimates from Coupled Atmosphere–Ocean Models, J. Clim., 21, 5135–5144, doi:10.1175/2008JCLI2239.1, 2008.

Evan, A. T., Heidinger, A. K., and Vimont D. J.: Arguments against a physical long-term trend in global ISCCP cloud amounts, Geophys. Res. Lett., 34, L04701, doi:10.1029/2006GL028083, 2007.

Fu, Q. and Liou, K. N.: On the Correlated k-Distribution Method for Radiative Transfer in Nonhomogeneous Atmospheres, J. Atmos. Sci., 49, 2139–2156, doi:10.1175/1520-0469(1992)049<2139:OTCDMF>2.0.CO;2, 1992.

Fu, Q. and Liou, K. N.: Parameterization of the Radiative Properties of Cirrus Clouds, J. Atmos. Sci., 50, 2008–2025, doi:10.1175/1520-0469(1993)050<2008:POTRPO>2.0.CO;2, 1993.

Garnier, A., Pelon, J., Dubuisson, P., Faivre, M., Chomette, O., Pascal, N., and Kratz, D. P.: Retrieval of cloud properties using CALIPSO Imaging Infrared Radiometer. Part I: effective emissivity and optical depth, J. Appl. Meteorol. Climatol., 51, 1407–1425, doi:10.1175/JAMC-D-11-0220.1, 2012.

Garnier, A., Pelon, J., Vaughan, M. A., Winker, D. M., Trepte, C. R., and Dubuisson, P.: Lidar multiple scattering factors inferred from CALIPSO lidar and IIR retrievals of semi-transparent cirrus cloud optical depths over oceans, Atmos. Meas. Tech., 8, 2759–2774, doi:10.5194/amt-8-2759-2015, 2015.

Guzman, R., Chepfer, H., Noel, V., Vaillant de Guélis, T., Kay, J. E., Raberanto, P., Cesana, G., Vaughan, M. A., and Winker, D. M.: Direct atmosphere opacity observations from CALIPSO provide new constraints on cloud-radiation interactions, J. Geophys. Res., 122, 1066–1085, doi:10.1002/2016JD025946, 2017.

Hansen, J., Lacis, A., Rind, D., Russell, G., Stone, P., Fung, I., Ruedy, R., and Lerner, J.: Climate sensitivity: Analysis of feedback mechanisms, Climate processes and climate sensitivity, Geophysical Monograph Series, vol. 29, J. E. Hansen and T. Takahashi, Washington, D. C., 1984.

Hartmann, D. L. and Larson, K.: An important constraint on tropical cloud-climate feedback, Geophys. Res. Lett., 29, 12-1–12-4, doi: 10.1029/2002GL015835, 2002.

Hartmann, D. L., Ockert-Bell, M. E., and Michelsen, M. L.: The Effect of Cloud Type on Earth's Energy Balance: Global Analysis, J. Clim., 5, 1281–1304, doi:10.1175/1520-0442(1992)005<1281:TEOCTO>2.0.CO;2, 1992.

Haynes, J. M., Marchand, R. T., Luo, Z., Bodas-Salcedo, A., and Stephens, G. L.: A multipurpose radar simulation package: QuickBeam, Bull. Am. Meteorol. Soc., 88, 1723–1727, doi:10.1175/BAMS-88-11-1723, 2007.

Henderson, D. S., L'Ecuyer, T., Stephens, G., Partain, P., and Sekiguchi, M.: A Multisensor Perspective on the Radiative Impacts of Clouds and Aerosols, J. Appl. Meteorol. Climatol., 52, 853–871, doi:10.1175/JAMC-D-12-025.1, 2013.

Holz, R. E., Ackerman, S. A., Nagle, F. W., Frey, R., Dutcher, S., Kuehn, R. E., Vaughan, M. A., and Baum, B.: Global Moderate Resolution Imaging Spectroradiometer (MODIS) cloud detection and height evaluation using CALIOP, J. Geophys. Res., 113, D00A19, doi:10.1029/2008JD009837, 2008.

Illingworth, A. J., Barker, H. W., Beljaars, A., Ceccaldi, M., Chepfer, H., Clerbaux, N., Cole, J., Delanoë, J., Domenech, C., Donovan, D. P., Fukuda, S., Hirakata, M., Hogan, R. J., Huenerbein, A., Kollias, P., Kubota, T., Nakajima, T., Nakajima, T. Y., Nishizawa, T., Ohno, Y., Okamoto, H., Oki, R., Sato, K., Satoh, M., Shephard, M. W., Velázquez-Blázquez, A., Wandinger, U., Wehr, T., and van Zadelhoff, G.-J.: The EarthCARE Satellite: The Next Step Forward in Global Measurements of Clouds, Aerosols, Precipitation, and Radiation, Bull. Am. Meteorol. Soc., 96, 1311–1332, doi:10.1175/BAMS-D-12-00227.1, 2014.

Kato, S., Rose, F. G., Sun-Mack, S., Miller, W. F., Chen, Y., Rutan, D. A., Stephens, G. L., Loeb, N. G., Minnis, P., Wielicki, B. A., Winker, D. M., Charlock, T. P., Stackhouse, P. W., Xu, K.-M., and Collins, W. D.: Improvements of top-of-atmosphere and surface irradiance computations with CALIPSO-, CloudSat-, and MODIS-derived cloud and aerosol properties, J. Geophys. Res., 116, D19209, doi:10.1029/2011JD016050, 2011.

Kay, J. E., Hillman, B. R., Klein, S. A., Zhang, Y., Medeiros, B., Pincus, R., Gettelman, A., Eaton, B., Boyle, J., Marchand, R., and Ackerman, T. P.: Exposing Global Cloud Biases in the Community Atmosphere Model (CAM) Using Satellite Observations and Their Corresponding Instrument Simulators, J. Clim., 25, 5190–5207, doi:10.1175/JCLI-D-11-00469.1, 2012.

Kiehl, J. T.: On the observed near cancellation between longwave and shortwave cloud forcing in tropical regions, J. Clim., 7, 559–565, doi: 10.1175/1520-0442(1994)007<0559:OTONCB>2.0.CO;2, 1994.

Klein, S. A. and Hall, A.: Emergent Constraints for Cloud Feedbacks, Curr. Clim. Change Rep., 1, 276–287, doi:10.1007/s40641-015-0027-1, 2015.

Klein, S. A. and Jakob, C.: Validation and sensitivities of frontal clouds simulated by the ECMWF model, Mon. Wea. Rev., 127, 2514–2531, doi:10.1175/1520-0493(1999)127<2514:VASOFC>2.0.CO;2, 1999.

Klein, S. A., Zhang, Y., Zelinka, M. D., Pincus, R., Boyle, J., and Gleckler, P. J.: Are climate model simulations of clouds improving? An evaluation using the ISCCP simulator, J. Geophys. Res., 118, 1329–1342, doi:10.1002/jgrd.50141, 2013.

Le Treut, H., Li, Z. X., and Forichon, M.: Sensitivity of the LMD general circulation model to greenhouse forcing associated with two different cloud water parameterizations, J. Clim., 7, 1827–1841, doi:10.1175/1520-0442(1994)007<1827:SOTLGC>2.0.CO;2, 1994.

L'Ecuyer, T. S., Wood, N. B., Haladay, T., Stephens, G. L., and Stackhouse, P. W.: Impact of clouds on atmospheric heating based on the R04 CloudSat fluxes and heating rates data set, J. Geophys. Res., 113, D00A15, doi:10.1029/2008JD009951, 2008.

Loeb, N. G., Wielicki, B. A., Doelling, D. R., Smith, G. L., Keyes, D. F., Kato, S., Manalo-Smith, N., and Wong, T.: Toward optimal closure of the Earth's top-of-atmosphere radiation budget, J. Clim., 22, 748–766, doi:10.1175/2008JCLI2637.1, 2009.

Mace, G. G, Houser, S, Benson, S., Klein, S. A., and Min, Q.: Critical Evaluation of the ISCCP Simulator Using Ground-Based Remote Sensing Data, J. Clim., 24, 1598–1612, doi:10.1175/2010JCLI3517.1, 2011.

Marchand, R. and Ackerman, T.: An analysis of cloud cover in multiscale modeling framework global climate model simulations using 4 and 1 km horizontal grids, J. Geophys. Res., 115, D16207, doi:10.1029/2009JD013423, 2010.

Marvel, K., Zelinka, M., Klein, S. A., Bonfils, C., Caldwell, P., Doutriaux, C., Santer, B. D., and Taylor, K. E.: External Influences on Modeled and Observed Cloud Trends, J. Clim., 28, 4820–4840, doi:10.1175/JCLI-D-14-00734.1, 2015.

Michele, S. D., McNally, T., Bauer, P., and Genkova, I.: Quality Assessment of Cloud-Top Height Estimates From Satellite IR Radiances Using the CALIPSO Lidar, IEEE Trans. Geosci. Remote Sens., 51, 2454–2464, doi:10.1109/TGRS.2012.2210721, 2013.

Nam, C., Bony, S., Dufresne, J.-L., and Chepfer, H.: The "too few, too bright" tropical low-cloud problem in CMIP5 models, Geophys. Res. Lett., 39, L21801, doi: 10.1029/2012GL053421, 2012.

Norris, J. R. and Evan A. T.: Empirical Removal of Artifacts from the ISCCP and PATMOS-x Satellite Cloud Records, J. Atmos. Ocean. Technol., 32, 691–702, doi:10.1175/JTECH-D-14-00058.1, 2015.

Norris, J. R., Allen, R. J., Evan, A. T., Zelinka, M. D., O'Dell, C. W., and Klein, S. A.: Evidence for climate change in the satellite cloud record, Nature, 536, 72–75, doi:10.1038/nature18273, 2016.

Ramanathan, V.: Interactions between Ice-Albedo, Lapse-Rate and Cloud-Top Feedbacks: An Analysis of the Nonlinear Response of a GCM Climate Model, J. Atmos. Sci., 34, 1885–1897, doi:10.1175/1520-0469(1977)034<1885:IBIALR>2.0.CO;2, 1977.

Rieger, V. S., Dietmüller, S., and Ponater, M.: Can feedback analysis be used to uncover the physical origin of climate sensitivity and efficacy differences?, Clim. Dyn., 1–14, doi:10.1007/s00382-016-3476-x, 2016.

Roca, R., Guzman, R., Lemond, J., Meijer, J., Picon, L., and Brogniez, H.: Tropical and extra-tropical influences on the distribution of free tropospheric humidity over the intertropical belt, Surv. Geophys., 33, 565–583, doi:10.1007/s10712-011-9169-4, 2012.

Rose, F. G., Rutan, D. A., Charlock, T., Smith, G. L., and Kato, S.: An Algorithm for the Constraining of Radiative Transfer Calculations to CERES-Observed Broadband Top-of-Atmosphere Irradiance, J. Atmos. Oceanic Technol., 30, 1091–1106, doi:10.1175/JTECH-D-12-00058.1, 2013.

Schneider, S. H.: Cloudiness as a Global Climatic Feedback Mechanism: The Effects on the Radiation Balance and Surface Temperature of Variations in Cloudiness, J. Atmos. Sci., 29, 1413–1422, doi:10.1175/1520-0469(1972)029<1413:CAAGCF>2.0.CO;2, 1972.

Shea, Y. L., Wielicki, B. A., Sun-Mack, S., and Minnis, P.: Quantifying the Dependence of Satellite Cloud Retrievals on Instrument Uncertainty, J. Clim., doi:10.1175/JCLI-D-16-0429.1, 2017.

Sherwood, S. C., Chae, J.-H., Minnis, P., and McGill, M.: Underestimation of deep convective cloud tops by thermal imagery, Geophys. Res. Lett., 31, L11102, doi:10.1029/2004GL019699, 2004.

Sherwood, S. C., Bony, S., Boucher, O., Bretherton, C., Forster, P. M., Gregory, J. M., and Stevens, B.: Adjustments in the Forcing-Feedback Framework for Understanding Climate Change, Bull. Am. Meteorol. Soc., 96, 217–228, doi:10.1175/BAMS-D-13-00167.1, 2015.

Soden, B. J., Held, I. M., Colman, R., Shell, K. M., Kiehl, J. T., and Shields, C. A.: Quantifying Climate Feedbacks Using Radiative Kernels, J. Clim., 21, 3504–3520, doi:10.1175/2007JCLI2110.1, 2008.

Spencer, R. W. and Braswell, W. D.: How Dry is the Tropical Free Troposphere? Implications for Global Warming Theory, Bull. Am. Meteorol. Soc., 78, 1097–1106, doi:10.1175/1520-0477(1997)078<1097:HDITTF>2.0.CO;2, 1997.

Stamnes, K., Tsay, S.-C., Wiscombe, W., and Jayaweera, K.: Numerically stable algorithm for discrete-ordinate-method radiative transfer in multiple scattering and emitting layered media, Appl. Opt., 27, 2502–2509, doi:10.1364/AO.27.002502, 1988.

Stephens, G. L., Vane, D. G., Boain, R. J., Mace, G. G., Sassen, K., Wang, Z., Illingworth, A. J., O'Connor, E. J., Rossow, W. B., Durden, S. L., Miller, S. D., Austin, R. T., Benedetti, A., and Mitrescu, C.: The CloudSat mission and the A-Train: A new dimension of space-based observations of clouds and precipitation, Bull. Am. Meteorol. Soc., 83, 1771–1790, doi:10.1175/BAMS-83-12-1771, 2002.

Stubenrauch, C. J., Cros, S., Guignard, A., and Lamquin, N.: A 6-year global cloud climatology from the Atmospheric InfraRed Sounder AIRS and a statistical analysis in synergy with CALIPSO and CloudSat, Atmos. Chem. Phys., 10, 7197–7214, doi:10.5194/acp-10-7197-2010, 2010.

Stubenrauch, C. J., Rossow, W. B., Kinne, S., Ackerman, S., Cesana, G., Chepfer, H., Di Girolamo, L., Getzewich, B., Guignard, A., Heidinger, A., Maddux, B. C., Menzel, W. P., Minnis, P., Pearl, C., Platnick, S., Poulsen, C., Riedi, J., Sun-Mack, S., Walther, A., Winker, D., Zeng, S., and Zhao, G.: Assessment of Global Cloud Datasets from Satellites: Project and Database Initiated by the GEWEX Radiation Panel, Bull. Am. Meteorol. Soc., 94, 1031–1049, doi:10.1175/BAMS-D-12-00117.1, 2013.

Su, H., Jiang, J. H., Zhai, C., Shen, T. J., Neelin, J. D., Stephens, G. L., and Yung, Y. L.: Weakening and strengthening structures in the Hadley Circulation change under global warming and implications for cloud response and climate sensitivity, J. Geophys. Res., 119, 5787–5805, doi:10.1002/2014JD021642, 2014.

Suarez, M. J., Bloom, S., daSilva, A., Dee, D., Bosilovich, M., Chern, J.-D., Pawson, S., Schubert, S., Sienkiewicz, M., Stajner, I., Tan, W.-W., and Wu, M.-L.: Documentation and validation of the Goddard Earth Observing System (GEOS) data assimilation system, version 4, 2005.

Taylor, K. E., Crucifix, M., Braconnot, P., Hewitt, C. D., Doutriaux, C., Broccoli, A. J., Mitchell, J. F. B., and Webb, M. J.: Estimating Shortwave Radiative Forcing and Response in Climate Models, J. Clim., 20, 2530–2543, doi:10.1175/JCLI4143.1, 2007.

Vaughan, M. A., Powell, K. A., Winker, D. M., Hostetler, C. A., Kuehn, R. E., Hunt, W. H., Getzewich, B. J., Young, S. A., Liu, Z., and McGill, M. J.: Fully Automated Detection of Cloud and Aerosol Layers in the CALIPSO Lidar Measurements, J. Atmos. Oceanic Technol., 26, 2034–2050, doi:10.1175/2009JTECHA1228.1, 2009.

Vial, J., Dufresne, J.-L., and Bony, S.: On the interpretation of inter-model spread in CMIP5 climate sensitivity estimates, Clim. Dyn., 41, 3339–3362, doi:10.1007/s00382-013-1725-9, 2013.

Wang, P.-H., Minnis, P., Wielicki, B. A., Wong, T., and Vann, L. B.: Satellite observations of long-term changes in tropical cloud and outgoing longwave radiation from 1985 to 1998, Geophys. Res. Lett., 29, 37-1–37-4, doi:10.1029/2001GL014264, 2002.

Watterson, I. G., Dix, M. R., and Colman, R. A.: A comparison of present and doubled CO2 climates and feedbacks simulated by three general circulation models, J. Geophys. Res., 104, 1943–1956, doi:10.1029/1998JD200049, 1999.

Webb, M. J., Lambert, F. H., and Gregory, J. M.: Origins of differences in climate sensitivity, forcing and feedback in climate models, Clim. Dyn., 40, 677–707, doi:10.1007/s00382-012-1336-x, 2013.

Wetherald, R. T. and Manabe, S.: Cloud Feedback Processes in a General Circulation Model, J. Atmos. Sci., 45, 1397–1416, doi:10.1175/1520-0469(1988)045<1397:CFPIAG>2.0.CO;2, 1988.

Wielicki, B. A., Young, D. F., Mlynczak, M. G., Thome, K. J., Leroy, S., Corliss, J., Anderson, J. G., Ao, C. O., Bantges, R., Best, F., Bowman, K., Brindley, H., Butler, J. J., Collins, W., Dykema, J. A., Doelling, D. R., Feldman, D. R., Fox, N., Huang, X., Holz, R., Huang, Y., Jin, Z., Jennings, D., Johnson, D. G., Jucks, K., Kato, S., Kirk-Davidoff, D. B., Knuteson, R., Kopp, G., Kratz, D. P., Liu, X., Lukashin, C., Mannucci, A. J., Phojanamongkolkij, N., Pilewskie, P., Ramaswamy, V., Revercomb, H., Rice, J., Roberts, Y., Roithmayr, C. M., Rose, F., Sandford, S., Shirley, E. L., Smith, W. L., Soden, B., Speth, P. W., Sun, W., Taylor, P. C., Tobin, D., and Xiong, X.: Achieving Climate Change Absolute Accuracy in Orbit, Bull. Am. Meteorol. Soc., 94, 1519–1539, doi:10.1175/BAMS-D-12-00149.1, 2013.

Williams, K. D. and Webb, M. J.: A quantitative performance assessment of cloud regimes in climate models, Clim. Dyn., 33, 141–157, doi:10.1007/s00382-008-0443-1, 2009.

Winker, D. M. et al.: The CALIPSO Mission: A Global 3D View of Aerosols and Clouds, Bull. Am. Meteorol. Soc., 91, 1211–1229, doi:10.1175/2010BAMS3009.1, 2010.

Yokohata, T., Emori, S., Nozawa, T., Tsushima, Y., Ogura, T., and Kimoto, M.: A simple scheme for climate feedback analysis, Geophys. Res. Lett., 32, L19703, doi:10.1029/2005GL023673, 2005.

Yue, Q., Kahn, B. H., Fetzer, E. J., Wong, S., Frey, R., and Meyer, K. G.: On the response of MODIS cloud coverage to global mean surface air temperature, J. Geophys. Res., 122, 966–979, doi:10.1002/2016JD025174, 2017.

Zelinka, M. D. and Hartmann, D. L.: The observed sensitivity of high clouds to mean surface temperature anomalies in the tropics, J. Geophys. Res., 116, D23103, doi:10.1029/2011JD016459, 2011.

Zelinka, M. D., Klein, S. A., and Hartmann, D. L.: Computing and Partitioning Cloud Feedbacks Using Cloud Property Histograms. Part I: Cloud Radiative Kernels, J. Clim., 25, 3715–3735, doi:10.1175/JCLI-D-11-00248.1, 2012.

Zelinka, M. D., Klein, S. A., and Hartmann, D. L.: Computing and partitioning cloud feedbacks using cloud property histograms. Part II: Attribution to changes in cloud amount, altitude, and optical depth, J. Clim., 25, 3736–3754, 2012.

Zelinka, M. D., Klein, S. A., Taylor, K. E., Andrews, T., Webb, M. J., Gregory, J. M., and Forster, P. M.: Contributions of Different Cloud Types to Feedbacks and Rapid Adjustments in CMIP5, J. Clim., 26, 5007–5027, doi:10.1175/JCLI-D-12-00555.1, 2013.

Zelinka, M. D., Zhou, C., and Klein, S. A.: Insights from a refined decomposition of cloud feedbacks, Geophys. Res. Lett., 43, 9259–9269, doi:10.1002/2016GL069917, 2016.

Zhang, M. H., Lin, W. Y., Klein, S. A., Bacmeister, J. T., Bony, S., Cederwall, R. T., Del Genio, A. D., Hack, J. J., Loeb, N. G., Lohmann, U., Minnis, P., Musat, I., Pincus, R., Stier, P., Suarez, M. J., Webb, M. J., Wu, J. B., Xie, S. C., Yao, M.-S., and Zhang, J. H.: Comparing clouds and their seasonal variations in 10 atmospheric general circulation models with satellite measurements, J. Geophys. Res., 110, D15S02, doi:10.1029/2004JD005021, 2005.

Zhang, Y., Rossow, W. B., Lacis, A. A., Oinas, V., and Mishchenko, M. I.: Calculation of radiative fluxes from the surface to top of atmosphere based on ISCCP and other global data sets: Refinements of the radiative transfer model and the input data, J. Geophys. Res., 109, D19105, doi:10.1029/2003JD004457, 2004.

Zhou, C., Zelinka, M. D., Dessler, A. E., and Yang P.: An Analysis of the Short-Term Cloud Feedback Using MODIS Data, J. Clim., 26, 4803–4815, doi:10.1175/JCLI-D-12-00547.1, 2013.